Neuronal Plasma Membrane Disruption in Traumatic Brain Injury

A Thesis

Presented to

The Academic Faculty

by

Gustavo R. Prado

In Partial Fulfillment

of the Requirements for the Degree

Doctor of Philosophy in the

School of Biomedical Engineering

Georgia Institute of Technology

July 2004

Copyright 2004 by Gustavo R. Prado

Neuronal Plasma Membrane Disruption in Traumatic Brain Injury

Approved by:

Dr. Michelle C. LaPlaca

Dr. Stephen P. DeWeerth

Dr. Edward Pettus

Dr. Steven M Potter

Dr. Mark R. Prausnitz

July 1. 2004

DEDICATION

I would like to thank my parents Alvaro and Vera for a lifetime of support and my wife Heather for making the last five years a great chapter in my life.

ACKNOWLEDGEMENTS

The author would like to acknowledge Jim Ross who manufactured the multi-electrode arrays and aided in techniques such as platinum plating employed in the manufacturing process as well as quantification of electrical outcome by software development. Ciara Caltagirone and Dr. Michael Schumm provided invaluable aid in the *in vivo* portion of this research with their expertise in animal experimentation. Dr. Mark R. Prausnitz, Dr. Pavel Kamaev, and Dr. Donna M. Geddes were pivotal in providing technical advice in the membrane disruption assays. Everyone in Dr. LaPlaca's laboratory was helpful in solving various technical issues throughout this process. John Graham and everyone else in the ME machine shop were instrumental in the facilitation in the manufacturing of the devices utilized in this study. This work was primarily funded by the Whitaker Foundation and the Institute of Bioengineering and Bioscience.

TABLE OF CONTENTS

LIST OF FIGURES

SUMMARY

During a traumatic insult to the brain, tissue is subjected to large stresses at high rates which often surpass cellular thresholds leading to cell dysfunction or death. Cellular events that occur at the time of and immediately after an insult are poorly understood. Immediately following traumatic brain injury (TBI), the neuronal plasma membrane may become disrupted and potentiate detrimental pathways by allowing extracellular contents to gain access to the cytosol. In the current study, neuronal plasma membrane disruption was assessed *in vivo* following moderate unilateral controlled cortical impact (CCI) in rats using a normally cell-impermeant fluorescent compound as a plasma membrane permeability marker. This fluorescent dye was injected into the CSF and allowed to diffuse into the brain. TBI caused a widespread acute disruption of neuronal membranes which was significantly different compared to uninjured brains. Affected cells were present in cortex and hippocampal regions. These findings were complemented by an *in vitro* model of TBI where membrane disruption was quantified and its mechanisms elucidated. Permeability marker(s) were added to neuronal cultures before the insult as indicators for increases in plasma membrane permeability. The percentage of cells containing the permeability marker was dependent on the molecular mass, as smaller molecules gained access to a higher percentage of cells than larger ones. Permeability increases were also positively correlated with the rate at which the insult was applied. Membrane disruption was transient, evidenced by a robust resealing within the first minute after the insult (assessed by adding permeability markers at different time points following the mechanical insult). In addition, membrane resealing was found to be dependent on extracellular Ca^{2+}, as chelation of the divalent ion abolished a significant

amount of resealing. Neurons depend on a tightly regulated ion concentration gradient across the plasma membrane, and mechanically-induced changes in membrane permeability can affect action potential firing, axonal signal conduction, and synapse function. We have investigated the effects of mechanically-induced plasma membrane disruptions on neuronal network electrical activity. We have developed a multielectrode array system that allows the study of electrical activity before, during, and after a traumatic insult to neurons. Endogenous electrical activity of neuronal cultures presented a heterogeneous response following mechanical insult. Moreover, spontaneous firing dysfunction induced by injury outlasted the presence of membrane disruptions. This study provides a multi-faceted approach to elucidate the role of neuronal plasma membrane disruptions in TBI and its functional consequences.

CHAPTER 1

INTRODUCTION

1.1 Mechanics of traumatic brain injury

Traumatic brain injury (TBI) arises from excessive mechanical stresses that are capable of generating strains which surpass tissue thresholds, leading to microscopic as well as macroscopic mechanical failure. A widely accepted injury criterion in head injury research, obtained initially from experiments on human cadavers, known as the Head Injury Criterion, shows that injury threshold depend on both acceleration of the head as well as duration of the onset of acceleration (Gurdjian et al., 1966). However, the type of acceleration (linear or angular) and the plane where the acceleration is induced both play important roles in tissue damage (Anderson, 1997). Ommaya et al. demonstrated that angular accelerations to brain tissue are particularly harmful (Ommaya and Gennarelli, 1974). These accelerations in animal preparations have been shown to produce shear strains which have been correlated to a large probability of concussion and presence of tissue damage such as axonal injury (Gennarelli et al., 1982). Holbourn, in earlier mechanical experiments, also found that shear deformation is the major type of deformation in TBI (Holbourn, 1943). More recent *in vitro* models of TBI, using fluid shear stress as a insult delivery method, have demonstrated that injury responses are dependent on the magnitude as well as the rate of stress loading to cells (LaPlaca et al., 1997). In addition, *in vitro* models using stretch-induced insult have shown that cell injury is dependent on stretch rate and magnitude. These observations are not surprising due to the viscoelastic nature of biological tissues.

1.2 Modeling TBI

TBI is a complex condition which consists of several parallel and serial cascades of events that are initially triggered by a mechanical insult to brain tissue and surrounding area. In order to study such complex condition, several different types of *in vivo* TBI models have been developed. Data from two models types will be discussed here. Both the fluid percussion model (McIntosh et al., 1989) and the cortical contusion model (Sutton et al., 1993) are widely used. The former produces a more diffuse injury and the latter a more local injury.

The complex responses seen following TBI vary according to the severity of insult and the area affected (Gennarelli, 1993). The heterogeneity of the brain tissue further adds complexity to the study of TBI (Prange and Margulies, 2002). For example, different types of brain tissue yield differential mechanical responses from the insult, which has been shown to be dependent on myelination level (white or grey matter) (Graham et al., 2000), cell type (Nawashiro et al. 1995), and tissue orientation (Graham et al., 2000; Nawashiro et al., 1995). Nawashiro et al., for example, have shown that CA3 hippocampal neurons selectively die from mild TBI followed by hypoxia, while neighboring tissue is spared. The study of TBI is further complicated by secondary responses to initial insult such as activation of intracellular biochemical cascades, systemic interactions with native tissue such as invasion of blood-born cells into injured area, and processes of cell death and recovery. These interactions manifest themselves at different time points. Research in several of these processes has elucidated many intricate aspects of this condition through the help of both *in vitro* and *in vivo* models of TBI.

In vitro models are useful tools which simplify multi-faceted problems with the help of an idealized controlled environment (Morrison et al., 1998). Furthermore these models are most relevant to the clinical setting when used to study short term or acute cellular responses. As time passes from initial insult, the lack of interactions and complexity of *in vitro* models will cause them to deviate further from *in vivo*. Conversely, events which occur shortly following mechanical injury will tend to reflect more accurately *in vivo* aspects of TBI.

1.3 Acute cellular response following TBI

Many cellular responses have been studied following TBI, including protein phosphorylation, protein breakdown (proteolysis), cell death via apoptosis and necrosis, and gene expression, among others. Many of these responses have been linked to intracellular Ca^{2+} disturbances. Extracellular Ca^{2+} influx into the cytosol of mechanically and chemically injured cells is one acute cellular event which has been extensively researched in both *in vitro* and *in vivo* TBI models (Cargill and Thibault, 1996; Geddes and Cargill, 2001; Gennarelli, 1993; LaPlaca et al., 1997; Tymianski and Tator, 1996; Weber et al., 1999; Wolf et al., 2001). Intracellular Ca^{2+} is known to be a ubiquitous secondary messenger implicated in many different cellular functions from cytoskeleton remodeling processes (Stewart et al., 1998) to fast triggering of vesicle docking (Detrait et al., 2000a; Detrait et al., 2000b). In order for Ca^{2+} to be an effective messenger, however, it is kept at very low intracellular concentrations. This is accomplished by active transport of the ion from the cytosol to the extracellular space or internal storage compartments such as the endoplasmic reticulum via ATPases and Na^{+} /Ca^{2+} exchangers. This active segregation produces a large concentration gradient of Ca^{2+} across the plasma

membrane. Therefore, if the plasma membrane becomes compromised, Ca^{2+} will diffuse down the gradient (Grembowicz et al., 1999). If membrane damage is severe enough, Ca^{2+} concentrations can quickly rise and overwhelm cellular mechanisms involved in ionic homeostasis. Persistent and high concentration of Ca^{2+} is the primary cause of certain cellular responses reported following TBI such as indiscriminate cytoskeletal proteolysis by activation enzymes such as calpain (Brana et al., 1999; Buki et al., 1999a; Newcomb-Fernandez et al., 2001; Pike et al., 2000; Stewart et al., 1998), endonuclease activation (Lewen et al., 2001), as well as activation of a range of other Ca^{2+}-mediated cascades, including the ones involving PKC, PKA (Raghupathi et al., 1995). Persistence of Ca^{2+} in the cell is also be responsible for mitochondrial damage (Albensi et al., 2000; Lifshitz et al., 2003; Pettus et al., 1994), energy depletion, and necrotic (Allen et al., 1999) as well as apoptotic (Yakovlev et al., 1997) cell death, all of which have been reported following TBI . Finally, increases of intracellular Ca^{2+} and/or extensive loss of membrane potential homeostasis due to TBI have been linked to increases of intracellular cAMP and the activation of early immediate genes such as c-fos, c-jun, and junB as early as five minutes post-injury (Raghupathi et al., 1995). Although intracellular Ca^{2+} increases have been implicated in most acute cellular responses, the acute entry method this ion is not fully understood. We propose that this entry of Ca^{2+}, at least acutely, is directly due to the increase in neuronal plasma membrane permeability increase due to disruptions caused by the mechanical stress. Although this research is not the first to propose such a mechanism (Geddes et al., 2003; Pettus et al., 1994; Pettus and Povlishock, 1996; Singleton and Povlishock, 2004; Singleton et al., 2002), it is the first

study to comprehensively elucidate the *acute* disruptions of the plasma membrane occurring following a mechanical insult in both *in vivo* as well as *in vitro* TBI models.

1.4 Current research

The current research objectives are to elucidate acute cellular events following a traumatic mechanical insult which can contribute to cell death and or dysfunction. We have evaluated the extent of plasma membrane disruption in the injured rat brain using an *in vivo* model of TBI. Also, the mechanisms of neuronal plasma membrane disruptions and subsequent resealing have been partially elucidated with the help of an *in vitro* model of TBI. Lastly, we have ascertained the electrical responses of neuronal cells following a mechanical trauma in which the plasma membrane is disrupted through extracellular recordings, using microelectrode array technology.

We have utilized a well-established *in vivo* model of TBI to accomplish the first objective in the current study. The CCI model produces a mostly focal injury caused by impact of a piston-like object onto the exposed dura mater of the rat. In order to evaluate the extent of the plasma membrane disruption in the injured brain a permeability marker was injected into the cerebrospinal fluid of the animal prior to the injury. The marker cannot gain access to cells that have an intact plasma membrane. It will, however, flood cells that present a membrane disruption and, if resealing occurs, the dye can then be trapped into the cellular compartment. We have confirmed a vast number of cells in different brain regions which have an increase in plasma membrane permeability, allowing the marker into the cell bodies followed by a subsequent membrane resealing which traps the marker in the cytosol.

In order to elucidate the temporal profile of the plasma membrane disruption induced by mechanical trauma and the subsequent resealing mechanism, we have utilized an *in vitro* model of TBI. We have developed a cell shearing device (CSID) capable of delivering high magnitudes of shear stress, at high rates, to neuronal cell cultures. We have validated the CSID, which is able of producing neuronal cellular death. We subsequently used sub-lethal injury parameters in the study of neuronal plasma membrane disruption. These parameters are capable of producing vast plasma membrane disruptions without increasing neuronal cell death at 24 hours post injury. Different characteristics of the plasma membrane resealing mechanism were elucidated, such as its calcium dependence and actin cytoskeleton involvement.

The electrical activity consequences of an increase in neuronal plasma membrane permeability driven by a mechanical insult have not been researched to date. This increase in neuronal plasma membrane permeability is hypothesized to disturb the ionic homeostasis of cells by allowing indiscriminate flux of ions across the membrane, directly affecting electrical activity. The spontaneous neuronal electrical activity responses following a mechanical trauma were evaluated. Upon modifications made to the CSID, we were capable of performing extracellular recordings of neuronal cultures before and immediately following an *in vitro* mechanical injury. This novel device allowed for first time insight in network electrical activity responses to a traumatic mechanical insult.

CHAPTER 2

TRAUMATIC INSULT INDUCES MEMBRANE DISRUPTIONS IN CELLS OF THE RAT BRAIN

2.1 Introduction

In order to fully understand the complex mechanisms triggered as a result of a traumatic insult to the brain, we must elucidate the acute events—also known as the primary injury. Research using *in vivo* traumatic brain injury (TBI) models has found that selective regions in the brain are more affected by the mechanical insult than others. For example, a vast presence of acute neuronal damage throughout brain areas such as certain regions of the hippocampal formation and cortex occurs as early as 10 minutes following fluid percussion (FP) injury (Carbonell and Grady, 1999; Hicks et al., 1996). In the hilar region of hippocampal formation, immediate early genes such as c-fos, c-jun, and junB have been reported to have increased induction within 5 minutes after FP injury. More recently, a transient loss of the microtubule-associated protein 2 (MAP-2) was reported 5 minutes following a moderate cortical contusion injury in mice (Huh et al., 2003). The trigger mechanisms which initiate these early cellular responses in neurons, however, have remained largely unexplored. Excitotoxicity is a major mechanism of injury which has been extensively studied and offered the potential explanation for the cell loss seen following TBI. This mechanism, which is triggered by an increase in the concentration of extracellular excitatory neurotransmitters, in particular glutamate, is believed to potentiate excess depolarization and it has been shown to be responsible for increases in intracellular Ca^{2+} (Koh et al., 1990; Sattler and Tymianski, 2000), proteolytic activity (Rami et al., 1997), and ultimately cell death (Munir et al., 1995). Using glutamate

concentrations obtained by microdialysis of the injured brain (Katayama et al., 1990), *in vitro* models of excitotoxicity have been able to reproduce the cell loss upon administration of glutamate to neuronal cultures (Munir et al., 1995). However, similar glutamate agonist levels were unable to induce the same cellular outcomes using *in vivo* excitotoxicity models, in which kainic acid (KA) was systemically injected. As discussed by Carbonnell et al., glutamate concentrations that eventually triggered cell loss in the brain were much larger than those found in TBI brains (Carbonell and Grady, 1999). Moreover, exitotoxicity insults using KA demonstrated delayed cell death for at least 3 hours after KA injection *in vivo,* which did not account for the acute cell injury mentioned above. This evidence points to additional mechanisms at work. Therefore, there is evidence that a much more widespread primary injury mechanism may trigger both acute cell damage as well as secondary injury mechanisms such as excitotoxicity. It is known that ionic currents occur immediately following trauma (Katayama et al., 1990) and are concomitant with an excessive excitatory neurotransmitter release in a positive feedback fashion. This mechanism is believed to be responsible for prolonged increases of intracellular Ca^{2+}, which has been shown to be a potential initiator of many detrimental pathways (Raghupathi et al., 1995). The question of how the initial ionic perturbation occurs, whether it is triggered by ion channels acting as stretch-activated channels or some other mechanism has remained unanswered.

We propose a novel mechanism that directly affects the somata of neurons and has the potential to lead to the rapid cellular damage occurring as early as minutes following trauma. We hypothesize that neuronal plasma membrane disruptions occur following TBI, causing an increase in plasma membrane permeability, which directly

affects the neurons at the somata level. Disruptions of the neuronal plasma membrane have the potential to trigger numerous detrimental events by allowing molecules and ions that are normally only present extracellularly inside the cell. We further hypothesize that certain areas, particularly the ones that have been shown to be more acutely vulnerable to experimental TBI (e.g., hippocampus), will be more affected than other brain regions, indicating that differential primary injury could be responsible to selectivity in cellular damage. A mechanism involving an increase in neuronal permeability due to plasma membrane disruptions caused by the mechanical insult may explain why excitotoxicity alone cannot be responsible for the cell damage seen following TBI (Carbonell and Grady, 1999).

The existence of an acute injury mechanism that would account for the initial large ionic currents postulated to occur after TBI, have been explored in relatively few studies of experimental TBI. These studies have shown alterations in the permeability of axonal plasma membranes in the cat brain as early as 5 minutes after FP injury (Pettus et al., 1994). The disruption of the axonal membrane was co-localized with alterations of cytoskeletal components such as compaction and misalignment of neurofilaments (Okonkwo et al., 1998; Pettus and Povlishock, 1996). Until recently, most of these studies focused on axonal membrane disruptions since FP insult produces a more diffuse injury compared to the controlled cortical impact (CCI) model and therefore diffuse axonal injury is a major manifestation of cell damage. Until a comprehensive study elucidated the fate of somata that presented axonal injury, it was unclear if the FP-induced axonal injury contributed to somata degeneration (Singleton et al., 2002). Singleton et al. have reported that traumatic axonal injury does not necessarily lead to

somata biochemical dysfunction and death even when injury is adjacent to cell bodies (Singleton et al., 2002). More relevant to this discussion, somatic plasma membranes have been shown to be directly compromised following FP injury when assessed at 2 hours post-injury (Singleton and Povlishock, 2004). Although the latter study points to a possible mechanism of primary somatic injury, there has not been an assessment of plasma membrane disruption of brain somata at time points within minutes of the insult, which may provide insight into the initial triggering mechanisms. Such a study would isolate the effects of the traumatic insult alone on neuronal plasma membrane integrity, negating other events such as swelling of brain tissue and neuronal plasma membrane breakdown which may occur in a delayed fashion.

The CCI is a model of focal TBI and it has been widely used in the past (Huh et al., 2003; Sutton et al., 1993). It consists of a pneumatic-driven piston which strikes the exposed dura mater of the rat brain. We have evaluated the membrane integrity of brain cells 10 minutes following a moderate insult evoked by a CCI device using a novel permeability marker. Lucifer yellow, the permeability marker used, is a relatively small molecule which is cell impermeant. An *in vitro* model of TBI and a cell wounding procedure were used to validate its ability to gain access into mechanically disturbed membranes and to stay in the cell once the membranes reseal. Following validation of Lucifer yellow, we have quantified the extent of cells with increased plasma membrane permeability in different injured brain regions. Our objective is to elucidate the extent and distribution of neuronal plasma membrane disruptions occurring acutely following experimental *in vivo* TBI at the somatic level— a potentially relevant primary injury mechanism for brain cell damage and death in TBI.

2.2 Materials and Methods

2.2.1 In vitro injury using Lucifer yellow as a permeability marker

Lucifer yellow (0.8 mg/mL of HBSS; Molecular Probes, Eugene, OR) was added to 7-day *in vitro* neuronal cell cultures (see Chapter 3 for culture details). Plasma membrane disruption was induced by scratching neuronal cultures with a 23-gauge needle or using the cell shearing injury device (see Chapter 3 for injury protocol).

2.2.2 Animal preparation

The initial surgical procedure consisted of permeability marker injection into the cerebrospinal fluid, as the marker cannot cross the blood brain barrier. Sprague-Dawley male rats (275 ± 25 g; Charles River, Wilmington, MA) were first anesthetized using 5% isoflurane/1000 mmHg O_2 in an induction chamber and maintained at 2-4% isoflurane/400 mmHg O_2. Fur was shaved from the head and rats were placed into a stereotactic apparatus and immobilized with standard ear bars. A 0.5 cm transverse incision was made at the base of the skull, exposing the atlanto-occipital membrane. The membrane was punctured and 4.0 cm of a polyethylene-10 tubing was inserted caudally into the subarachnoid space. A 50 µL Hamilton syringe (Reno, NV) attached to a 30-gauge needle was connected with the tubing and was used to inject permeability marker (20 µL of 4% w/v in 1 minute). Five minutes were allotted to elapse before the tubing was slowly removed. Severed muscle was sutured back and the skin incision was closed using 2-3 staples. Animals were put back in cages and permeability marker was allowed to diffuse into the brain for two hours.

2.2.3 Cortical contusion injury

Animals were re-anesthetized with isoflurane (5% induction, 2-4% maintenance) and placed in the sterotactic apparatus where a midline incision was made to expose the skull, which was then scraped and dried. A 6 mm diameter craniectomy was performed over the left fronto-parietal cortex, with the center 3.0 mm posterior to the bregma and 3.0 mm lateral to the midline. The skull flap was removed and the impactor rod (5 mm) of the CCI device was positioned over the dura mater at a 15º angle and impacted the brain at a velocity of 4.5 m/s to a depth of 2.0 mm. There were a total of 4 injured animals (n=4). Sham injured animals (n=2) underwent marker injection followed by craniectomy procedure. Uninjured animals (n=2) underwent marker injection only.

2.2.4 Post-injury processing

Animals were allowed to survive for 8 minutes, followed by an overdose of sodium pentobarbital (60 mg/kg; intraperitoneal injection). Animals were perfused intracardially with 120 mL PBS followed by 120 mL of 4% paraformaldehyde and 0.1% glutaldehyde in PBS at 4ºC. Brains were carefully removed from animals and placed in the fixative solution for 2 days at 4ºC in the absence of light. Brains were placed in 30% w/v sucrose (Sigma) in PBS for 2 days or until they were infiltrated. Brains were then placed in plastic molds (Electron Microscopy Sciences, Hatfield, PA) which were subsequently filled with OCT (Sakura, Torrence, CA) and frozen in liquid nitrogen and kept at -80ºC. Brain sections were cut in a Cryostat at 20 µm thick and placed on microscope slides.

2.2.5 Somata membrane disruption quantification

Micrographs of the hippocampal areas CA1-3, and dentate gyrus, cerebral cortex, and thalamus were taken from injured, sham-injured, and uninjured rat brains. Micrographs were captured on a Nikon TE-300 microscope (Tokyo, Japan) or, when specified, a Zeiss confocal microscope (Oberkochen, Germany). A total of 3 coronal sections were analyzed per brain. Five regions of the brain (medial cerebral cortex , CA1, CA2, CA3, and dentate gyrus of the hippocampal formation) per section were photographed. The number of positive cells were quantified in each region and normalized by the total number of positive cells in that section. Sections were visualized using TRTC-conjugated FluoroNissl (Molecular Probes, Eugene, OR) as a counterstain for neuronal cells.

2.3 Results and Discussion

2.3.1 In vitro validation of Lucifer yellow as a permeability marker

Lucifer yellow has been extensively used as a neuronal tracer. It is impermeant to cells, and it is usually microinjected into the cytoplasm, where the dye quickly diffuses throughout the neurites belonging to that cell (Duval et al., 2002; Lubke et al., 1997). More recently, Lucifer yellow has been used as a resealing marker where it was employed to quantify resealing rate of transected axons *in vivo* (Howard et al., 1999). Our *in vitro* characterization of Lucifer yellow as a permeability marker showed that the dye was capable of gaining access into injured neural cells but remained outside cells in uninjured cultures. Because of its smaller size, Lucifer yellow (457 Da) is noticeably more sensitive than calcein (640 Da). Using Lucifer yellow also resulted in a visibly larger range in uptake amounts from cell to cell as well as extensive presence within

neurites (Figure 2.1). The Lucifer yellow used in our studies can be easily fixed, unlike calcein, with paraformaldehyde and glutaldehyde solution, which immobilizes the dye and preserves its fluorescence. Although Lucifer yellow has advantages over other dyes such as calcein, it is incapable of staying inside cells for flow cytometry quantification, unless it is fixed before cell removal from the substrate. For these reasons, calcein was the predominant permeability marker in *in vitro* plasma membrane disruption quantification experiments (see Chapter 3), while Lucifer yellow was used for the *in vivo* studies presented here.

2.3.2 Plasma membrane disruption in the injured brain

Lucifer yellow was diffused throughout the brain at two hours. There was, however a noticeable gradient of Lucifer yellow concentration which was higher at the ventral areas of the brain and lower laterally and dorsally at the cerebral cortex. Although such a gradient was present, it did not affect the analysis of positive cells since the amount of Lucifer yellow or the fluorescent intensity of cells was not quantified. Moreover, the gradient was macroscopic and microscopic sections assessed did not present noticeable background non-uniformity. Positive cells were easily distinguished from negative cells although the uptake observed *in vivo* did present a concentration gradient on a cell-to-cell comparison amongst neighboring cells, indicating differential levels of membrane disruptions.

Plasma membrane disruption was present in many areas of the injured brain, evidenced by the presence of Lucifer yellow–containing cells. Uptake of the permeability marker, however, varied significantly according to the area assessed. We have analyzed the extent of Lucifer yellow positive cells in the hippocampal areas of the CA1, CA2,

CA3, and dentate gyrus as well as the cerebral cortex on the ipsilateral and contralateral sides of the injury site (Figure 2.2 and 2.3). In the hippocampal formation, the areas containing the highest number of Lucifer yellow-containing cells were both the ipsilateral and contralateral dentate gyrus. Other more ventral areas of the ipsilateral hippocampal formation, including the CA2 and CA3 regions, presented significantly larger number of positive cells than the ipsilateral CA1 region. When comparing ipsilateral and contralateral dentate gyrus formations, the ventral-medial region of the dentate gyrus is the region with most asymmetry with respect to Lucifer yellow uptake (Figure 2.4). This is surprising since more distal areas were expected to have more differential uptake when comparing the impacted and unimpacted side.

The positive cells in the cerebral cortex as well as the hippocampal formation of the injured rat brains presented a continuum of intracellular concentrations of Lucifer yellow (Figure 2.5). This is evidence of a diverse severity in the membrane disruptions experienced by these cells at the time of the mechanical insult. More surprising yet is the presence of cells with high uptake of the permeability marker immediately adjacent to cells that contain no dye. This phenomenon was notably observed in the hippocampal formation and to a lesser degree in the cerebral cortex. The spatial uptake profile in the cortex presented a more gradual level of uptake within neighboring cells as compared to the hippocampal formation, which presented less gradual spatial uptake (Figure 2.5). Moreover, cells containing highest levels of Lucifer yellow presented a distinct shrunken morphology when compared with unaffected neighboring cells. Morphological changes seen co-localized with uptake of Lucifer yellow also shows gradation which seems to correlate to the amount of Lucifer yellow contained in the somata. In addition to the

shrunken and elongated morphology, positive cells also consistently presented diminished Nissl staining (Figure 2.6). Similar morphological changes have been reported also at 10 minutes following FP injury through an independent method of staining tissue with acid fuchsin (Hicks et al., 1996).

Complex patterns of cellular uptake of Lucifer yellow were present in most sections of the cerebral cortex (Figure 2.7) in spite of the even background fluorescence, ruling out the possibility of this phenomenon being due to a gradient of the permeability marker available extracellularly. These patterns suggest complex strain fields during CCI. In the hippocampal formation, specifically in the hilar region of the dentate gyrus, evidence of complex strains also exists, where regions of positive cells suddenly end without noticeable changes in tissue characteristics such as cell density. The number of positive cells is highest in the dentate gyrus and lowest in the CA1 region (Figure 2.8). This phenomenon could be due to the assumed prevalence of compressive stresses immediately below the impact site compared to more complex stress fields predicted towards the edges of the impact. Compressive stresses and strains have being reported to be less detrimental than shear strains (Gennarelli et al., 1982; Holbourn, 1943). Both ipsilateral and contralateral dentate gyrus regions were vastly affected. Unexpectedly, the hippocampal region closest to the impact site, the CA1 region, presented the fewest number of positive cells. These results may indicate that, the heterogeneity of the area immediately below the impact site, which presents tissues with different cellular alignment, myelination levels, and mechanical properties, can contribute to differential injury susceptibility (Prange and Margulies, 2002). Prange et al. has reported that, at rapid deformations, inhomogeneity of tissue can yield stress and strain concentrations

that may affect injury patterns. More evidence that complex strain fields are present in experimental *in vivo* TBI comes from finite element analysis studies which take tissue inhomogeneity into account. These studies have shown that shear strain can vary widely in different parts of the rat brain immediately following a weight-drop injury (Unpublished data from King et al., Wayne State University).

The results presented here support findings of a recently published study which has reported plasma membrane disruptions at the somata level following FP injury (Singleton and Povlishock, 2004). Singleton et al., however, did not evaluate membrane disruptions at time points earlier than 2 hours post-injury. Also, the smallest permeability marker used by Singleton et al. was 10 kDa. The current study showed an immediate plasma membrane disruption at the somata level, which differentially affects neurons throughout the brain following a CCI injury. This study also points to a mechanism for post-injury early ionic homeostasis disruption which may be a triggering mechanism to secondary detrimental pathways. Results from the current study also have implications in what causes differential susceptibility of certain areas of the brain following TBI and can contribute to the elucidation of preferential cell death found in certain areas. The extent of cells with disrupted membranes far exceeds the cell death known to occur in this injury regime. Therefore, this marker of injury is a sensitive one and may be a better indicator of potential cell dysfunction either temporary or permanent than an indicator of cell death. Since we hypothesize that cells containing Lucifer yellow have altered ionic balance for an unknown length of time, the extent of positive cells may be a reflection of the extent of dysfunctional cells present acutely after CCI.

The temporal profile of the disruptions is difficult to quantify, since injection of permeability marker needs to be made hours before injury in order to allow proper diffusion into the parenchyma. In order to further understand how long disruptions last and any potential resealing mechanism, one must take advantage of an *in vitro* model that can allow rapid manipulations of the presence of the permeability marker into the extracellular medium. By combining the advantages of both *in vitro* and *in vivo* models, we can evaluate *in vivo*-relevant cellular responses with the depth that an idealized *in vitro* environment provides.

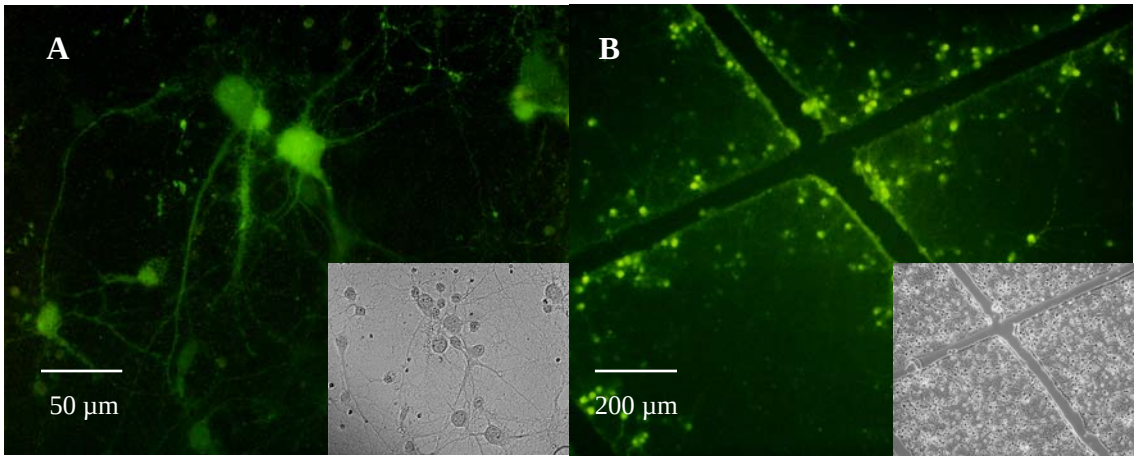

Figure 2.1. Lucifer yellow gained access to neurons in two modes of membrane disruption *in vitro*. Micrographs show permeability marker entrapped by resealing mechanism following fluid shear stress (A) and needle scratching-induced injury (B) in *in vitro* neuronal cultures. Visualization of membrane disruption in injured neuronal cultures was possible by applying the insult when Lucifer yellow was present in the extracellular medium and then rinsing the marker. Differential uptake of Lucifer yellow is seen in this fluorescence micrograph (A). Fluid shear stress-induced injury parameter was 140 dynes/cm^2, 300 ms impulse duration, and 20 ms rise time.

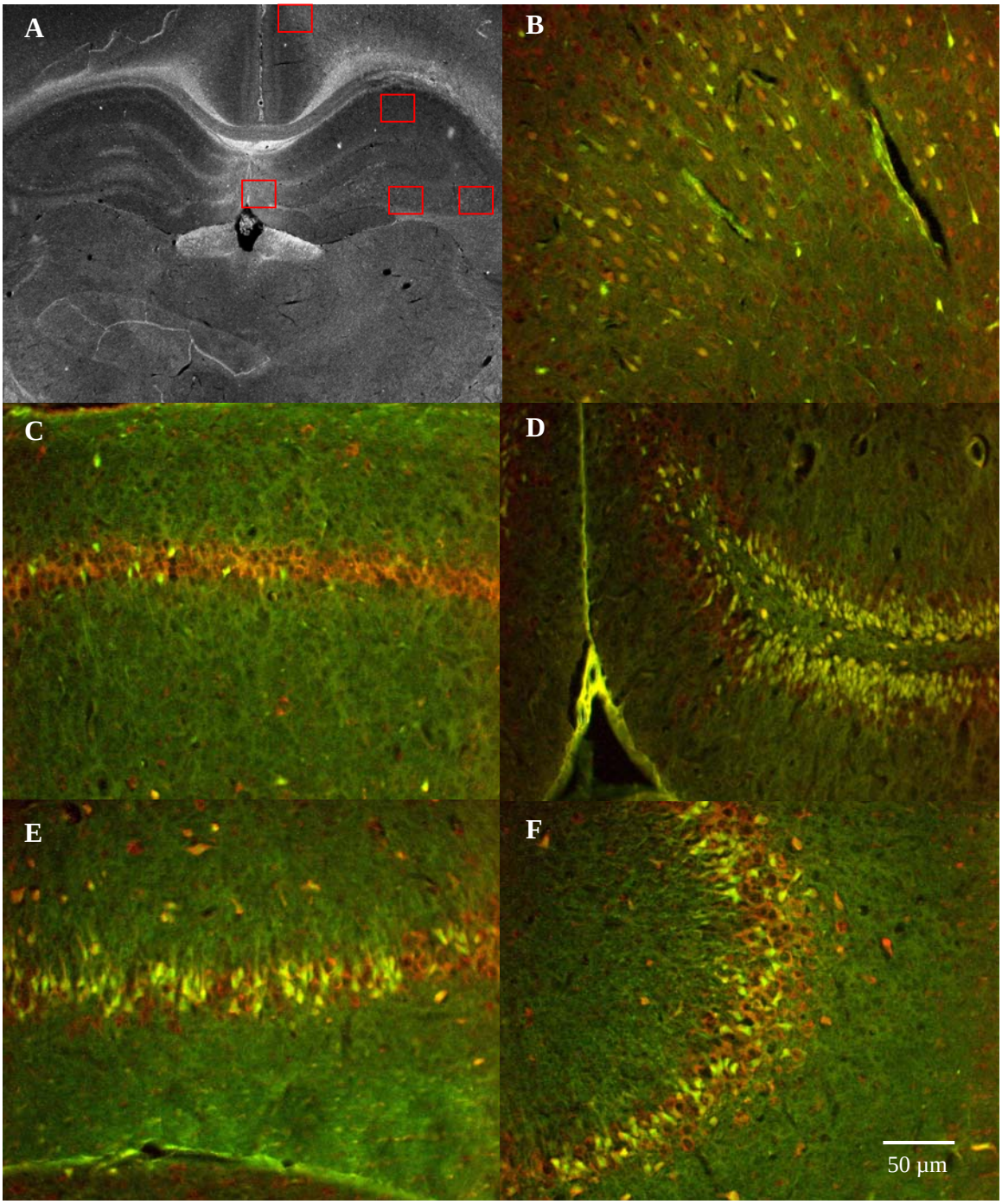

Figure 2.2. Ipsilateral regions of the injured rat brain contain widespread Lucifer yellow cellular uptake. (A) Low magnification bright field micrograph shows where subsequent photographs were taken (red boxes). (B) Cerebral cortex presented a heterogeneous uptake pattern. (C) Hippocampal CA1 region contained the lowest number of positive cells. (D) In contrast, the dentate gyrus presented a comparatively high number of positive cells. (E, F) The CA3 region also contained affected cells.

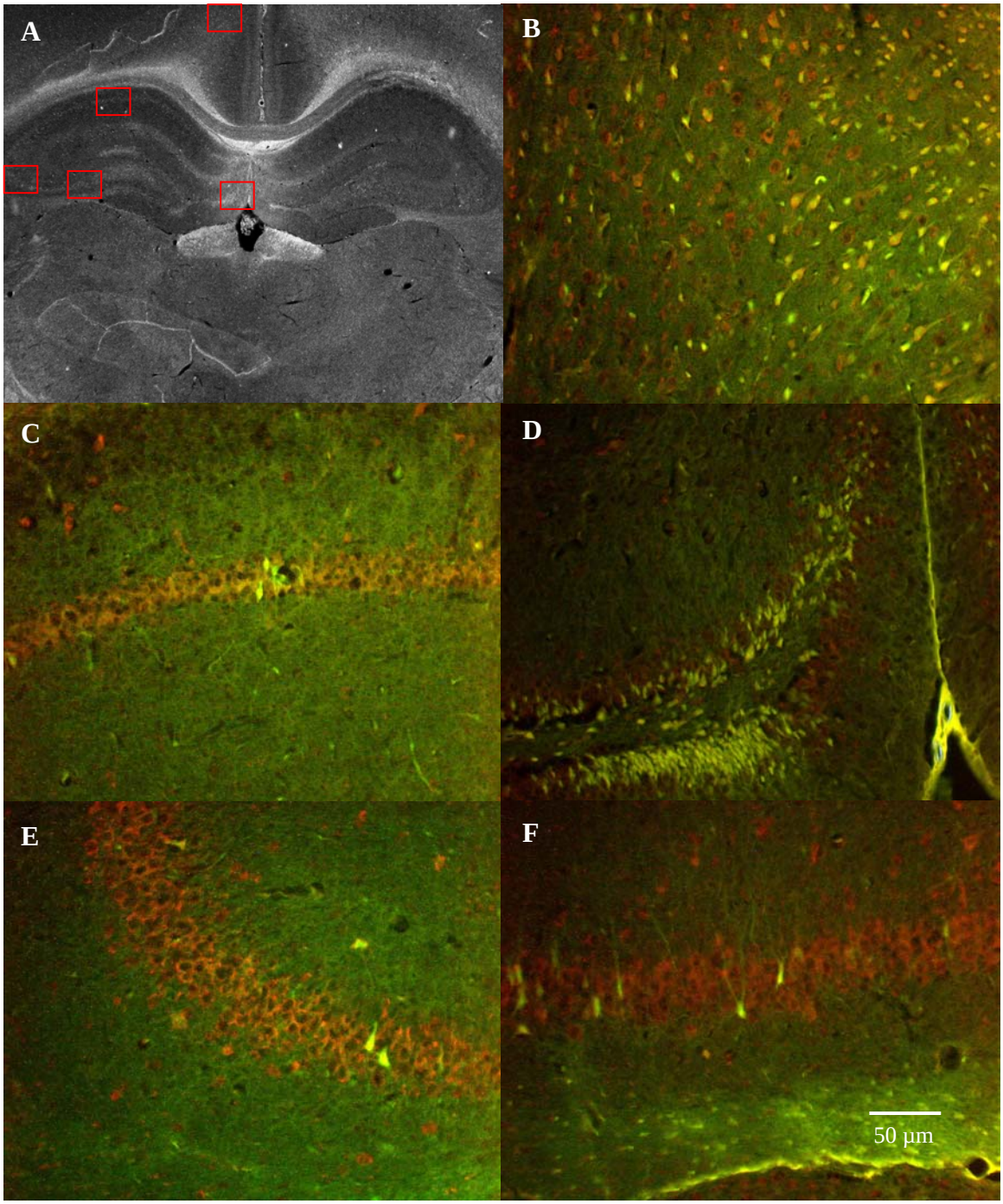

Figure 2.3. Contralateral regions of the rat injured brain. (A) Low magnification bright field micrograph shows where subsequent photographs were taken (red boxes). (B) Region of the cerebral cortex assessed presented a heterogeneous uptake pattern. (C) As in the ipsilateral side, hippocampal CA1 region contained few positive cells. (D) The contralateral dentate gyrus presented vast number of positive cells. (E, F) The CA3 region contralateral to the injury presented few positive cells and the greatest contrast when compared to the corresponding ipsilateral regions.

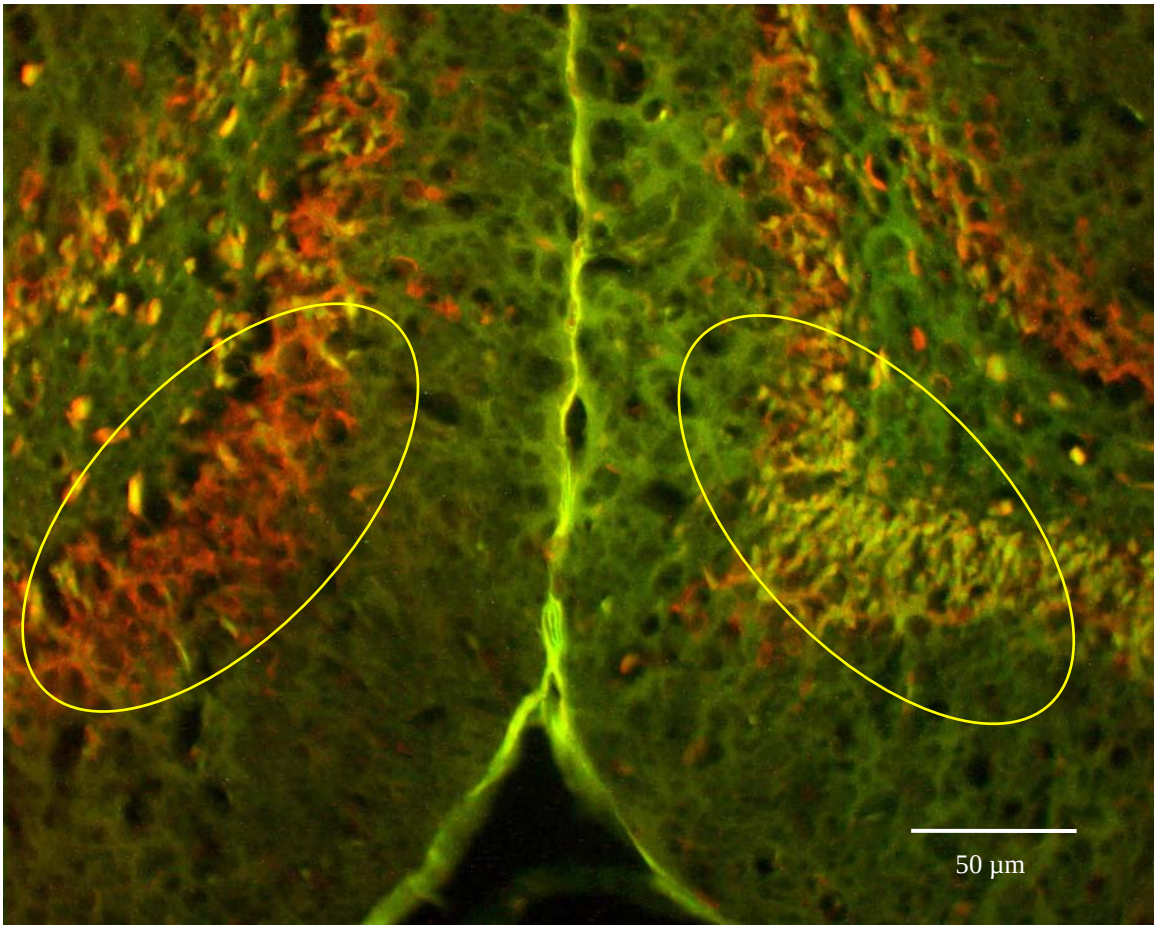

Figure 2.4. Dentate gyrus ipsilateral to the injury site contains more positive cells than the contralateral structure. The medial-ventral portions (enclosed by ellipse) of the ipsilateral dentate gyrus presents more positive cells than the same area in the contralateral side (left).

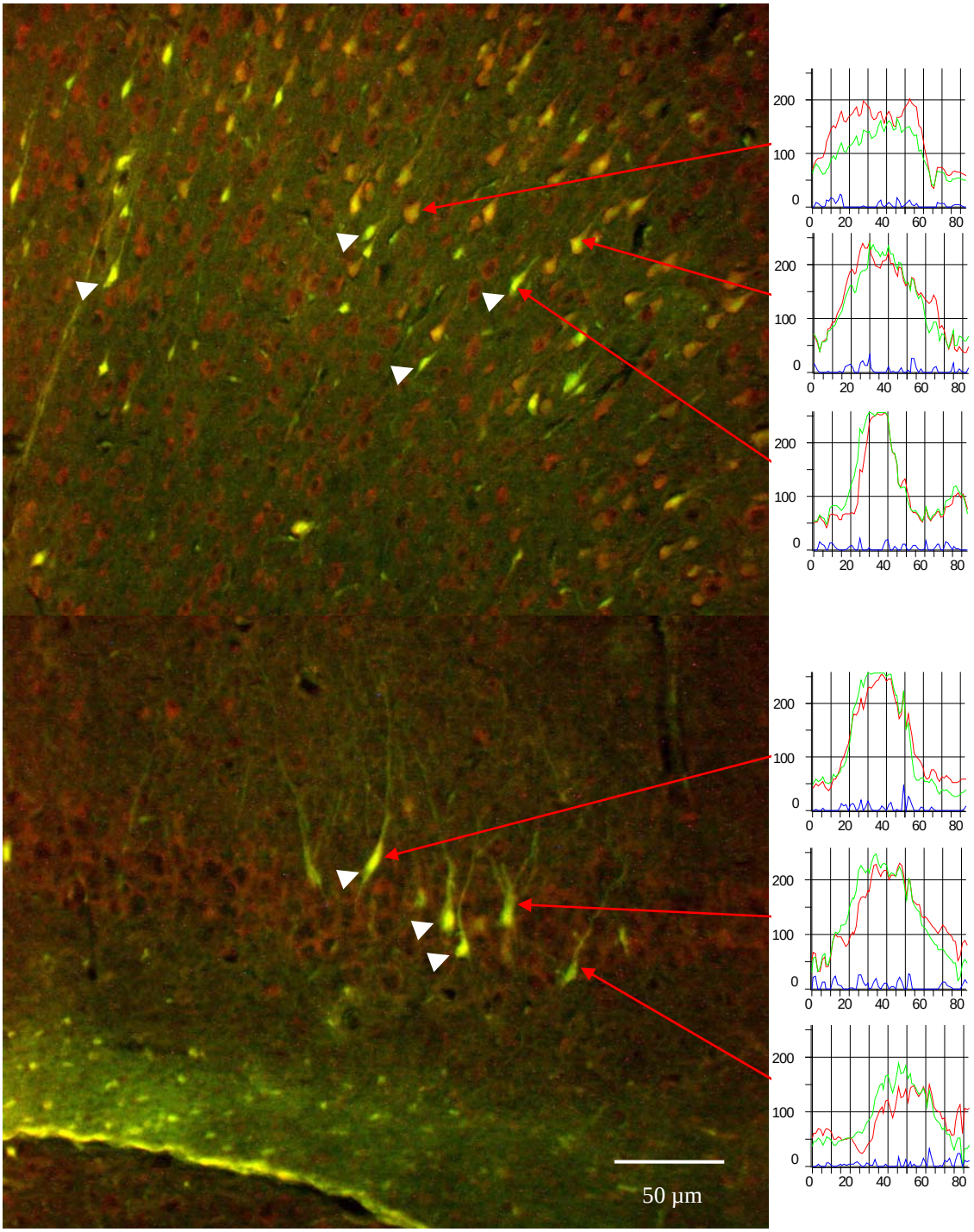

Figure 2.5. Differential uptake of Lucifer yellow is present in the cerebral cortex and in the hippocampus. Arrows denote the sampled cells which have their fluorescent intensity depicted in the histograms on the right. (A) Ipsilateral cerebral cortex. (B) Contralateral CA3. X-axis in histograms denote length of line profile used to evaluate intensity. Y-axis denote pixel intensity values (0-255). Note that the cells containing highest concentrations of Lucifer yellow present a shrunken and elongated morphology (arrowheads).

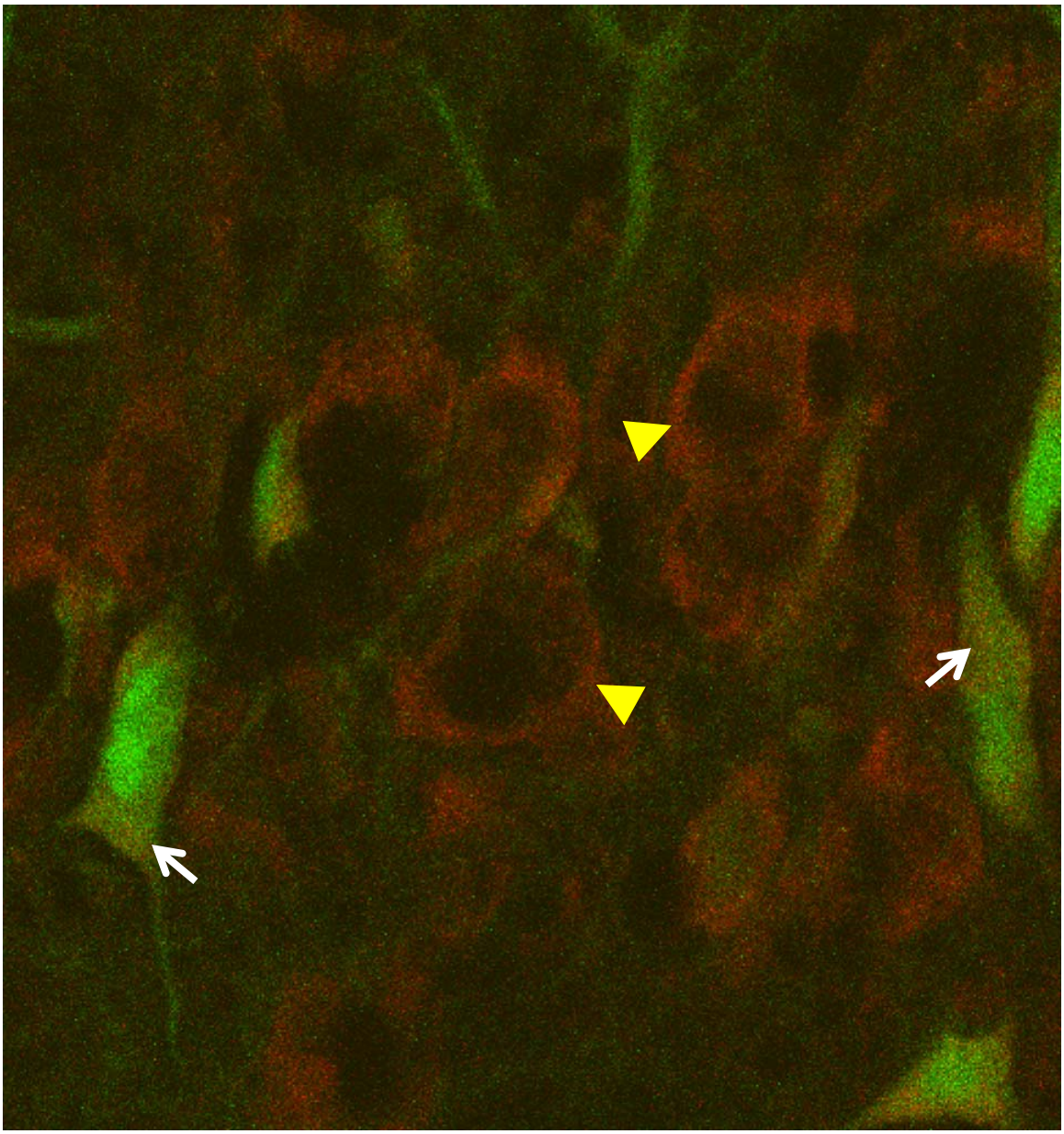

Figure 2.6. High magnification of Lucifer yellow-containing cells. Neighboring cells that did not contain Lucifer yellow presented relatively circular and larger somata (arrowheads). Positive cells presented the characteristic shrunken and elongated morphology, containing less Nissl staining in the cytoplasm than neighboring ones. Note also the compacted nuclear shape that the positive cells present. Micrograph obtained from CA3 hippocampal region contralateral to impact following staining for Nissl bodies (red) by confocal microscopy.

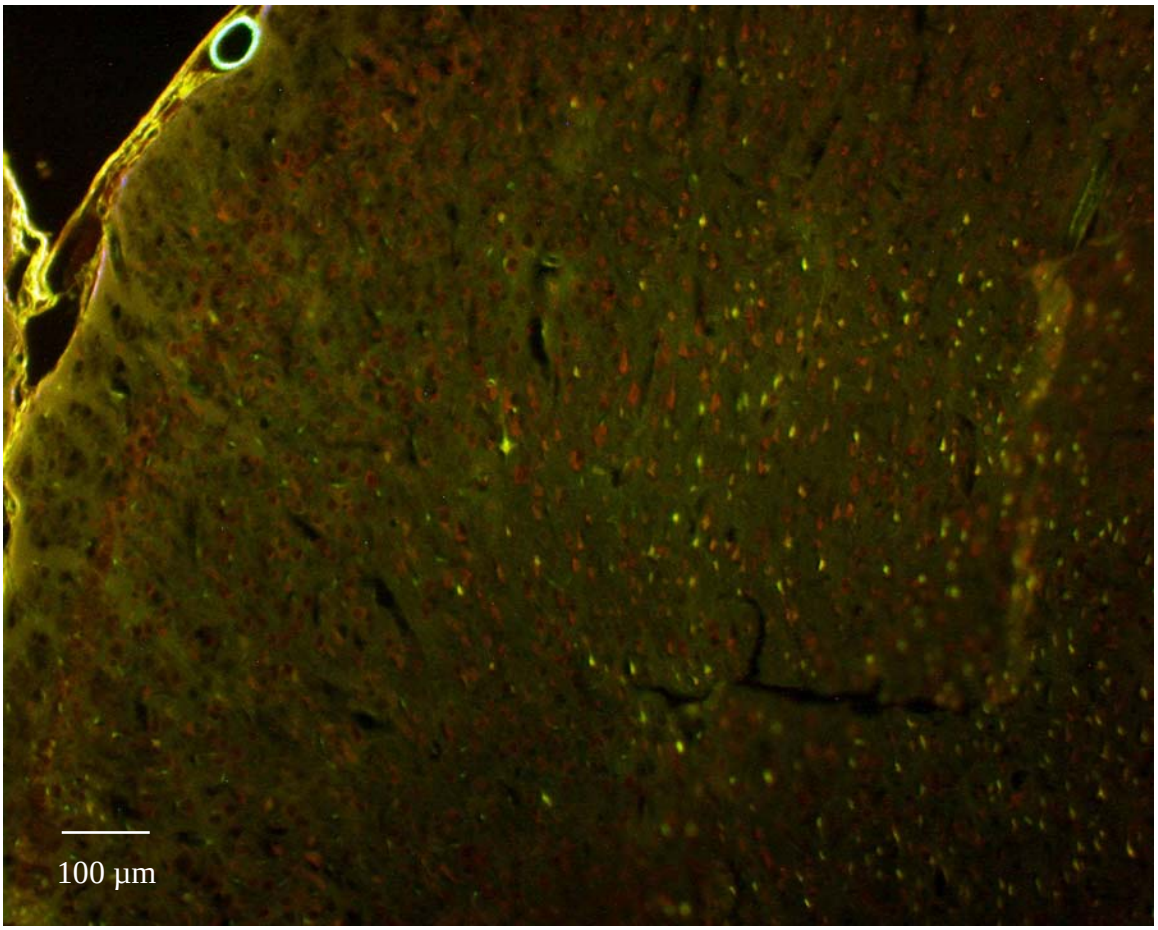

Figure 2.7. Differential uptake patterns can be seen in the medial cerebral cortex. Background fluorescence indicate even presence of Lucifer yellow in the area assessed. Coronal section from the ipsilateral medial cerebral cortex.

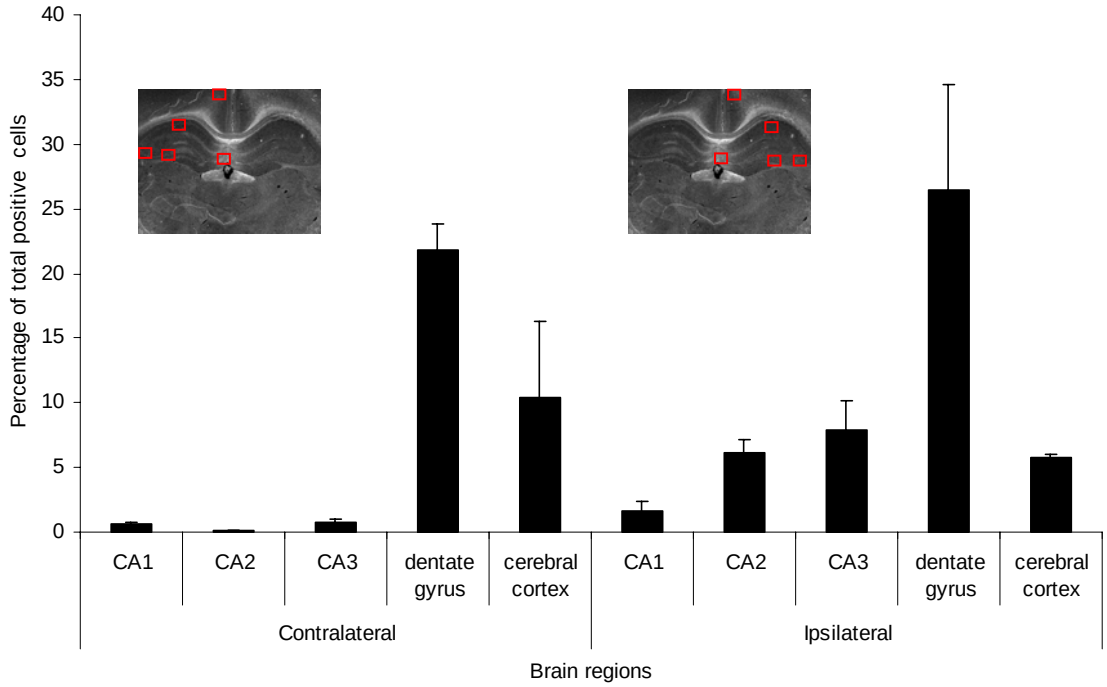

Figure 2.8. Distribution of positive cells in an injured rat brain. Number of positive cells assessed in the injured brain were normalized by the total number of positive cells in that section. Normalized values were then averaged over 3 different levels. Brain region was a significant factor ($p<0.0001$) as well as injury side ($p<0.05$). The interaction of the both factors was also significant ($p<0.05$), by 2-way ANOVA.

CHAPTER 3

NEURONAL PLASMA MEMBRANE IS TRANSIENTLY DISRUPTED BY A TRAUMATIC INSULT

3.1 Abstract

The acute response of neurons subjected to traumatic loading is poorly understood, although it may involve plasma membrane disruption. We have utilized an *in vitro* traumatic neuronal injury model to investigate plasma membrane integrity immediately following a sub lethal, uniform mechanical insult—high rate fluid shear stress. Normally cell-impermeant fluorescent molecules (calcein and fluorescein-conjugated dextran) were added to neuronal cultures before the insult as markers for increases in plasma membrane permeability. The percentage of cells containing the permeability marker was dependent on the molecular mass, as smaller molecules gained access to a higher percentage of cells than larger ones. Permeability increases were also positively correlated with the rate at which the insult was applied. Membrane disruption was transient, evidenced by a robust resealing within the first minute after the insult (assessed by adding permeability markers at different time points following the mechanical insult). In addition, membrane resealing was found to be dependent on extracellular Ca^{2+}, as chelation of the divalent ion abolished a significant amount of resealing for at least 2 minutes post-insult. Chelation of intracellular Ca^{2+} caused a decrease in resealing when cultures were injured in normal extracellular Ca^{2+}. However, injury following chelation of both extracellular and intracellular Ca^{2+} caused a diminished permeability increase due to the insult and a recovery in resealing. Flooding

of the cytosol with Ca^{2+} ions prior to injury using the ionophore A23187 did not affect resealing. Treatment of neuronal cultures with jasplakinolide, which stabilizes filamentous actin, reduced permeability increases to calcein, while latrunculin-B, an actin depolymerizing agent, reduced the increase in plasma membrane permeability and increased resealing. This study gives insight into the dynamics of neuronal membrane disruption, which consists of varying defect sizes. In addition membrane defects are subject to subsequent resealing, which was found to be calcium dependent, and involve actin in a role that differs from non-neuronal cells. Calpain activity was not found to affect this mechanism. Taken together, these data lead to a better understanding of the acute response of a large population of cells subjected to a rapid traumatic event.

3.2 Introduction

3.2.1 TBI and increases in permeability

Traumatic brain injury (TBI) arises from excessive mechanical stresses in the brain and subsequent strains that surpass tissue thresholds, leading to macroscopic as well as microscopic failure. Although mechanical insults can directly kill cells by surpassing structural thresholds, the plasma membrane of moderately disturbed cells (i.e. in lower strain regions) may become affected in more subtle ways, such as becoming transiently permeable from non-specific membrane disruptions. These membrane disruptions may play an important role in cellular injury in mild TBI, in which widespread cell death is absent, yet functional deficits may be present (Lewen et al., 1999; McIntosh et al., 1989). One of the earliest biophysical events observed after experimental *in vivo* TBI is an increase in neuronal plasma membrane permeability (Pettus et al. 1994; Pettus et al. 1996). Axonal plasma membrane disruption due to traumatic insult was observed

following horseradish peroxidase (HRP) injection in the cerebrospinal fluid of cats before fluid percussion to the brain (Pettus et al., 1994; Pettus and Povlishock, 1996). These studies demonstrated that HRP, a normally cell-impermeant molecule, was able to gain access to the axolemma of neurons. More recently, the transient nature of plasma membrane permeability changes was demonstrated in an *in vitro* stretch injury model (Geddes et al., 2003). Other cellular events such as activation of proteolytic enzymes including calpain, which may be triggered by increases of intracellular Ca^{2+} due to increases in permeability, have been shown to play an intimate role in the process of neuronal cell death (Rami et al., 1997; Villa et al., 1998). Although this body of evidence points to an important role that neuronal plasma membrane permeability disruption may have as an initial event following TBI, the process by which the plasma membrane becomes compromised as well as the mechanisms that promote resealing have remained largely unexplored.

3.2.2 Non-neuronal permeability studies

Mechanical disruption of the plasma membrane has been extensively studied in non-neuronal cell types, which may provide insight into such processes in a traumatic neuronal injury setting. Neurons in the central nervous system do not normally experience high magnitudes of mechanical stress as do cells in other tissues (e.g., epithelial and muscle cells), yet the biophysical mechanisms identified from the response of non-neuronal cells to plasma membrane disruptions may point to potential key mechanisms of disruption and resealing. Stresses generated by cavitation of microbubbles due to ultrasound energy have been shown to be responsible for increases in membrane permeability as well as death of prostate cancer cells (Guzman et al., 2001a; Guzman et

al., 2001b) and corneal endothelial cells (Saito et al., 1999), in a severity dependent manner. The resealing events following membrane disruptions have also been studied in many cell types. Extrusion of egg cells through a syringe needle, that generates high fluid shear stresses, also causes disturbances in the plasma membrane and leads to resealing in the presence of extracellular Ca^{2+} (McNeil and Baker, 2001). This resealing mechanism, first proposed by McNeil (McNeil et al., 2000) and later refined (McNeil, 2002), is initiated by extracellular Ca^{2+} influx through tears or pores of the plasma membrane, leading to depolymerization of the actin cortical cytoskeleton. Subsequently, the depolymerized cytoskeleton allows docking and fusion of vesicles such as lysosomes to each other and to the plasma membrane, thereby promoting resealing by either patching up the tear (McNeil, 2002; McNeil and Baker, 2001; Miyake et al., 2001; Terasaki et al., 1997) or by decreasing membrane tension (Togo et al., 2000).

3.2.3 Commonalities between non-neuronal permeability changes and TBI

Many of the immediate cellular responses commonly shown to occur in neuronal cells following a mechanical insult may be triggered in part by an increase of plasma membrane permeability. Responses such as the immediate efflux of intracellular lactate dehydrogenase (LDH) following insult *in vitro* (Ellis et al., 1995; Geddes et al., 2003; LaPlaca et al., 1997), influx of extracellular Ca^{2+} (Geddes and Cargill, 2001; LaPlaca et al., 1997; LaPlaca and Thibault, 1998), and *in vivo* mass depolarization of neurons (Katayama et al., 1990; Yoshino et al., 1991) may be caused by non-specific neuronal plasma membrane disruptions. Also, changes in expression of immediate early genes such as c-fos have been reported to be acute responses of both neural cells *in vivo* (Raghupathi et al., 1995) and non-neuronal cells *in vitro* (Grembowicz et al., 1999)

following a mechanical insult. The latter study found a requirement of plasma membrane disruption for the gene expression changes to occur.

3.2.4 Current study

The purpose of the current study is to resolve some of the mechanisms such as calcium dependency, actin cytoskeleton involvement, calpain activity as well as the role of bilayer fluidity in neuronal plasma membrane permeability alterations and resealing following a traumatic mechanical injury. Our *in vitro* TBI model consists of injuring cortical neurons cultured on glass plates using fluid as a medium to deliver stress to the cells. We have designed a device based on a cone-plate viscometer, which is capable of delivering high rates of shear stress uniformly throughout a cell population. This system allows us to apply controlled insults to neurons and measure plasma membrane permeability over time and under varying conditions.

3.3 Materials and Methods

3.3.1 Neuronal cell culture

Cortices were dissected from embryonic day 18 Sprague-Dawley rats (Charles River, Wilmington, MA**),** rinsed with Hanks' balanced salt solution (HBSS; Invitrogen, Carlsbad, CA) without Ca^{2+}/Mg^{2+} followed by incubation with trypsin (2.5 g/L plus 1 mM EDTA; Invitrogen) for 10 minutes. Trypsin solution was then removed and tissue was rinsed twice with DMEM containing 10% fetal bovine serum. Cortices were then dissociated in a solution of Neurobasal medium (Invitrogen) containing DNAse (0.15 mg/ml; Invitrogen) by brief agitation. Cells were counted and seeded (density=1.00-1.25x10^5 cells/cm^2) onto customized glass plates for the cell shearing injury device (CSID). Prior to cell seeding, glass plates were briefly flamed and subsequently coated

with a poly-L-lysine solution (0.0023% w/v; Sigma, St. Louis, MO) for at least 12 hours at 37˚C, 95% relative humidity. Cells were cultured in Neurobasal medium supplemented with B-27 (2% v/v; Invitrogen), Glutamax (0.5 mM; Invitrogen), and 1000 units/L of penicillin/ 1 mg/L of streptomycin/ 2.5 µg/L of amphotericin (Sigma) and used at 7 days *in vitro* (DIV). This serum-free medium ensured that the culture remained a neuronal with minimum astrocyte proliferation (Evans et al., 1998). The resulting cell phenotype by this seeding and culturing method has been established to yield 90-95% neurons (confirmed by immunostaining for neuronal-specific cytoskeletal markers such as tau-5), with the remaining cells exhibiting morphological characteristics of glial cells (verified by GFAP immunostaining). In addition, cells at 7 DIV also exhibited electrical bursts, as assessed using microelectrode arrays (data not shown). Also, cells cultured this length of time have maximum adherence to the substratum and will hence respond to the mechanical insult in a more reproducible way than cells that may not be well adhered. Astrocytes were also separately cultured as control cells for the actin visualization studies. These cells were obtained from postnatal day 0-1 rats. Astrocytes were obtained in a similar procedure described above for neuronal cell harvesting. Astrocyte purification was accomplished by using serum containing medium (DMEM/10% FBS) and by mechanically knocking off neuronal and microglial cells from cultures before passing. Cultures were passed at least four times before cells were used in the experiment.

3.3.2 Injury protocol

Neuronal cell cultures were subjected to a high magnitude, short duration pulse of fluid shear stress using the CSID. The CSID consists of a servo motor-driven cone (0.5º)

that rotates on top of the cell culture surface. Fluid (shearing buffer) between the cone and cell plate transfers the momentum from the rotating cone to the plate where cells are seeded, producing a uniform shear stress across the culture plate.

Specifically, experiments were conducted by removing culture plates from the incubator, rinsing them with HBSS (with or without Ca^{2+}/Mg^{2+}), and mounted them in the CSID. The cone was lowered until its apex contacted the center of cell plate. Shearing buffer (HBSS with or without Ca^{2+}/Mg^{2+} and permeability markers) was added through a perfusion port in order to fill the gap between the cone and the plate. The insult parameters of shear stress magnitude and duration were 140 dynes/cm^2 and 300 milliseconds, respectively. Unless otherwise stated the rise time, which is defined to be the length of time for the cone to reach maximum velocity, was 20 milliseconds. Cells were immediately removed from the CSID and subjected to permeability assessment. Groups of 4-8 culture plates were used for each condition.

3.3.3 Plasma membrane permeability assessment following mechanical insult

The shearing buffer consisted of HBSS with Ca^{2+}/Mg^{2+} and either calcein (629 Da; $3.2x10^{-4}$ M; Sigma) or fluorescein-5-isothiocyanate (FITC) conjugated dextran (10^{-4} M) molecules of different sizes (42 and 464 kDa; Sigma). Cells were incubated at 37°C in the buffer containing the permeability marker for 10 minutes following injury. Sham groups were placed in the CSID and loaded with the shearing buffer after the cone was lowered as with the injured group, but the cone did not rotate. Shams were also incubated for 10 minutes with the shearing buffer and marker after they were taken from the CSID. Uninjured controls were cultures that were not placed in the CSID, but were exposed to shearing buffer containing the permeability marker for 10 minutes. These plates were

used to establish zero percent uptake. In order to reveal the resealing time course, cultures were sheared without the presence of a permeability marker, which was then added to cells at 1, 2, and 10 minutes after injury (calcein only). Calcein or FITC-conjugated dextrans were in contact with cells for a total of 10 minutes for all groups (Figure 3.1A). Following incubation with the permeability marker, all plates were rinsed with HBSS.

3.3.4 Chelation of extracellular Ca^{2+}

A Ca^{2+}-free extracellular environment was attained by rinsing cells with HBSS without Ca^{2+}/Mg^{2+} and using shearing buffer supplemented with 1mM EGTA (a Ca^{+2} chelator; Sigma) and calcein (Figure 3.1B).

3.3.5 Chelation of intracellular Ca^{2+}

Dimethyl BAPTA-AM (Molecular Probes Inc., Eugene, OR) is a potent cell-permeant Ca^{2+} chelator. Cells were pretreated for 75 minutes with 60 µM of dimethyl BAPTA-AM in HBSS containing Ca^{2+}/Mg^{2+}. Cultures were then rinsed three times with HBBS with or without Ca^{2+}/Mg^{2+}. Cells were then mechanically injured with the CSID with appropriate shearing buffer containing calcein (Figure 3.1B). For the evaluation of the resealing profile, cells were injured without the permeability marker, which was then added one minute following insult. Ca^{2+}-free shearing buffer, when used, also contained 1mM EGTA.

3.3.6 Intracellular cation flooding

Cell cultures were pretreated with the ionophores A23187 and gramicidin for 10 minutes in HBSS prior to injury. A23187 concentrations used were 0.1 and 1 µM. Gramicidin was used at both 0.1 and 1 µg/mL (Molecular Probes).

3.3.7 Actin polymerization and depolymerization

Actin polymerization was promoted by pretreating cell cultures with jasplakinolide (5 µM; Molecular Probes) for 5 minutes. A separate set of cultures were used to probe the role of actin in resealing following the application of shear stress in unperturbed cultures (jasplakinolide added 1 minute after the insult for 5 minutes). Actin depolymerization was promoted by pretreatment of cell cultures with latrunculin-B (25 µM; Sigma) for 60 minutes. In both cases, chemical treatments were followed by rinses with HBSS containing Ca^{2+}/Mg^{2+} prior to injury (Figure 3.1B).

3.3.8 Actin cytoskeleton visualization

Both filamentous actin (f-actin) and globular actin (g-actin) were visualized in neurons and astrocytes. Cell cultures were treated with HBSS (negative control; 1 hour incubation), gramicidin, BAPTA-AM, latrunculin-B, and jasplakinolide (same concentrations and exposure as described above). Cells were then rinsed with PBS and fixed in 3.7% formaldehyde at 4ºC for 10 minutes. Immunocytochemistry was accomplishing using an actin antibody capable of detecting both f and g-actin (Chemicon, Temecula, CA).

3.3.9 Calpain inhibition

Calpain activity was inhibited by 25 µM AK295 (in HBSS) pretreatment for 120 minutes. Cultures were rinsed with HBSS. Injuries were performed in normal extracellular Ca^{2+} concentrations. AK295 was donated by Dr. Powers, Georgia Institute of Technology.

3.3.10 Membrane fluidity perturbation

Plasma membrane fluidity was increased by pretreatment of neuronal cultures with 40-200 mM of benzyl alcohol for 60 minutes (Sigma).

3.3.11 Quantification of plasma membrane permeability and statistical analysis

To analyze the degree of plasma membrane permeability changes, cell cultures that were subjected to the above protocols were rinsed with HBSS containing Ca^{2+}/Mg^{2+} and then treated with trypsin (2.5 mg/mL) followed by removal from the glass plates via gentle scraping. Trypsin was removed from cells following centrifugation at 1000 g for 10 minutes at 4°C. Pellets containing cells were then resuspended in phosphate buffered saline (PBS, pH=7.4, 4°C). Ten minutes before suspended cells were counted, propidium iodine (PI; 1.0 mg/mL; Molecular Probes) and Hoechst 33342 (0.5 mg/mL; Molecular Probes) were added. A Beckton Dickinson LSR Flow Cytometer was then used to determine fluorescent intensity from at least 10,000 cells per sample. Using WinMDI (Scripps, San Diego, CA) flow cytometry quantification software, live cells were gated from the rest of the particles in solution using a side-scatter versus forward scatter dot plot. In order to ensure that only live cells were being read, Texas Red and UV histograms were used to exclude cells that were permeable to PI and cells that had more intense Hoechst emission which would indicate apoptotic cells. Subsequently, the intensity of individual cells gated in the latter step was displayed in a histogram of FITC intensity (~533 nm emission) (Figure 3.2a). Using a similar permeability quantification method previously published (Miyake et al., 2001), data analysis was accomplished by first fitting the FITC histograms obtained from uninjured control samples with a Gaussian curve, using Origin Software (OriginLab Corp., Northampton, MA). The center (peak value) and standard deviation of the normal distribution curve was then used to find the

threshold for the given experiment. The threshold was defined as the peak of the uninjured control Gaussian curve plus two standard deviations to the right, which excludes approximately 95% of that population assuming a normally distributed curve. The average threshold for uninjured control samples was used to define the percentage of positive cells in treatment groups. Positive cells were defined to be cells located to the right of the threshold (Figure 3.2b). The uptake ratio was quantified for experiments with chemical pretreatments. The uptake ratio is defined as the percentage of positive cells at 1 minute following insult normalized by the percentage of positive cells at 0 minute. These ratios are only shown when the percentage positive cells at 1 minute is significantly different than the values at 0 minute, and they were used to compare the resealing phenomenon independent of initial insult. Even when using this semi-quantitative method, there were some variations in the baseline of experiments. Each experiment was repeated at least three times and contained untreated, uninjured and injured, controls that were compared to treated groups in order to account for day-to-day variations of flow cytometry baselines. Statistical analysis was accomplished by analysis of variance (ANOVA), followed by Tukey's pairwise comparison.

3.4 Results

3.4.1 Neuronal membrane permeability increases due to mechanical insult

Shear stress-induced insult did not cause significant cell death in parallel cultures observed up to 24 hours following insult (data not shown). Cells assayed for presence of permeability markers excluded PI, indicating complete resealing and viability at that time.

Fluid shear stress-induced mechanical insults caused an acute increase in neuronal plasma membrane permeability. This increase was dependent on the size of the molecule used as the permeability marker ($p<0.05$; Figure 3.3). Injured neurons presented good neurite attachment, preserving most of the fine network arbor after insult (Figure 3.4A). The calcein uptake within a culture was not uniform, and we commonly found neighboring cells containing varying amounts of calcein (Figure 3.4B). The temporal profile of neuronal membrane permeability to calcein indicated that resealing occurs rapidly following this insult (Figure 3.5). The percentage of cells positive for calcein was reduced fourfold within the first minute. A smaller portion of the cell population, however, remained permeable to calcein for at least 2 minutes. By 10 minutes the percent of positive cells was not statistically different than uninjured controls ($p>0.05$). Furthermore, the increase in permeability to calcein was rate dependent, with higher rate insults causing a larger increase in membrane permeability than lower rates. Sham groups also exhibited increased membrane permeability, albeit significantly less than injured ones. This was due to the shear stress generated by addition of the shearing buffer in the CSID, causing some calcein uptake.

3.4.2 Role of Ca^{2+} in neuronal plasma membrane resealing

Neuronal plasma membrane resealing was dependent on the presence of extracellular Ca^{2+}. Chelation of Ca^{2+} by EGTA resulted in the loss of resealing ability by a large percentage of neurons. As much as 10 minutes elapsed before a significant amount of resealing was observed. Even at 10 minutes, however, the percentage of positive cells was still elevated compared to uninjured controls (Figure 3.6A). Also, qualitative observations showed that chelation of extracellular Ca^{2+} caused a consistent

increase in the amount of calcein contained in positive cells at 0 minute. This was evidenced by the large number of cells forming a second peak to the right of FITC-intensity histograms (Fig 3.6B).

The role of intracellular Ca^{2+} in neuronal plasma membrane disruption and resealing following injury was elucidated by chelating intracellular Ca^{2+} stores. Pretreatment with dimethyl BAPTA-AM followed by injury in the presence of extracellular Ca^{2+} resulted in no change in calcein uptake when the marker was present during injury as compared to the untreated group (Figure 3.7). However, resealing of neuronal plasma membranes was affected by intracellular chelation of Ca^{2+}. Pretreatment with dimethyl BAPTA-AM compromised plasma membrane resealing when the insult took place in the presence of extracellular Ca^{+2}. This was demonstrated by a higher uptake ratio in the treated group when calcein was added 1 minute following injury compared to the untreated group. Interestingly, pretreatment with dimethyl BAPTA-AM followed by chelation of extracellular Ca^{2+} using EGTA and subsequent injury yielded unexpected results. In the total absence of the divalent cation inside and outside the cells, they regained, at least in part, the ability to reseal following injury instead of a hypothesized exacerbation of the inability to reseal (Figure 3.8). Pretreatment in such conditions resulted in a lower percentage of positive cells at the time of injury. Resealing was positively affected by the pretreatment with BAPTA-AM, which was evidenced by the uptake ratio of 0.45 while the ratio in the untreated group was 0.74. Dimethysulfoxide (DMSO; Sigma), the vehicle for dimethyl BAPTA-AM (0.06% v/v), has been reported to increase resealing of plasma membrane at low extracellular Ca^{2+} concentrations (Shi et al., 2001). However, control experiments using cells that were

pretreated with DMSO only (0.06% v/v) were not significantly different than the non-treatment group (data not shown). Also, similar results were found when using FITC-conjugated dextran molecules as permeability markers (data not shown), indicating that this phenomenon is not a result of calcein interaction with the treatment.

To further explore the role of intracellular Ca^{2+} in membrane disruption and resealing, cells were flooded with Ca^{2+} prior to injury by pretreatment with A23187. This ionophore forms selective channels in the plasma membrane which allows only Ca^{2+} into the cell (Doebler, 2000). The peptide gramicidin is also a ionophore, although it allows the indiscriminate passage of cations through its channels (Shapovalov et al., 1999). Pretreatment with gramicidin and A23187 pretreatment did not affect the temporal profile of neuronal plasma membrane disruption at the concentrations used (Figure 3.9). Although there were no changes in the percent of positive cells in pretreated cultures, both ionophores caused positive cells to significantly gain more calcein than untreated groups at 0 minute (data not shown).

3.4.3 Role of actin cytoskeleton in neuronal plasma membrane resealing

The actin cytoskeleton has been shown to play a crucial role in the resealing of mammalian cells (Miyake et al., 2001). In order to elucidate the role of actin in neuronal plasma membrane disruption and subsequent resealing from fluid shear stress injury, actin was chemically perturbed using jasplakinolide, a powerful, cell permeant, stabilizer of filamentous actin (f-actin) (Bubb et al., 1994), which promotes actin polymerization (Bubb et al., 1994; Miyake et al., 2001). Jasplakinolide treatment was hypothesized to decrease resealing since its effects on actin are believed to obstruct the cytosolic vesicles docking with the plasma membrane—a crucial step in resealing (Miyake et al., 2001).

However both pretreatment and treatment following injury did not deter resealing of neuronal plasma membrane (Figure 3.10, 3.11). Pretreatment with jasplakinolide caused a reduction of positive cells at the time of injury (Figure 3.10). However, uptake ratios of both untreated and treated groups were not affected. Post-treatment of jasplakinolide caused a decrease in positive cells at 1 minute following insult (Figure 3.11). Similar results were seen when using fluorescent dextrans as permeability markers (data not shown). To further elucidate the role of the cortical actin cytoskeleton in resealing, we used a compound that promotes actin depolymerization. Latrunculin-B pretreatment decreased uptake of calcein at 0 minutes and it induced a smaller number of positive cells at 1 minute following injury. The pretreated uptake ratio was not different when compared to the untreated group (Figure 3.12).

3.4.4 Actin cytoskeleton visualization

In order to elucidate the effects of some of the chemical treatments employed in this study, visualization of actin present in neurons was accomplished by immunocytochemistry (Figure 3.13). Parallel astrocytic cultures were used as a cell controls. Basal levels of actin bundles were profoundly different between astrocytes and neurons. Astrocytes presented extensive amount of actin bundles throughout the cytoplasm. Neurons lacked such stress fibers and only presented a diffuse signal within the cytoplasm, indicating a modest presence of f-actin. Chemical treatments in neurons did not produce noticeable changes in cell morphology and actin architecture. However, astrocyte cultures treated with latrunculin-B and jasplakinolide showed dramatic changes in cortical actin architecture as well as cell morphology. Jasplakinolide treatment caused a widespread presence of deformed nuclei and loss of orderly actin-positive structures.

Latrunculin-B treatment caused every astrocyte in treated culture to present shrunken morphology as well as a loss of orderly stress fibers within the cytoplasma.

3.4.5 Role of calpain in onset of membrane disruption and subsequent resealing

Cultures pretreated with the widely characterized, broad-range, cell-permeant calpain inhibitor AK295 (James et al., 1998; Saatman et al., 1996) did not affect the initial plasma membrane disruption or the resealing profile when compared to untreated controls (Figure 3.14).

3.4.6 Role of the plasma membrane fluidity

Benzyl alcohol has been shown to interact with the lipid bilayer thereby lowering its viscosity and increasing its fluidity (Gordon et al., 1980). Only the highest concentration of benzyl alcohol pretreatment used (80 mM) resulted in alterations in the neuronal plasma membrane permeability temporal profile. At this concentration, benzyl alcohol caused a reduction in the percent of positive cells when the permeability marker was present, when compared to untreated groups. The same concentration caused an increase in the percent of positive cells when the permeability marker was added at 1 minute (Figure 3.15).

3.5 Discussion

Fluid shear stress-induced mechanical trauma in neurons causes a significant flux of extracellular molecules into the cell through a disturbed plasma membrane. We hypothesize that such changes in permeability result from excessive plasma membrane strain arising from the mechanical insult and subsequent non-specific membrane disruptions. *In vitro* TBI models have shown that substantial plasma membrane strains arise from large stresses characteristic of this type of injury (LaPlaca and Thibault, 1997).

By varying the size and the molecular mass of the permeability marker we were able to show differential uptake of the marker based on its molecular mass and/or size. The entry of the marker is directly due to the physical insult and the mechanism appears to be non-specific. Although significant plasma membrane disruptions occurred in the neurons as a result of mechanical insult, we did not observe increases in cell death at 6 and 24 hours post-injury in neuronal cultures subjected to the same insult parameters as those shown to increase permeability. This implies that these insult parameters are sub-lethal, yet the links between acute membrane disruption and potential cell dysfunction are not known.

We have analyzed parallel cultures with a LSM 510 confocal microscope (Zeiss, Germany) in order to verify that the marker molecules were present within the cells (images not shown). Immediately following injury, we have observed an overwhelming majority of the calcein trapped inside the cells to be present in the soma, with relatively few neurites containing the molecule. This is hypothesized to be caused by the nature of the insult. Neuronal cells cultured on flat surfaces have their somata resting relatively higher from the plating surface than the neurites, making the cell bodies more vulnerable and prone to deformation from a fluid shear stress insult from the apical surface (versus, for instance, a substrate stretch insult). This spatial variation may result in a differential strain distribution, which is supported by previous data from our laboratory, demonstrating that plasma membrane strains can be significantly larger at the cell bodies than at adjacent neurites during a traumatic mechanical insult (LaPlaca and Thibault, 1997). Most of the calcein observed within neurites was emanating from the somata. Therefore, the somata are likely the entry points for the markers examined in this model. This evidence points to an increase in plasma membrane permeability due to the

mechanical disruption which is not dependent on the transection of neurites, albeit further studies are needed to confirm this assertion.

The rate dependency of the increase in plasma membrane permeability can be attributed to the viscoelastic properties of cells. The shorter rise time insult results in a more severe injury since it loads the stress more rapidly, allowing less time for relaxation, and increasing membrane disruptions due to excessive stresses at the plasma membrane level. Higher rates caused an increase in the percentage of cells that were permeable to calcein. This observation corroborates results from other *in vitro* models that show that the rate of applied insults to the cells is an important parameter that potentiates the severity of the injury (Geddes and Cargill, 2001; Geddes et al., 2003; LaPlaca and Thibault, 1997). The placement of culture plates into the CSID is hypothesized to have produced, by itself, some plasma membrane disruption because of the shear stress induced as shearing buffer is introduced to the gap between the cone and cell substrate, despite care taken during placement and buffer filling. We consider this type of injury to be due to quasi-static cell loading. The mechanisms of permeability increases in sham cultures, however, are hypothesized to be the same as those produced when the cone is rotated, but to a lower extent. If, for example, the buffer containing calcein is added to the cells too rapidly (i.e. by pipetting to close to the cells), we have observed increases in the percent of positive cells in these “uninjured cultures”. Also, we have not been able to induce higher percentages of positive cells than the ones reported here even when increasing the duration of the insult (data not shown). The injury parameters reported here are the minimum stress magnitudes that evoke increases in plasma membrane permeability at the rates used. Other combinations of parameters may cause similar

perturbations to the plasma membrane, although they might not be relevant to the study of TBI, which is known to occur from high rate insults.

The observed resealing phenomenon was found to be initiated within the first minute following injury, which is comparable to resealing times reported in cell wounding studies in non-neuronal cells (Togo et al., 2000). This resealing process can be shown by the dramatic reduction in the percentage of cells containing calcein when the marker is added to cells 1 minute post-insult. The resealing process occurred rapidly, as no difference in permeability to calcein between injured and uninjured cultures was observed when the marker was added 10 minutes post injury. The resealing process was impaired when Ca^{2+} and Mg^{2+} were removed from the extracellular buffer. The importance of extracellular Ca^{2+} for resealing of the plasma membrane has been demonstrated in numerous studies using both neurons and other cell types. Many resealing studies using neural cells have examined nerve transection and subsequent axonal resealing (Howard et al., 1999; Spira et al., 1996), which have demonstrated a dependency on extracellular $Ca^{2+}$for the resealing process. In studies involving non-neuronal cells, extracellular Ca^{2+} has also been found to be a major participant in membrane resealing following plasma membrane disruption (McNeil and Terasaki, 2001; Terasaki et al., 1997). This is the first report, to our knowledge, that a similar Ca^{2+} dependency in membrane repair was exhibited in cortical neurons subjected to a uniform mechanical insult.

The chelation of intracellular Ca^{2+} stores prior to the insult while extracellular Ca^{2+} was unchanged also limited resealing, demonstrating that ions stored inside the cells may play a role in the repair mechanism following mechanical disruption of the neuronal

plasma membrane. Dimethyl BAPTA-AM-treated cells injured in normal extracellular Ca^{2+} presented limited resealing at 1 minute following injury, which could be explained by the capability of cytosolic BAPTA to rapidly chelate Ca^{2+} (Ko et al., 2001) as it enters the injured cells, thereby reducing the number of divalent ions on which resealing has been shown to be dependent. Dimethyl BAPTA-AM-treated cells demonstrated a "regained" ability to reseal without extracellular Ca^{2+} as seen in Figure 3.8. The significantly smaller ratio of positive cells at 1 minute over 0 minute in treated groups when compared to untreated groups make a compelling case that neurons are resealing in these conditions even if the onset of injury was affected by a unknown synergy between BAPTA-AM pretreatment and subsequent EGTA contact, since separate treatment with the two chemicals does not result in decrease in vulnerability to mechanical disruption (Figure 3.6 and 3.7). This suggests that increased resealing may play a role in this phenomenon, affecting both 0 and 1 minute values of permeabilty. Chelation of intracellular Ca^{2+} by dimethyl BAPTA-AM has been shown to promote decoupling of the actin cytoskeleton and transmembrane adhesion proteins (Ko et al., 2001). This decoupling may reduce plasma membrane tension, in much the same way that actin-depolymerization agents such as cytochalasin-D have been shown to reduce tension and facilitate resealing (Togo et al., 1999). Furthermore, reduced membrane tension may be a primary requirement for resealing (Togo et al., 1999). This evidence may explain why chelation of both intracellular and extracellular Ca^{2+} resulted in a "regained" ability of the cells to reseal. This explanation, however, contrasts with the results obtained when only extracellular Ca^{2+} is chelated. If membrane tension, lowered by dimethyl BAPTA-AM, was the sole requirement for resealing, then we would not expect that the influx of

extracellular Ca^{2+} into the cell would interfere with this mechanism. It may be possible that changes in the Ca^{2+} gradient across the plasma membrane, which is perturbed upon intracellular chelation, may play a role in the resealing process, albeit we cannot rule out other unknown mechanisms triggered by the intracellular Ca^{2+} chelation.

Treatment of neuronal cultures with the actin polymerization promoter jasplakinolide before the mechanical insult resulted in a decrease in the percentage of positive cells within injured cultures. This was true even when accounting for the shift to the left in FITC-intensity seen in histograms of treated cultures. This shift is probably due to the diminished ability of jasplakinolide-treated cells to uptake extracellular contents (pinocytosis), which is responsible for the first peak seen in the obtained histograms (Saito et al., 1999) (see Figure 3.2 for an example of a histogram of an untreated culture). However, with the latter results alone, we can not rule out that this decrease of percentage in positive cells was not due to the changes in mechanical properties that such treatment could possibly cause to the cells, making them less (or more) vulnerable to the mechanical insult since the treatment occurred before injury. To remedy this possible artifact, and to isolate the role of actin polymerization in the membrane resealing process alone, we took advantage of the diminished ability of cells to reseal when extracellular Ca^{2+} is removed. By injuring cultures in low/no extracellular Ca^{2+} before jasplakinolide treatment we ensured that cells were injured as much as untreated groups and that a relatively large percentage of cells remained permeable throughout the treatment time. Post-treatment of jasplakinolide while membranes were still permeable to calcein allowed us to evaluate the calcium-dependent resealing mechanism of these cultures, a process which was initiated as soon as calcein and extracellular Ca^{2+} were added to cultures

(Figure 3.11). The results of this series of experiments confirmed the findings of the previous experiments where cells were treated before the insult. We conclude that jasplakinolide treatment reduces the percentage of positive cells due to the mechanical insult and does not diminish resealing as evidenced both by the constant uptake ratio in the pretreatment experiment and by the smaller percent of positive cells when cultures were treated after the onset of the mechanical insult. Jasplakinolide treatment of endothelial cells has been reported to decrease resealing of those cells when subjected to scratch-wounding (Miyake et al., 2001). The nature of this type of cell wounding is, however, different than the one used in the present study. Furthermore, the reduced presence of actin in neuronal cells, evidenced by the presence of relatively few stress fibers, as opposed to the abundant f-actin structures present in other cell types such as astrocytes may point to the reasons why the role of actin polymerization in resealing may differ in neurons.

Latrunculin-B is known to be a powerful actin depolymerization agent (Thurmond et al., 2003; Wakatsuki et al., 2001). Disturbing the actin cytoskeleton with latrunculin-B had a significant effect on mechanically-induced membrane disruptions. The relative decrease in permeability compared to the untreated group may be due to a decrease of cytoskeleton/membrane interactions which is known to occur upon actin depolymerization (Ko et al., 2001), making these cells less vulnerable to the insult. Also, depolymerization of the actin cytoskeleton has been shown to facilitate resealing, which may have affected the percentages of permeable cells obtained both at 0 and 1 minute post-insult, although the uptake ratios were the same (Miyake et al., 2001; Togo et al., 2000). This may be due to the fact that a less stiff cytoskeleton allows for the plasma

membrane to reseal faster by passive means, which can occur even in the absence of extracellular Ca^{2+} (Togo et al., 1999; Togo et al., 2000). Also, this slower calcium-independent mechanism is evident in our results of the temporal profile of resealing under low extracellular Ca^{2+} conditions. Similar mechanisms have been reported by Togo et al. where pretreatment of cells with cytochalasin-D has been shown to decrease plasma membrane tension in some cell types, which is thought be a necessary step for resealing to occur (Togo et al., 1999; Togo et al., 2000). Our results suggest that even though neuronal plasma membrane permeability presents many similarities with other models of cell wounding, there are distinctive disparities. Although we have shown significant alterations in disruption and resealing due to changes in actin cytoskeleton polymerization levels in neuronal cells, they are not all common to other cell types. The role of actin cytoskeleton remains to be defined in neuronal plasma membrane disruption and resealing.

Calpain activity has been shown to be necessary in basic cellular functions, including cell locomotion and migration (Carragher and Frame, 2002; Potter et al., 1998). Calpain activation has also been shown to be intimately related to events occurring during neuronal cell death following TBI and stroke (Buki et al., 1999a; Buki et al., 1999b; Kampfl et al., 1997; Newcomb-Fernandez et al., 2001; Pike et al., 2000). Pathological increases in intracellular concentrations of Ca^{2+} are thought to activate this enzyme in a uncontrolled fashion, which has been shown to be critical to cell degeneration in both necrosis and apoptosis (Rami et al., 1997; Villa et al., 1998). Calpain activity may have yet another role, albeit less researched. Calpain activation is hypothesized to play a beneficial role acutely following nerve transection (Howard et al.,

1999). Howard et al. have found that calpain inhibition provoked a reduction of resealed axons following transection. Calpain inhibition was expected to cause a reduction in the percentage of resealed neurons 1 minute following insult when compared to the untreated group. This was not the case in our model. Although many similarities exist between axotomy injury models and the model presented in this manuscript, such as resealing dependency in extracellular Ca^{2+}, there also exist many differences. Axotomy produces disruptions larger in scale than the plasma membrane disruptions in our model, as evidenced by the time scale for full resealing of 60 to 120 minutes reported in transection studies (Howard et al., 1999) versus 1 minute in our studies. We can reasonably assume that calpain activation plays a more important role in axotomy models by ridding the axonal membrane of cytoskeleton connections, thereby promoting actin depolymerization, making it possible for the bilayer to collapse on itself. This is a possibility since calpain activation has been reported to induce the detachment of the actin cytoskeleton from focal adhesions by cleavage of linker proteins such as paxillin and talin (Carragher and Frame, 2002). A similar effect, although not necessarily involving the same mechanisms, has been reported following transection of the giant squid axon, where the axolemma content elution was required in order for axonal resealing to occur (Gallant, 1988). We hypothesize that the differences between our results and the axotomy studies arise from the differences in size of the membrane disruptions caused by the CSID, which are too small compared to a complete axotomy to benefit from calpain activity, explaining why blocking this enzyme did not affect the resealing.

Plasma membrane fluidity is known to affect many biophysical as well as biochemical cellular functions, including modulation of G-protein activity while anchored in the plasma membrane (Gudi et al., 1998; Haidekker et al., 2000). Benzyl alcohol concentration in the order of 40 mM has been shown to produce significant changes in lipid bilayer fluidity in reconstituted liposomal vesicles (Gordon et al., 1980). In the context of this research, an increase in fluidity was expected to influence the passive resealing mechanism which is benefited by a thermodynamically favorable process where the hydrophobic and hydrophilic components of the phospholipids are most stable in a bilayer form (McNeil and Steinhardt, 1997). By lowering the viscosity of the plasma membrane (increasing fluidity), benzyl alcohol pretreatment was expected to facilitate resealing by increasing the chances of the torn leaflet to coalesce back into a continuous sheet. However, the pretreatment with the alcohol did not produce higher rates of resealing with the injury parameters employed. The highest concentration of benzyl alcohol reported here caused a change in the permeability profile that does not necessarily point to an increase in resealing since the percentage of positive cells seen 1 minute following injury was not significantly different than the 0 minute group. This phenomenon may be most likely attributed to a possible permanent breach of the plasma membrane due to a combination of alcohol treatment which actually weakened the bilayer at the high concentrations and insult, resulting in part of the cell population that could not trap calcein within the cytosol.

These findings may have an important impact in the study of TBI, as normal electrical function in neurons depends on a tightly regulated ionic concentration gradient across the plasma membrane, which is likely to be altered as a result of increased

permeability. Plasma membrane disruption may also cause a dramatic perturbation in other cellular functions, given that molecules much larger than ions are able to cross the plasma membrane. It is not known how these cells are affected by a potential loss in ion homeostasis or how the temporal recovery profile contributes to ultimate function. Future work will elucidate how membrane disruption correlates to these and other known cellular responses such as activation of proteolytic enzymes as well as alterations in electrophysiological activity.

A)

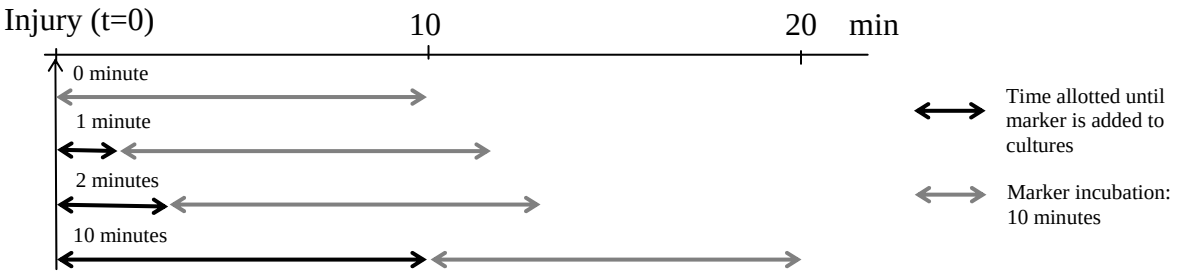

B)

Permeability Marker	Time allotted after injury for addition (minutes)			
	0	1	2	10
Calcein	N,B,E,EB,J,L	N,B,E,EB,J,L	N	N
FITC-Dextrans (42kDa and 464kDa)	N	-	-	-

Figure 3.1. (A) Timeline of neuronal plasma membrane assessment. To temporally assess permeability following mechanical insult calcein was present during injury or added at 1, 2, or 10 minutes following shear stress application. Incubation of cells with calcein ($3.2x10^{-4}$ M) was 10 minutes for all groups. (B) Summary of the experimental condition and the type of permeability marker added at different times following insult. N= no treatment, B= dimethyl BAPTA-AM, J= jasplakinolide, L= latrunculin-B, E= EGTA, EB= EGTA + dimethyl BAPTA-AM. See Methods for treatment durations.

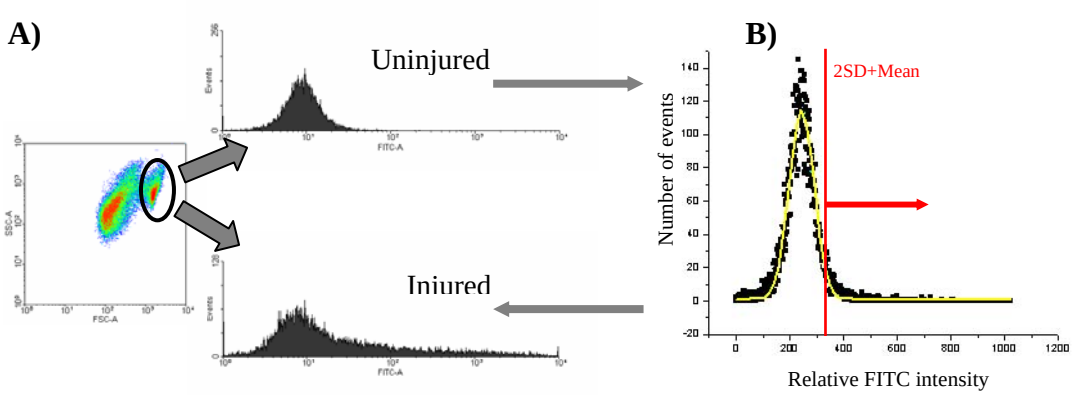

Figure 3.2. Quantification of percent of positive cells using flow cytometry data. (A) Histograms on the left were representative fluorescent data from uninjured populations (upper) and injured ones (lower). (B) Threshold of uptake was assigned from examination of the Gaussian distribution for uninjured controls. Cells that present higher fluorescence than the threshold (vertical line) were considered positive cells.

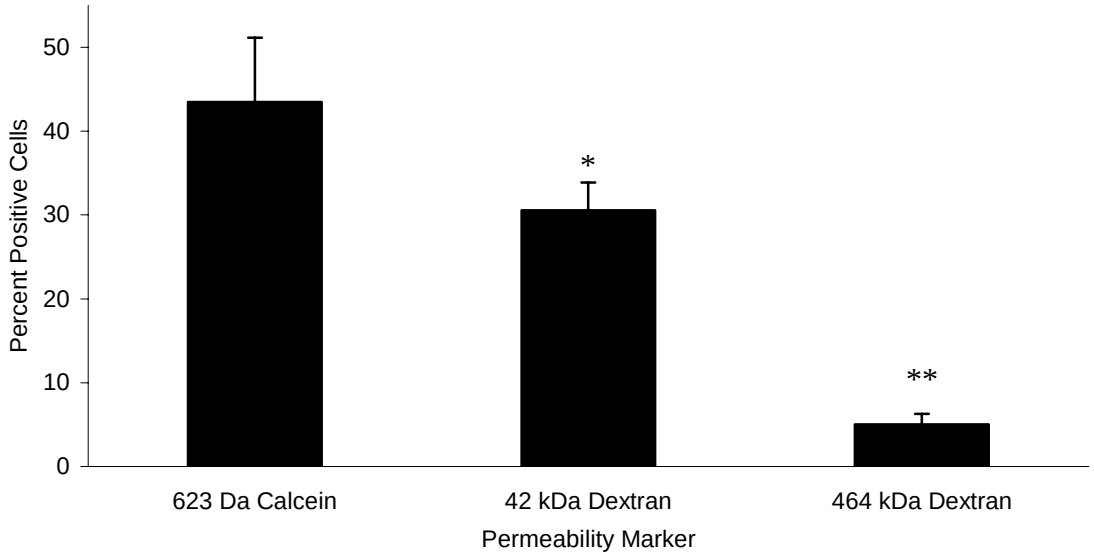

Figure 3.3. Percent positive cells decreased as the size of the marker molecule increased following equal mechanical insult (140 dynes/cm^2 shear stress magnitude, 20 ms rise time). Permeability markers were present during injury. Dextran concentrations were 10^{-5} M. *Significantly different from calcein group ($p<0.05$), and **42kDa group ($p<0.0005$) group. Error bars represent SD. n=3-5 cultures/group.

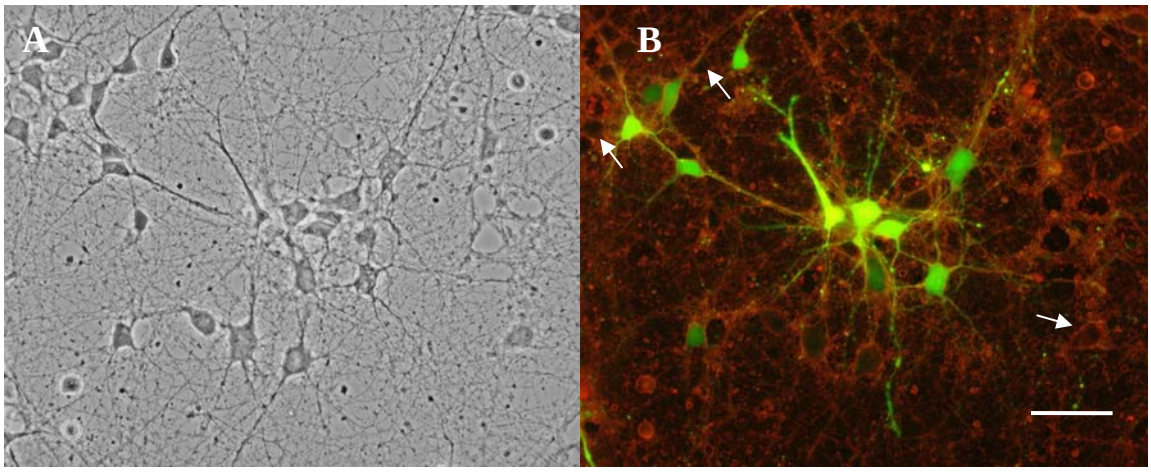

Figure 3.4. Representative neuronal culture injured in the presence of the fluorescent permeability marker calcein. (A) Phase micrograph shows preservation of cellular integrity following insult. (B) Fluorescence micrograph of the same field shows cells which contained calcein (EM ~520 nm). Notice the differential uptake of calcein within cells (white arrows highlight examples of cells with no uptake). Cultures were treated with a 50 µg/mL solution of Di-8 ANEPPS (red) for 10 minutes as a counterstain. Injury parameters: shear stress= 140 dynes/cm^2; rise time= 20 ms. Scale bar= 50 µm.

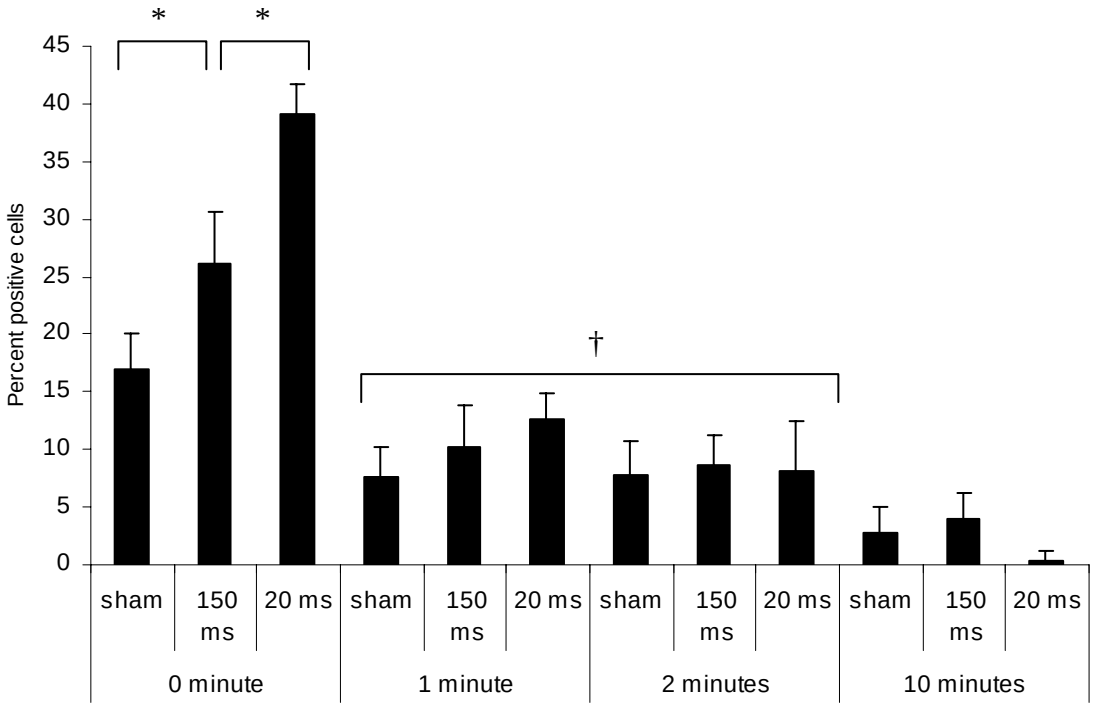

Figure 3.5. Percent of positive cells was highest when calcein was present during injury (0 minute). This increase was rate dependent. Cells rapidly resealed following injury, reducing the percentage of positive cells fourfold within the first minute. Total calcein incubation time was 10 minutes for all samples. Shear stress for all injuries: 140 dynes/cm^2; rise times: 20 and 150 ms. *Significantly different $p<0.001$. †Significantly different from uninjured controls (zero percent uptake; not shown) $p<0.05$. Error bars represent standard deviation (SD). n=4-5 cultures/group.

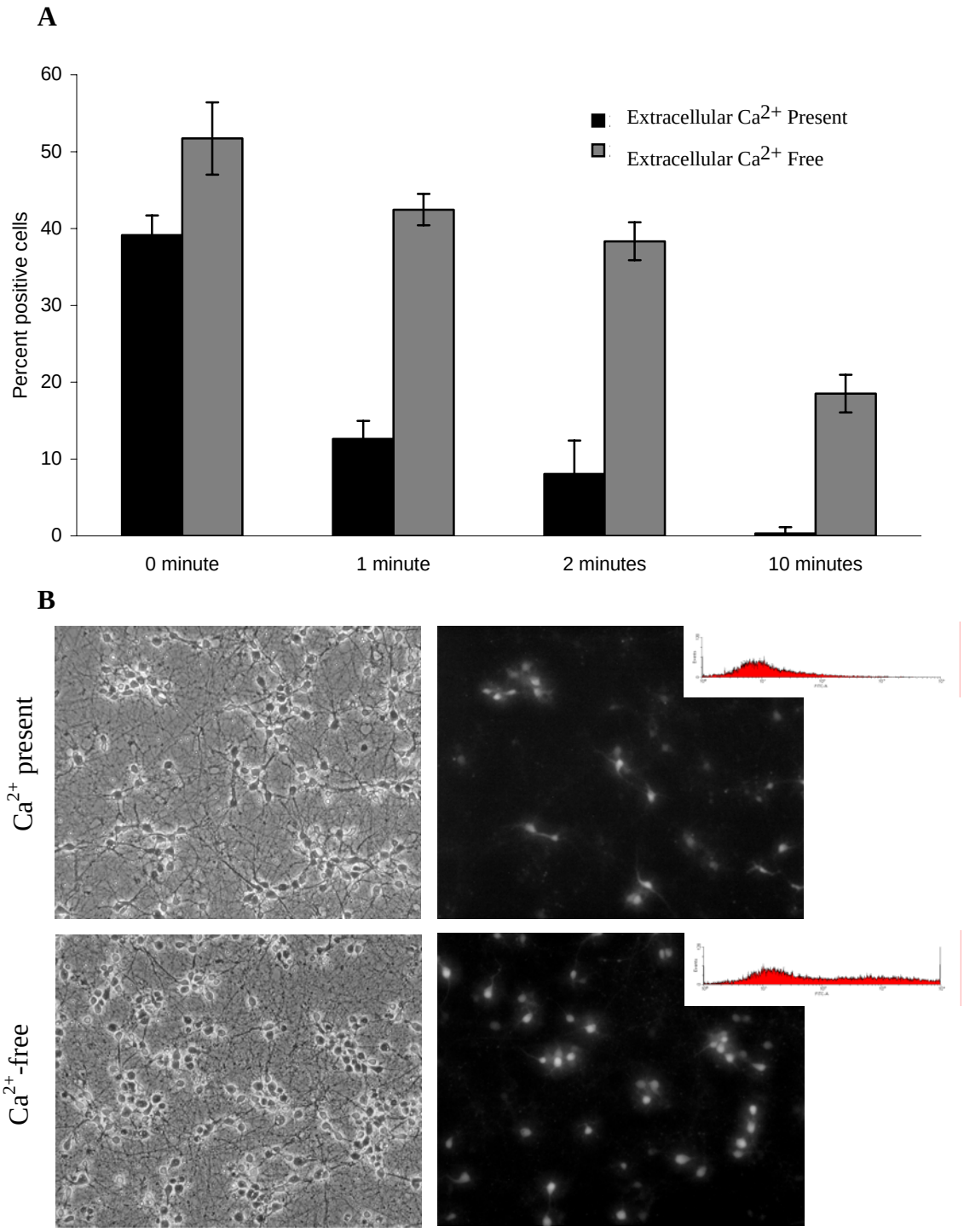

Figure 3.6. (A) Dependence of neuronal plasma membrane resealing on extracellular Ca^{2+}. The ability of a large percentage of neuronal cells to rapidly reseal within the first minute was lost in the absence of extracellular Ca^{2+}. Even though the average percentage of positive cells at 10 minutes was reduced by about one third of the permeability level seen when the marker was present during injury, this value was still significantly larger than uninjured controls. Total calcein incubation was 10 minutes for all samples. Ca^{2+}-

free samples were injured and incubated in HBSS buffer containing 1 mM EGTA with or without calcein. For all injuries: Shear stress= 140 dynes/cm^2, rise time= 20 ms. General linear model shows that both extracellular Ca^{2+} and time of marker introduction are significant variables ($p<0.0001$ for both). Error bars represent SD. n=4-5 cultures/group. (B) Removal of extracellular Ca^{2+} causes an increase in the amount of calcein molecules that gain access into injured cells. Representative phase (left) and fluorescent (right; EM ~530 nm) micrographs of injured cultures in normal and low Ca^{2+} show higher intensity of positive cells injured in the absence of the ion. Representative histograms obtained from flowcytometry in each condition are shown of the right.

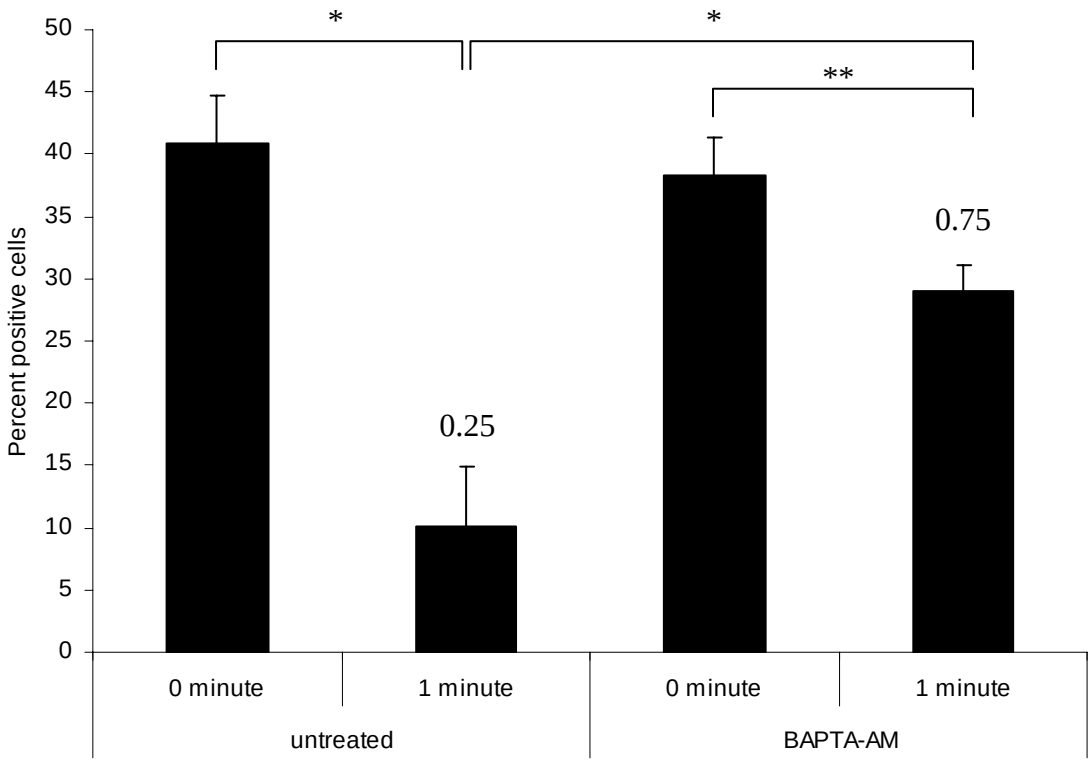

Figure 3.7. BAPTA-AM pretreatment did not have an effect on the increase of permeability due to the mechanical insult under normal extracellular Ca^{2+}. Resealing, however, was affected by intracellular chelation of Ca^{2+}, resulting in a larger percentage of cells that did not reseal to calcein entry by 1 minute after insult when compared to untreated group (* $p<0.0001$; ** $p<0.05$). Uptake ratios are seen on top of 1 minute groups Error bars represent SD. n=4-5 cultures/group.

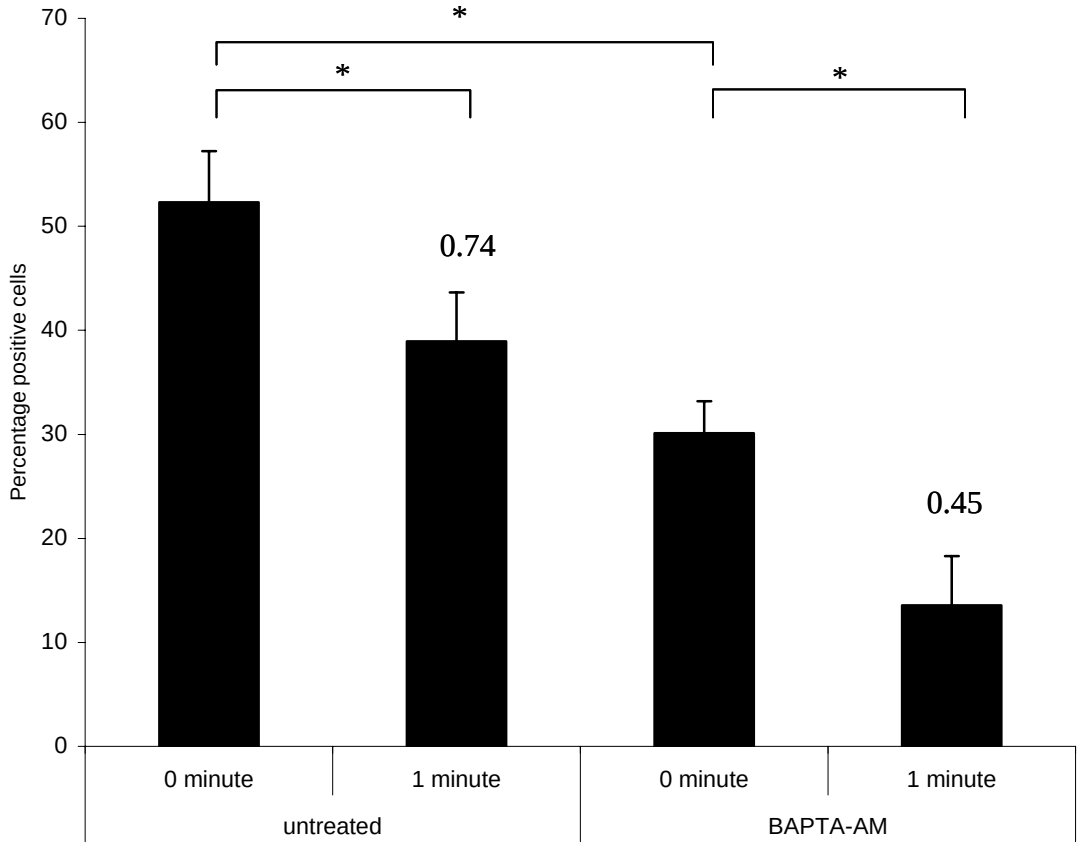

Figure 3.8. In the absence of extracellular Ca^{2+} during shearing, BAPTA-AM pretreatment reduced the permeability increase due to mechanical insult when compared to untreated group (* $p<0.0001$), also sheared in absence of extracellular Ca^{2+}. Pretreatment also increased resealing, which is manifested by the lower percentage of positive cells to calcein 1 minute after insult compared to untreated group. Uptake ratios are seen on top of 1 minute groups. Error bars represent SD. n=8 cultures/group.

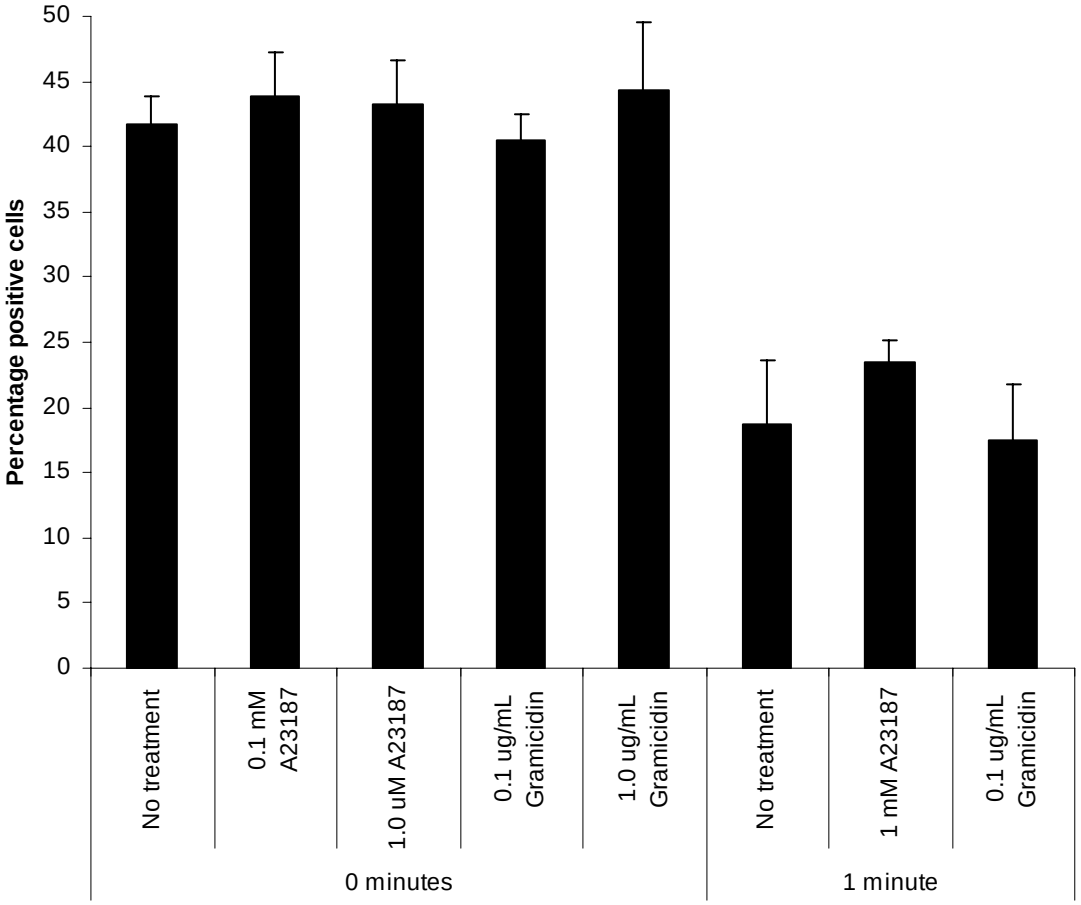

Figure 3.9. Ionophore pretreatment did not change the temporal profile of membrane disruption. (n=4-5)

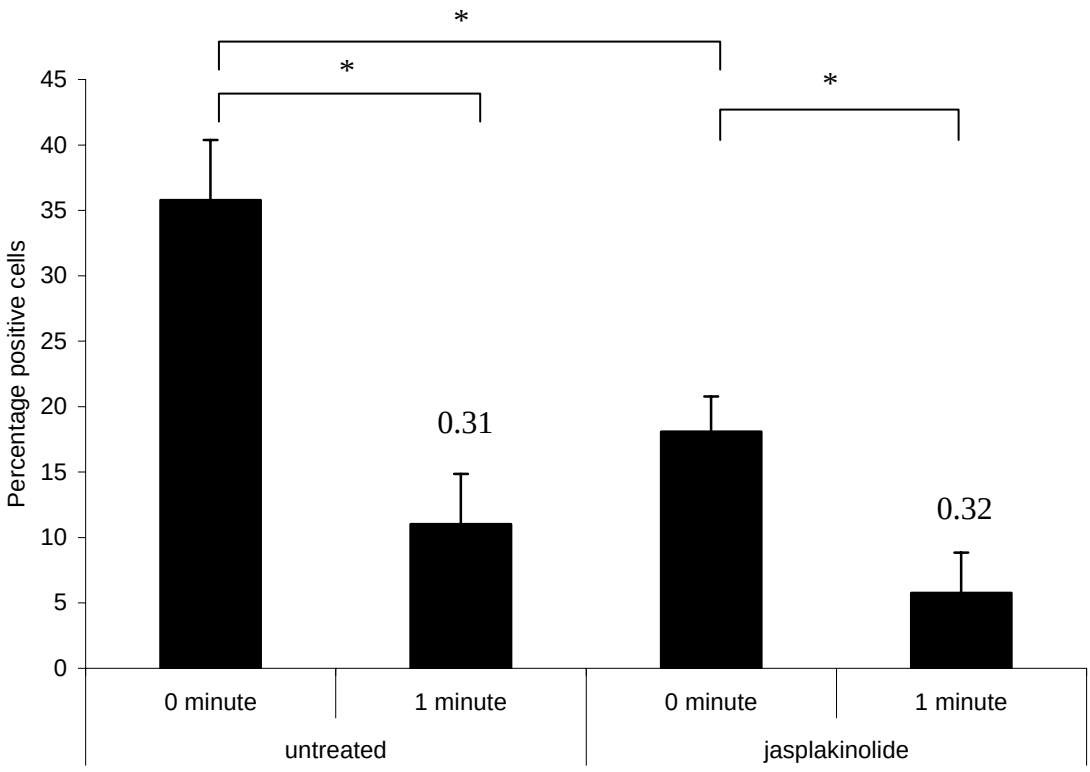

Figure 3.10. Pretreatment with jasplakinolide reduced increases in the percentage of positive cells to calcein due to mechanical insult (* $p<0.0005$). Pretreatment did not have an effect in the cellular resealing when compared to untreated cultures at 1 minute. Uptake ratios are seen on top of 1 minute groups. Error bars represent SD. n=3-5 cultures/group.

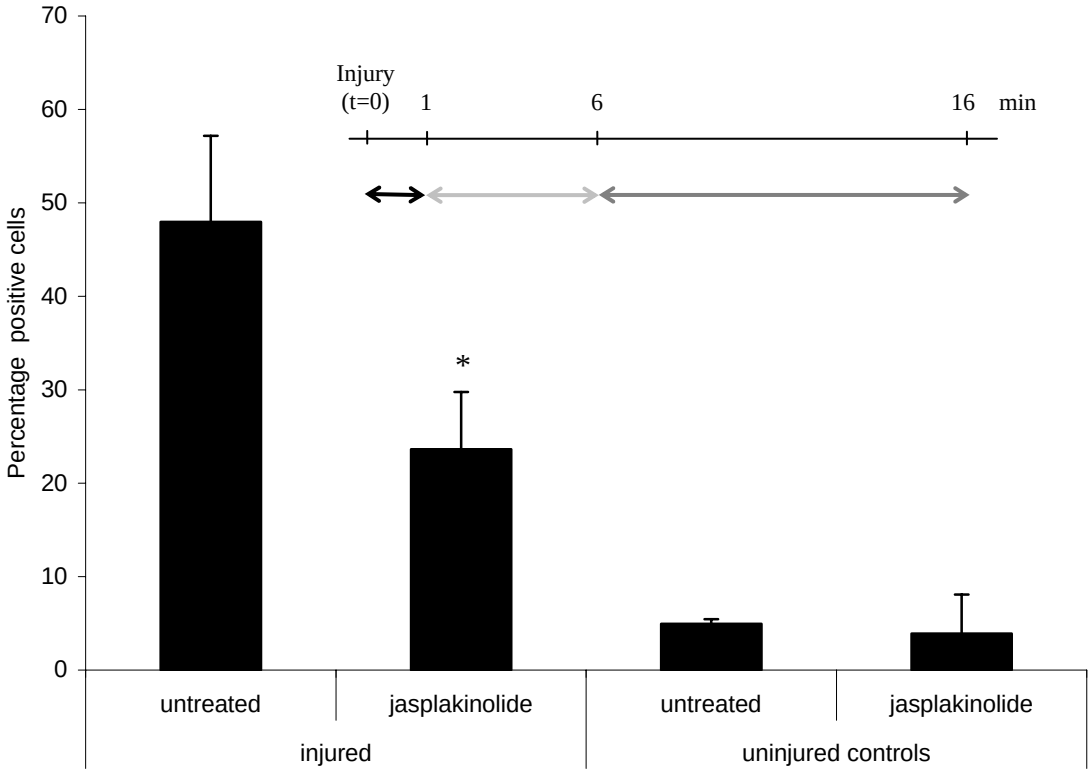

Figure 3.11. Treatment of jasplakinolide after insult induced cell resealing, which is evidenced by the lower percentage of positive cells to calcein when the marker is added after treatment when compared to untreated group ($p<0.005$). Chart shows time course of this experiment. Black arrow indicates time between insult and addition of jasplakinolide, light grey indicates jasplakinolide treatment, and dark grey indicates calcein incubation. The injured data were not subtracted from uninjured control values in this experiment. Uninjured controls are displayed on the right and show that treatment alone did not significantly change uptake levels. Error bars represent SD. n=4-5 cultures/group.

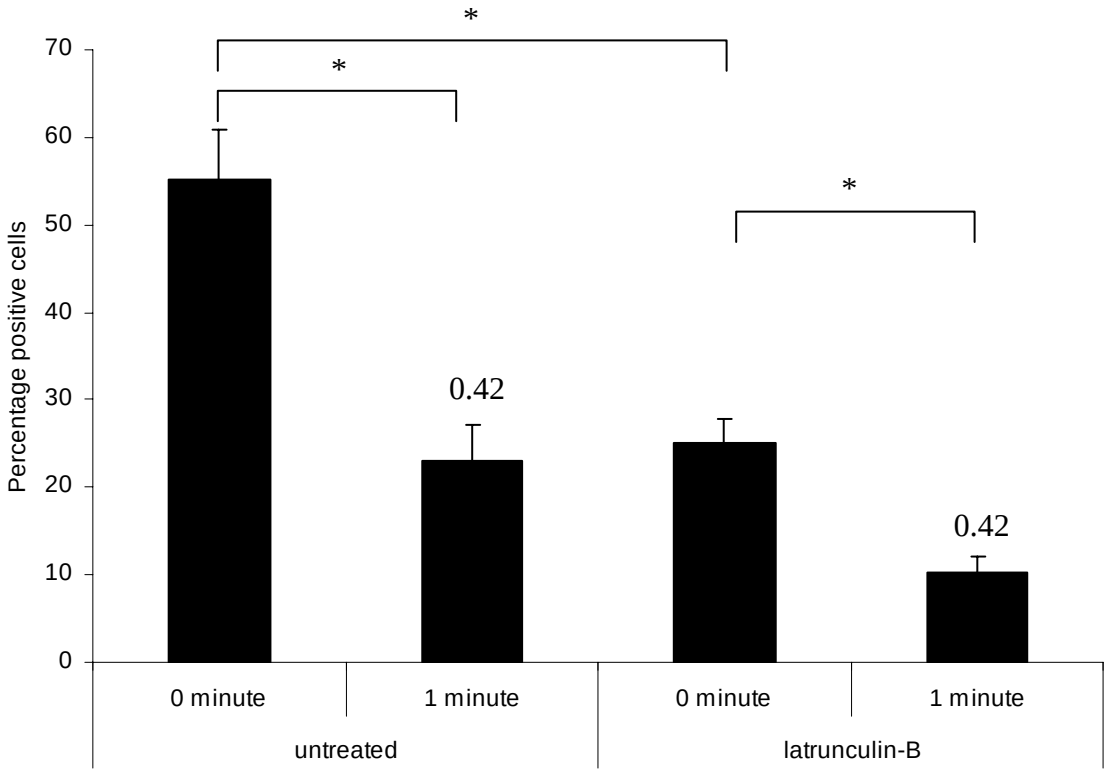

Figure 3.12. Pretreatment with latrunculin-B reduced the increase in percentage of positive cells due to mechanical insult when compared to untreated group (* $p<0.0001$). Latrunculin-B-treated group contained less positive cells at 1 minute, although the uptake ratios were the same for treated and untreated groups at that time. Error bars represent SD. n=3-4 cultures/group.

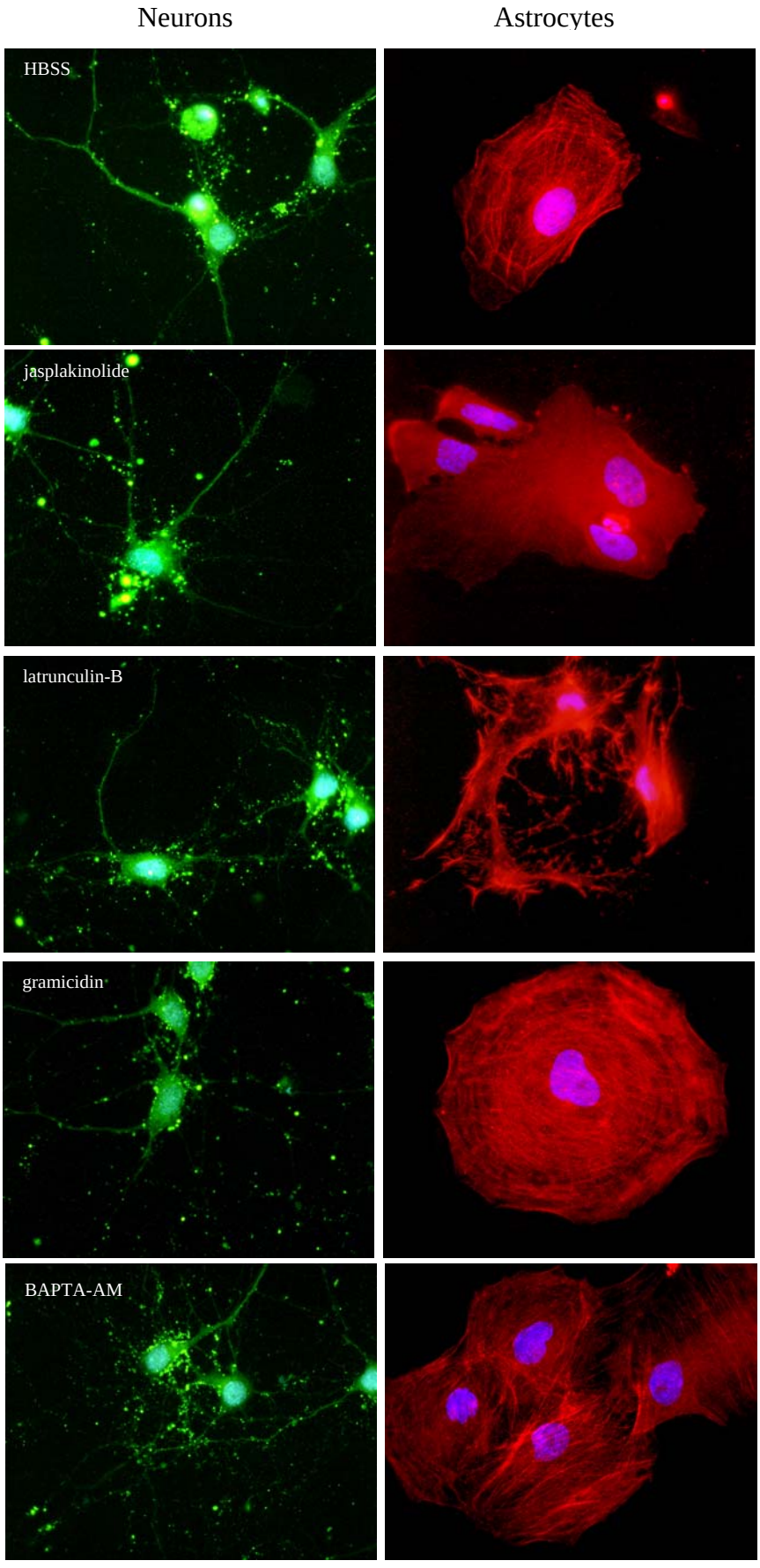
Neurons
Astrocytes
HBSS
jasplakinolide
latrunculin-B
gramicidin
BAPTA-AM

Figure 3.13. Actin visualization in neurons and astrocytes. Neuronal and astrocytic cultures underwent chemical treatments for the same length of time as in previous experiments. Cells were fixed and an actin antibody was used to visualize both filamentous and globular actin. Jasplakinolide and latrunculin-B produced severe changes of actin cytoskeleton in astrocytes. Neurons presented no visually detectable stress fibers that were readily found in astrocytes.

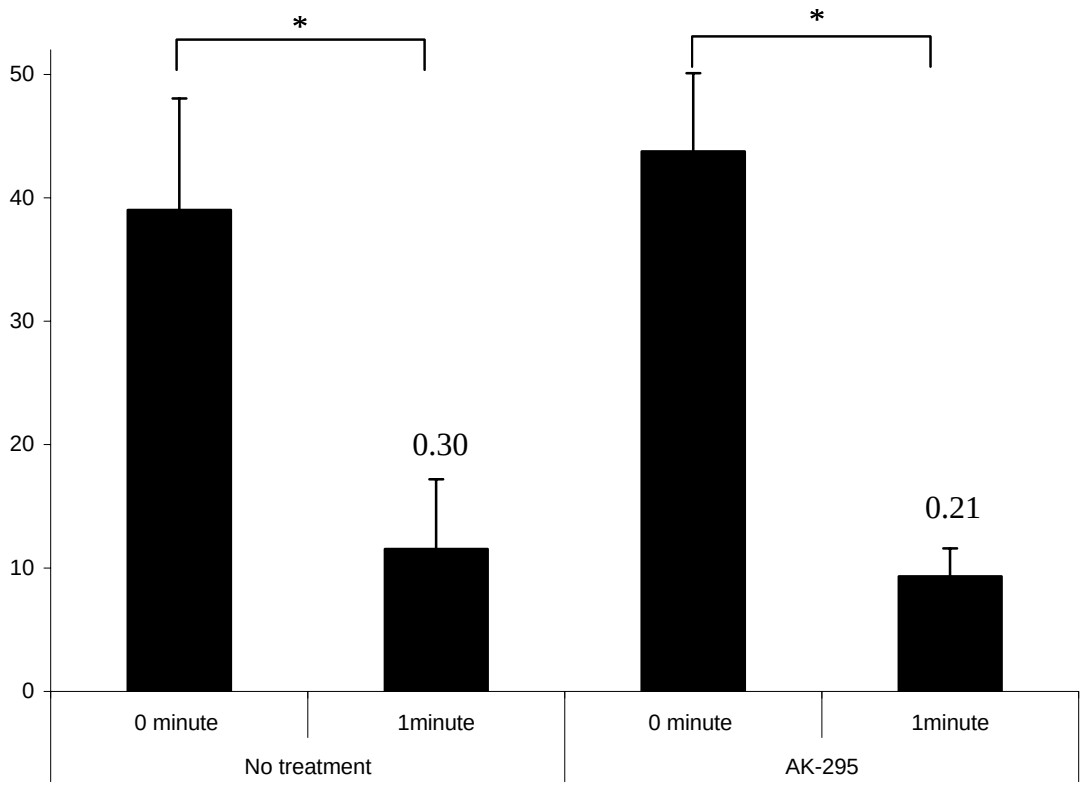

Figure 3.14. Calpain inhibition did not affect plasma membrane disruption or resealing. Pretreatment with 10 mM AK295 did not affect the initial plasma membrane disruption. Resealing mechanism was present in treated cultures and was not significantly different than untreated ones (* $p<0.0005$; n=4-5). Uptake ratios are seen on top of 1 minute groups. Error bars represent SD.

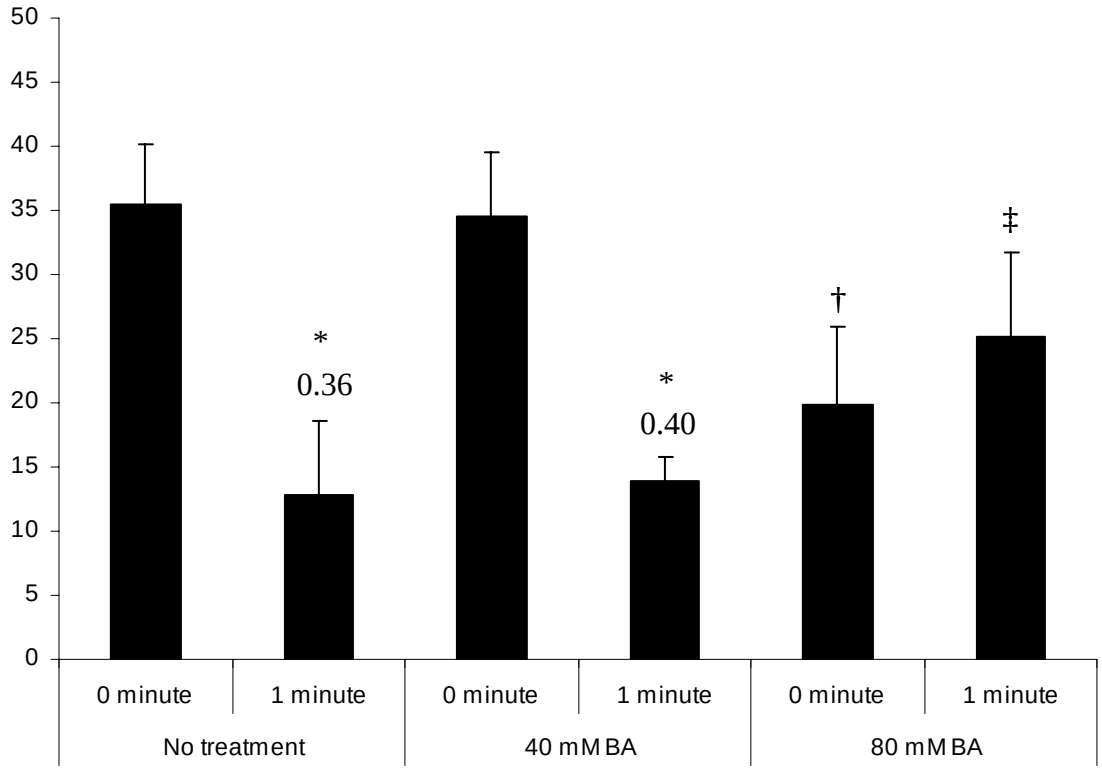

Figure 3.15. High concentrations of benzyl alcohol pretreatment disturbed both initial plasma membrane disruption as well as the resealing mechanism. 40 mM benzyl alcohol pretreatment did not affect initial plasma membrane disruption or resealing (* significantly different from 0 minute; $p<0.0001$). The higher concentration of benzyl alcohol (80 mM) resulted in significantly less positive cells at the time of insult († $p<0.005$) as well as an arrest in the resealing mechanism (‡ $p<0.05$) when compared to untreated and 40 mM benzyl alcohol pretreated groups.

CHAPTER 4

NEURONAL ELECTRICAL ACTIVITY FOLLOWING *IN VITRO* MECHANICAL INJURY

4.1 Introduction

4.1.1Electrophysiological disturbances following traumatic brain injury (TBI)

The neuronal plasma membrane plays a crucial role in cell function, maintaining ionic gradients used for a variety of processes ranging from action potential production to neurotransmitter transport. Therefore if the plasma membrane lipid bilayer, normally impermeable to ions, becomes compromised (even in a transient fashion) it may lead to neuronal dysfunction. Electrophysiological function is the ultimate attribute of a healthy neuronal cell. TBI-induced electrophysiological disturbances *in vitro* have not been extensively researched. While a few studies have evaluated aspects of electrophysiological changes in individual cells following mild/moderate *in vitro* TBI (Goforth et al., 1999; Zhang et al., 1996), network properties such as overall changes in endogenous activity following such insults have not been investigated. Although classic intracellular electrophysiological measurements can elucidate many aspects of neuronal functionality following TBI, these studies do not examine cell interactions within a network after an insult. Also, due to complex and time-consuming techniques, intracellular recordings cannot elucidate acute changes in electrical parameters in the seconds following insult. Moreover, characteristics of a neuronal network such as synapse strength, signal spread, and spread velocity, cannot be revealed by investigating one cell at a time. Extracellular electrical recordings through the use of multielectrode

array (MEA) technology, however, will give new insight into network properties changes that may occur following a traumatic neuronal injury. Such network properties may be more relevant than changes seen in a single cell, as even the simplest behavior in an animal involves extensive cell-to-cell interaction. We hypothesize that the cellular dysfunction reported following TBI, such as reduction in AMPA receptor desensitization in a sub population of cells (Goforth et al., 1999), compounds with cell-to-cell alterations to ultimately yield network property changes. Also, we hypothesize that plasma membrane permeability changes have a direct effect on neuronal network properties. It is hypothesized that, following a permeability increase, neuronal function will be affected as a result of massive diffusion of ions across the lipid bilayer until plasma membrane disruption is repaired. However, it may be that the electric as well as biochemical functionality of these cells can be affected long after the membrane permeability has returned to basal levels due to initiation of secondary events. For example, high levels of intracellular Ca^{2+} may be a trigger for secondary events following experimental TBI such as activation of numerous cellular pathways that may induce short (Raghupathi et al., 1995) and long term changes in neurons, including cell death (Hicks et al., 1996).

4.1.2 Extracellular measurement using MEAs

We have designed a new system that integrates our cell shearing injury device (CSID) with a commercially available MEA system able to measure extracellular electrical activity from neuronal cultures (Multi Channel Systems, Germany). This hybrid device is capable of monitoring extracellular neuronal electrical activity, including parameters such as firing rate, burst rate, burst interval, and others, which can be accomplished before, during, and following traumatic injury. Also, cultures were injured

directly in the MEA, avoiding time-consuming manipulations such as the ones needed in intracellular electrophysiology, which renders acute measurements impossible. Injury parameters were sub-lethal and were the same used in Chapter 3. The injury MEAs (*i*MEAs) in this study were custom-made in house with a unique electrode array position. Commercially available MEAs consist of a 50x50 mm square glass plates that contain 60 electrodes at the center, where cells are cultured. The CSID uses a rotating cone that contacts the center of the plate (MEA surface), therefore commercially available MEAs would be unacceptable for this application. The custom MEA pattern was designed with the electrodes placed off center to accommodate the CSID specifications. Briefly, the *i*MEAs were fabricated using a relatively thicker insulating layer of the photoresist SU-8 (3.5μm; dielectric=3-4) than commercially available MEAs, which use a relatively thin layer of silicon nitride (1μm; dielectric=7-8) as an insulator. This feature reduced capacitive coupling between cells and gold tracts which run below the surface. *i*MEAs also benefited from electroplated platinum electrodes with about half of the impedance of the TiN interface used in commercial MEAs (at 1 kHz). Platinum was plated in an ultrasonic environment in order to improve adhesion and life of the electrodes.

4.1.3 Extracellular recording background

In vitro neuronal networks of rat neonatal cells exhibit electric activity as early as three days following cell seeding (Kamioka et al., 1996). This initial spontaneous activity is believed to be localized and present with little or no propagation since synapses are still developing at that stage. Early activity, however, has been shown to be responsive to currents generated via NMDA, AMPA, GABAa, and fast-sodium ionotropic receptors, demonstrating early expression of these receptors (Kamioka et al., 1996). At

approximately four days *in vitro* (DIV), neuronal cultures begin to exhibit signal propagation, indicating the strengthening of synapses. Propagation speeds become faster as the cultures mature. At approximately the same time, cultures begin exhibiting spontaneous bursts of activity that propagate across the MEA (Kamioka et al., 1996). In the current study, we have shown that neuronal cultures present spontaneous bursting activity occurring readily at 10 DIV. This endogenous activity can serve as a health indicator for the entire network. We have quantified burst intervals, firing frequency, and firing within burst before and after mechanical insults of two severities. Spontaneous electrical activity, burst intervals, in particular, has been extensively characterized in developing and mature neuronal cultures (Tateno et al., 2002).

4.2 Materials and Methods

4.2.1 CSID-iMEA hybrid system

Modifications were made to the original CSID (see Appendix A) in order to make live extracellular electrical recordings possible. First, support brackets were machined from polycarbonate to attach the pre-amplifier to the CSID. The pre-amplifier used is commercially available (MEA1060-2 amplifier, Multi Channel Systems, Germany) and it was placed below the main stage of the CSID. The original CSID cell plate receptacle was modified in order to accommodate the pre-amplifier (Figure 4.1). The CSID's cone shaft was also extended in order to accommodate the lower cell surface.

*i*MEAs were designed with similar patterns to commercially available MEAs (64 electrodes separated by 200 μm in a square matrix) with the exception that the array itself was not in the center of the dish. The array of electrodes was designed to have a radial distance of 0.9 cm from the center in order to accommodate the CSID (Fig 4.2). The

fabrication of the MEA component, which employs two masks, involved conventional surface micromachining technology (Figure 4.3). Briefly, photoresist was patterned to define the MEA wiring. Layers of titanium and gold were sequentially e-beam evaporated with the undesired portions lifted off in acetone. The SU-8 was patterned to form the openings to the contact pads, and electrodes. The SU-8 served as both the electroplating mold for the platinum black electrodes and as the final insulation layer. Platinum was electroplated into the SU-8 molds under ultrasonic conditions, which effectively removes loosely adherent platinum deposits to ensure long lasting adhesion (Marrese, 1987). The thick SU-8 insulator, coupled with the low impedance of the platinum electrodes, provided a larger signal-to-noise ratio than commercially available arrays. *i*MEAs were then cured in an oven at 90ºC for 24 hours. Subsequently, *i*MEAs were submerged in de-ionized water for at least 48 hours in order to rid the cell-contacting surfaces of any toxic residue from the manufacturing. Once *i*MEAs were cured and rinsed, custom-cut polycarbonate rings (3.2 cm OD, 2.8 cm ID, 0.8 cm deep) were attached to *i*MEA surfaces using Sylgard 184 (Dow Corning, Midland, MI).

4.2.2 Neuronal cell culture in iMEA

Neuronal cortical cells were obtained from embryonic day 18 Sprague-Dawley rats (Charles River, Wilmington, MA**),** rinsed with Hanks' balanced salt solution (HBSS; Invitrogen, Carlsbad, CA) without Ca^{2+}/Mg^{2+} followed by incubation with trypsin (2.5 g/L plus 1 mM EDTA; Invitrogen) for 10 minutes. Trypsin solution was then removed and tissue was rinsed twice with DMEM containing 10% fetal bovine serum. Cortices were then dissociated in a solution of Neurobasal medium (Invitrogen) containing DNAse (0.15 mg/ml; Invitrogen) by brief agitation. Cells were counted and seeded

(density=1.25-2.0x10^5 cells/cm^2) onto *i*MEAs. Prior to cell seeding, *i*MEAs were rinsed with de-ionized water for 24 hours, briefly rinsed with 70% ethyl alcohol and allowed to dry in a sterile environment. *i*MEAs were then briefly flamed and allowed to return to room temperature. Poly-L-lysine (0.0023% w/v; Sigma, St. Louis, MO) was added to cover surface area of *i*MEAs for at least 12 hours at 37˚C, 95% relative humidity.

4.2.3 Fluid shear stress-induced mechanical injury

Neuronal cell cultures were subjected to a high magnitude, short duration, pulse of fluid shear stress using the CSID. The CSID consists of a servo motor-driven cone (0.5º) that rotates on top of the cell culture surface. Fluid (shearing buffer) between the cone and cell plate transfers the momentum from the rotating cone towards the plate where cells are seeded, producing a uniform shear stress across the culture plate.

Specifically, experiments were conducted by removing the *i*MEA from the incubator and rinsing it with HBSS twice. HBSS (0.5 mL) was left in the *i*MEA as the shearing buffer. A micrograph was then taken from the array of *i*MEA before it was placed in the CSID using a TE 300 microscope (Nikon, Japan). The *i*MEA was first placed in the pre-amplifier which was then attached to the CSID. The cone was slowly lowered until its apex contacted the center of *i*MEA. The insult parameters of shear stress magnitude and duration were 140 dynes/cm^2 and 300 milliseconds, respectively. The rise times, which are defined to be the length of time for the cone to reach maximum velocity, were either 20 or 150 milliseconds, which were categorized as high and low injury levels, respectively. The *i*MEA was then removed from the CSID and photographed while under the microscope. In some cases calcein (629 Da; 3.2x10^{-4} M; Sigma) was added to the shearing buffer as a neuronal permeability marker. In these cases the *i*MEAs were also

photographed under fluorescent light (~530 EM) after calcein was rinsed. In long term readings (24 hours following injury), Neurobasal medium was returned to the *i*MEA.

4.2.4 Electrical recording

At 10 DIV, *i*MEAs were placed in the pre-amplifier which was then attached to the CSID. Neurons were cultured until day 14 if they did not present burst activity earlier. Electrical activity of neuronal cultures was recorded for 10 minutes prior to mechanical-induced injury as well as the subsequent 10 minutes with MC Rack software (Multi Channel Systems). In some cases recordings also were made at 24 hours post injury.

4.2.5 Ionophore treatment

Both gramicidin and A23187 ionophores (Molecular Probes, Eugene, OR) were used. The *i*MEAs were taken from the incubator and rinsed three times with HBSS. HBSS (1.0 mL) was left in the *i*MEAs cell chamber. The *i*MEAs were placed in the amplifier and electrical activity was recorded for at least 10 minutes. A 2X ionophore solution in HBSS was prepared and 1.0 mL of the solution was slowly added after a new electrical recording was started. Adding 1mL of a 2X solution to the existing HBSS in the *i*MEA ensured proper and even dilution throughout the cell chamber.

4.2.6 Electrical activity quantification

Burst activity was detected by MCRack software (Multi Channel Systems). Activity was separated into 10 ms bins. The obtained files were then loaded onto a MATLAB routine where detection of bursts was accomplished by Butterworth low pass filtering techniques (2-5 Hz). A threshold was manually assigned above which bursts were detected. The parameters quantified in this study were firing frequency [action potentials/s], burst interval [s], and firing within burst [action potentials/burst]. A

temporal profile of array activity was then constructed with recordings from *i*MEAs at the first 10 minutes following the insult. Both overall activity during the 10 minutes following injury and 100 second increments within those 10 minutes were compared to activity recorded before insult. Some of the *i*MEAs cultures were also evaluated at 24 hours following insult. Statistical analysis was performed using ANOVA, comparing activity levels of 10 minutes before injury with either 100 seconds intervals or the total 10 minutes of activity following injury. Error bars in all figures represent standard deviation (SD).

4.3 Results and Discussion

4.3.1 Mechanical insult-induced neuronal plasma membrane permeability

Membrane disruption due to mechanical insult was assessed in 10 DIV cultures on *i*MEAs and 7 DIV cultures in cell plates (cultures used in Chapter 3) in a side-by-side fashion. Membrane disruptions in both types of neuronal cultures were not significantly different from each other as evidenced by similar calcein cellular uptake (Figure 4.4). These results validate the presence of similar membrane disruption in both types of cultures which ensured that subsequent electrical activity evaluations following a mechanical insult in *i*MEAs may be correlated with plasma membrane disruptions profiles from experiments in Chapter 3. Figure 4.5 shows representative micrographs taken before injury and immediately after in both phase and fluorescent modes. Neuronal cultures appeared morphologically normal immediately following insult. Note the presence of different amounts of calcein in cell bodies throughout the array area (Fig 4.5C).

4.3.2 Endogenous activity of cortical neuronal cultures

Electrical activity of neuronal cultures was evaluated at 10-14 days in culture, according to level of spontaneous activity. Most *i*MEA cultures presented several active electrodes at day 10 DIV. At that time cells were well adhered and presented a well developed network of neurites. *i*MEA recordings of uninjured cultures yielded a heterogeneous activity among different cultures as well as among electrodes within the same culture. A typical spatial activity within a cultured dish is shown in Figure 4.6. Although all three parameters assessed varied considerably among electrodes of the same culture, they did not significantly change with time during the periods evaluated (Figure 4.7). This was an expected outcome as other studies have reported similar results from neuronal networks of this age, when firing patterns have not yet become completely synchronous within a culture (Tateno et al., 2002). In the same study, Tateno et al. also found that although there was significant variation of burst intervals amongst cultures, there was little tendency in variation within recordings.

4.3.3 Mechanical insult-induced electrical disruptions

Mechanical insult to cortical neuronal cultures induced immediate electrical activity changes. The CSID-*i*MEA system has made it possible, for the first time, to continuously monitor neuronal electrical activity before and immediately after a mechanical insult. Figure 4.8 shows this capability with a recording sample of an injured culture, depicting one electrical parameter (burst interval) averaged every 50 seconds before and after injury. The figure also shows a common outcome for burst interval following injury, characterized by an increase in magnitude and variability. However, electrical activity responses were heterogeneous and varied in different electrodes within

the same array. A compilation of the outcome averaged over the first 10 minutes following injury of all electrodes which presented spontaneous electrical activity before the mechanical insult in this study is shown in Figure 4.9A. Only statistically significant ($P<0.001$) and changes greater than 20% in magnitude were considered significant changes. Cultures injured at rise times of 20 ms (high injury level) presented more immediate changes in electrical activity than did cultures injured at 150 ms rise time (low injury level). In addition, the high injury level induced a larger percentage of electrodes to exhibit complete cessation of activity as compared to low injury levels. Moreover, the low injury level insult produced a more heterogeneous response, including electrodes that presented increases, decreases, and no significant changes in overall electrical activity within the first 10 minutes following injury. Although the number of electrodes that were categorized under “no change” in overall activity within the first 10 minutes was high, changes were seen when averages of electrical outcome was made in shorter time increments. The incremental temporal evaluation of activity using 100 second bin reveal significant changes in electrical activity within the first 10 minutes following injury (Figure 4.10). Therefore, by averaging electrodes that presented an initial decrease of burst interval immediately after the insult followed by an increase in this same parameter may hide interesting dynamical processes within that time frame. As we quantified the overall 10 minute comparison, many of these variations were hidden and dismissed as statistical variability. For this reason, quantification of the temporal profile in 100 second increments during the 10 minutes following injury was performed in all electrodes that showed electrical activity (data not shown). Figure 4.10 illustrates the gradual shift in electrical activity in all three electrical parameters during the 10 minute interval

following insult, indicating complex interactions within the network as opposed to perturbation in activity simply due to immediate detachment of neurons at the time of the insult. Other *i*MEAs presented two distinct parts in their electrical response. The first was an immediate increase in the means of burst intervals followed by a second and delayed response of a further increase of magnitude accompanied by an increase in variability hundreds of seconds later (Figure 4.11). In summary, the most prevalent acute electrical responses seen following insults were both an immediate or a combination of sudden and delayed increase in burst interval which was also usually accompanied by and an increase in burst interval variability. This outcome was usually accompanied by a decrease in firing within bursts.

4.3.4 Ionophore-induced electrical disruptions

The hypothesis that neuronal permeability increases after a mechanical insult contributes to electrical perturbations within the network by affecting cellular ion homeostasis can be partially tested with the use of ionophores. Ionophores are molecules that embed themselves into the lipid bilayer and are capable of forming temporary pores, allowing ions to pass through. Gramicidin is an antibiotic-peptide that embeds itself within a single lipid leaflet of the bilayer. One molecule is not large enough to create an pore by itself. These molecules drift within the membrane and momentarily create a complete pore whenever they coincide at the same planar location (Sawyer et al., 1989). Gramicidin-induced pores are specific to cations, allowing passage of Ca^{2+}, Na^{+}, and K^{+} (Doebler, 2000). This ionophore is capable of depolarizing neuronal cells at low concentrations (1 µg/mL) (Doebler, 2000). A23187 is a Ca^{2+}-specific ionophore, and it is

commonly used to load Ca^{2+} into cells as a positive control in Ca^{2+} visualization studies using Fura-2 (Mills and Kater, 1990).

Ionophore treatment caused several similar electrical responses seen following a mechanical insult. A23187 treatment at concentrations of 1.0 µM caused a destabilization of burst intervals, resulting in an increase in the magnitude as well as variability in this parameter in 86% of recorded electrodes (Fig 4.9C). Gramicidin treatment at concentrations as low as 0.1 µg/mL caused sudden and complete cessation of electrical activity within 2 minutes of addition. At 0.01 µg/mL, gramicidin caused perturbed electrical activity for several hundred seconds until it overwhelmed neuronal cells which ceased activity. At these concentrations, gramicidin treatment caused a similar response seen in 36% of electrodes injured at 150 ms rise times. This response consisted in an immediate decrease in burst intervals followed by an increase in magnitude and variability of the same parameter. Also, gramicidin treatment caused a similar temporal response to mechanical injured cultures in many treated electrodes, consisting of two-parts as discussed in the last section. First, immediate and relatively small but significant increases in the burst intervals occurred followed by a gradual increase in magnitude and variability of this parameter (Figure 4.12). Figures 4.11 and 4.12 show the averaged electrical responses within one *i*MEA injured at 150 ms rise time and one culture treated with 0.01 µg/mL of gramicidin, respectively. The dramatic increase in burst interval in a delayed fashion is evident in both cases. At that concentration, however, ionophore-treated cultures could not sustain activity for longer than 400 seconds. These results show similarities in electrical responses caused by ionic homeostasis disruptions caused by ionophore treatments with the electrical responses observed after a mechanical insult.

These results provide further evidence that neuronal plasma membrane disruptions occurring due to a mechanical trauma are, at least in part, responsible for electrical activity disturbances. Although ionophores can provide a link between trauma-induced membrane disruptions and electrical activity responses seen in mechanically injured cultures, care needs to be taken when comparing a chemical treatment to a mechanical trauma as their temporal action differ. Unlike mechanically-induced alterations in electrical activity, ionophore addition to neuronal cells had a delayed effect. Perturbations in network activity took several seconds after addition of these molecules to become evident and no immediate cessation of electrical activity was seen. Doebler et al. presented similar results, where addition of gramicidin took minutes to depolarize NG108-15 cells (Doebler, 2000). Moreover, removing the action of the ionophores involved multiple rinses and required extra time for the molecules to diffuse away from the plasma membrane. So, unlike the fast acting pulse of mechanical stress which subsides within the order of one second, due to viscous forces dictating the fluid environment (Blackman et al., 2000), the ionophore action, even if causing a similar mechanism of destabilizing the ionic homeostasis of cells, had a significantly different temporal action. These constraints in the use of ionophores often caused cells to be overcome with the ionic flux, which lead them to cease electrical activity within minutes. Only extremely low concentrations (on the order of 0.0001 μ/mL) were able to modulate the electrical activity without causing cessation of firing in the short term (Figure 4.13). Higher concentrations (>0.01μg/mL) of ionophore treatment caused complete neuronal cell death at 24 hours, even upon rinsing of cultures following recordings. Cell death was not quantified in these experiments, but inspection of cultures yielded vast neuronal cell

death and sparing of cells presenting glial morphology. Concentrations less than or equal to 0.01µg/mL did not cause neuronal cell death when cultures were rinsed after recordings were complete (see section 4.3.7).

4.3.5 Extracellular Ca^{2+} and electrical activity

In studies presented in Chapter 3 we demonstrated the importance of the extracellular Ca^{2+} in the resealing of neuronal plasma membrane following a mechanical trauma. Chelation of extracellular Ca^{2+} greatly deters the resealing of membranes, but it remained unknown if removal of this ion can be otherwise detrimental to neuronal cultures. Extracellular Ca^{2+} was removed from *i*MEA cultures by rinses with HBSS without Ca^{2+}/ Mg^{2+}. The electrical activity was abolished immediately since extracellular Ca^{2+} is necessary in the release of neurotransmitters (Martin, 2003) as well as in pacemaker currents responsible for rhythmic firing in different neuronal networks (Harris-Warrick, 2002). Ca^{2+} was returned to the *i*MEAs by rinses with HBSS. The return in neuronal electric activity required at least 500 seconds (Figure 4.14). An overshoot was detected in both firing rate and firing within bursts from 500 seconds until the end of recordings. These results suggest that Ca^{2+} removal, for short amounts of time, does not seem to inflict abrupt cell dysfunction although long term outcome was not evaluated and consequences to the overshoot in firing rate are not known.

4.3.6 Heterogeneity in electrical responses

Similar to single-cell electrophysiological studies following a traumatic event (Goforth et al., 1999), our study yielded results that were heterogeneous in nature. While a subset of the population of electrodes evaluated presented unchanged activity, other subsets showed dramatic changes. Although we applied a uniform insult throughout the

injured cultures, the morphological variability within the population of cultured neurons was potentially responsible to the heterogeneous electrical response reported here. Cells presenting different morphological profiles will be more or less vulnerable to the fluid shear stress-induced injury. Morphological differences also correlate to differing levels of cell adhesion to the substrate, which further increases variability in injury susceptibility (see Appendix B for more details).

4.3.7 Long term outcome in mechanically injured cultures

Most cultures injured at rise times of 150 ms were still active at 24 hours post-insult. This is contrasted with the lack of electrical inactivity at 24 hours in most of the arrays injured at rise times of 20 ms (Figure 4.9B). This finding underscores the importance of evaluating electrical activity of *in vitro* cultures in cell injury models. Cultures that may appear otherwise healthy could present a complete or partial cessation of electrical activity and other dysfunctions. An example of an injured culture activity 10 minutes and 24 hours following insult can be seen in Figure 4.15. This is a representative *i*MEA which shows heterogeneity amongst electrodes before and after injury. Changes due to injury are significant ones, however. Electrical activity at 24 hours following injury changed dramatically compared to both before and immediately after insult was applied. In order to elucidate mechanisms responsible for electrical changes seen in these electrodes, detailed microphotographs of the same *i*MEA at 24 hours were compared before injury. The microphotographs show an unexpected and dramatic remodeling of cultures occurring around the electrodes evaluated. This is evidenced by the migration of many cells around electrodes. Although this finding may point to an injury-induced remodeling of the network, we did not have uninjured controls of the same maturity level

for comparison. Also, although viability was not assessed in these experiments, cell death does not seem to be increased in this particular culture. These results show that a short lasting change in neuronal plasma membrane permeability may evoke long-term changes in network activity. These changes may occur due to triggering of secondary events by the initial insult, which may consist of sensitization and desensitization ionic channels as reported by Goforth et al. (Goforth et al., 1999) as well as long-lasting synaptic strengthening and weakening. Ionophore treatment at concentrations of 0.01 μg/mL also caused long-term electrical changes in neuronal cultures (Figure 4.17). This is evidence that a temporary increase in permeability to ions by ionophore can cause long-term electrical changes similar to the ones observed following mechanical injury.

It is important to recognize the difficulties in drawing conclusions from long term measurements such as the 24 hour time points. 10-14 DIV neuronal cultures have been shown to be in a developing state with regards to the electrical activity, when burst intervals have shown to decrease as cultures mature (Tateno et al., 2002). Therefore, care needs to be taken when concluding that the mechanical insult only was responsible for long-term changes.

4.4 Conclusions

This study is the first report in which network electrical activity is assessed following mechanical trauma. We have shown that membrane disruption occurs in a large percentage of cells within the *i*MEA. Also, we have demonstrated concomitant alterations in neuronal plasma membrane permeability and spontaneous electrical activity perturbations. Although the initial electrical response may be triggered by the change in permeability of neurons, other mechanisms such as loss of cells and synaptic

disconnections together with secondary cascades triggered by the initial insult can contribute to electrical responses seen. Results from ionophore treatments showed that many of the electrical responses due to increase in permeability to cations are similar to the responses observed following a mechanical insult.

This study underscores the difficulty in accessing neuronal injury in TBI models. Neuronal cellular responses to a mechanical insult are varied and complex. A network of neurons can appear morphologically healthy, but it can be electrically nonfunctional. The results obtained in this study elucidated a yet different and equally important manner to assess neuronal injury. This assessment is significant as it does not depend only on the health of individual neurons, but the network as a whole. This new dimension of outcome is often neglected in both *in vitro* as well as *in vivo* models of TBI and other CNS disorders. Quantification of cell viability and activation of different types of enzymes are done on a cell by cell basis, but the electrical health of network is, to our knowledge, never assessed. Although information about which enzymatic cascades are triggered inside a cell following a mechanical insult can be crucial in the potential treatment of TBI, equal amount of effort should be made in the understanding of network dynamics in TBI. For example, does the native brain tissue network have a rerouting response once an area becomes impaired? Can such mechanism be facilitated with drug or surgical interventions? Thus, this study has the potential to be an important step towards the understanding of complex electrical interactions following TBI.

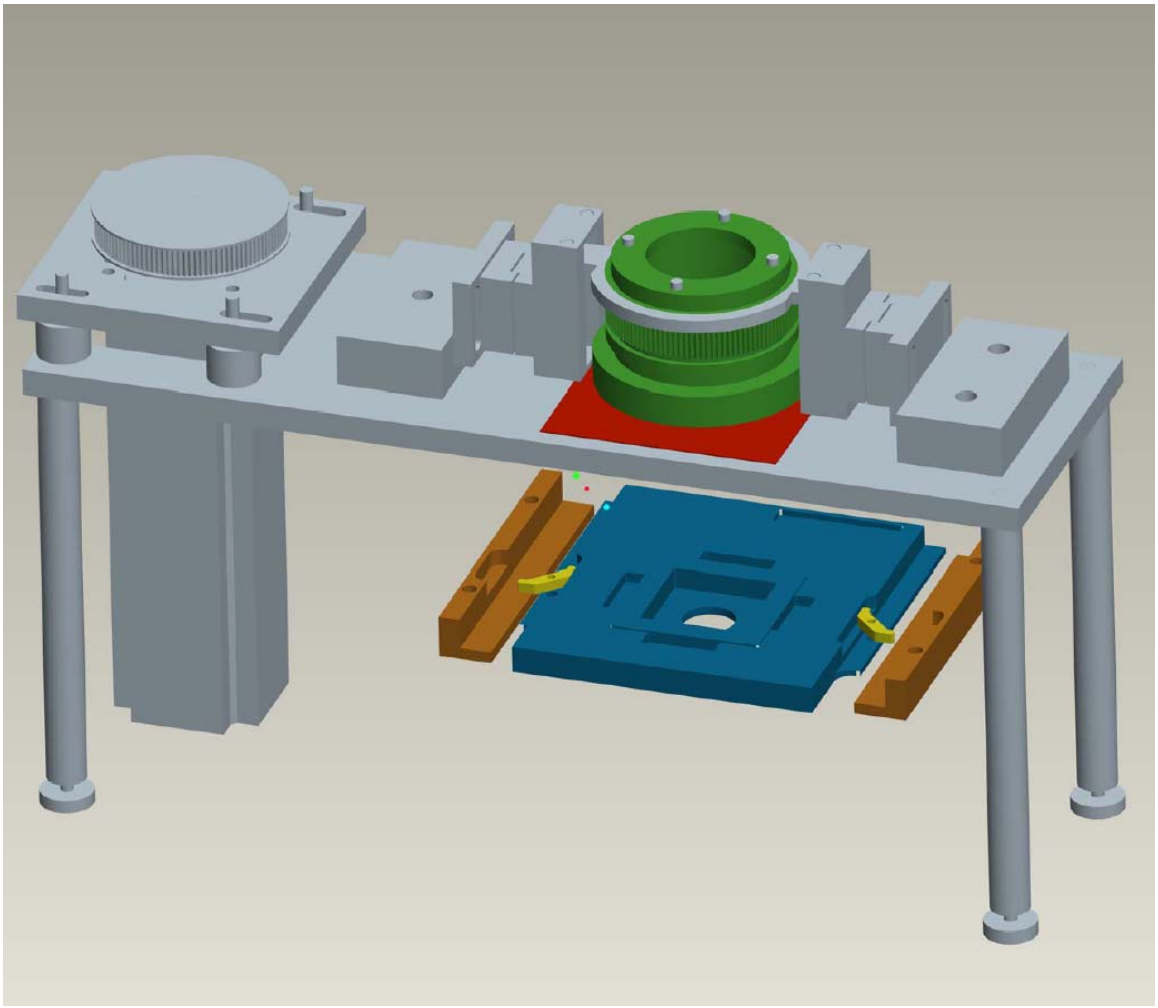

Figure 4.1. Modifications to the original CSID. Parts in color represent where modifications were made to the CSID. The rotating shaft of the device was modified to accommodate the lower surface of the *i*MEAs (green). The cell plate holder was replaced with the pre-amplifier receptacle (red). The pre-amplifier (blue) was secured to the device by polycarbonate braces (brown).

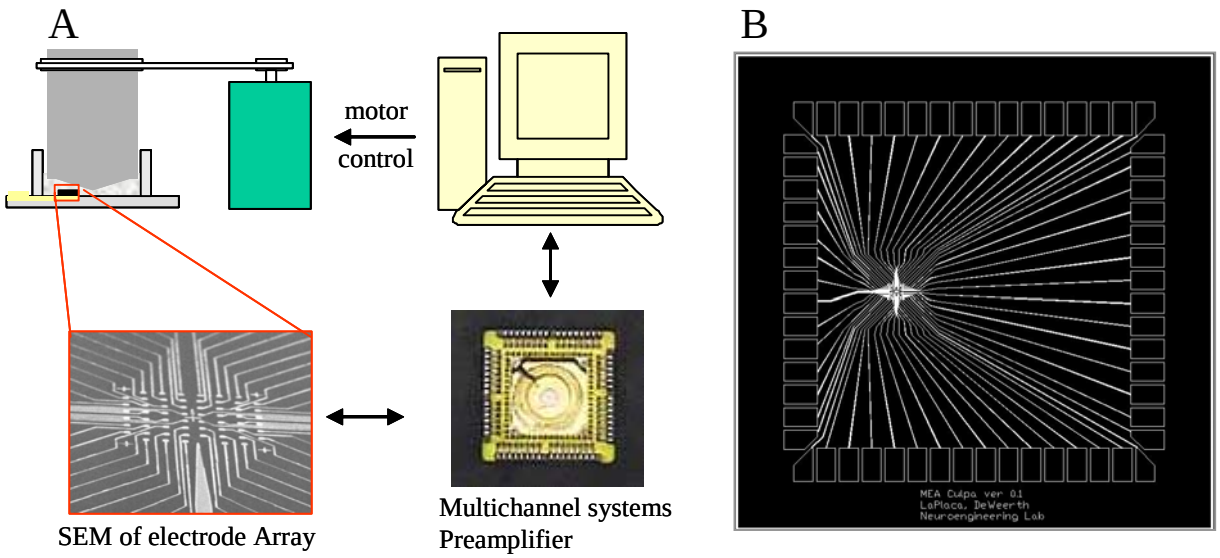

Figure 4.2. Schematics of the *i*MEA system. Microelectrode array embedded in the CSID is connected to a pre-amplifier which relays the signals from the MEA to the computer (A). Custom made *i*MEA geometry where array is placed off-center (B).

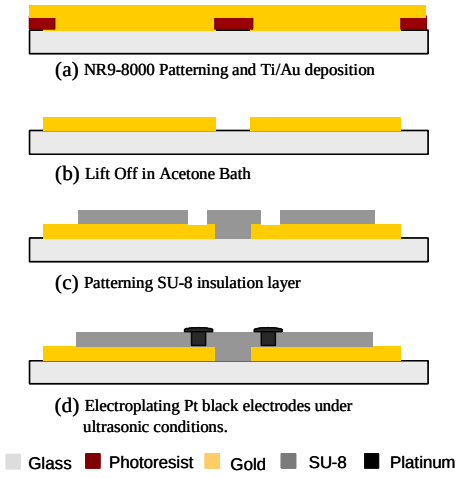

Figure 4.3. Micro fabrication of *i*MEA.

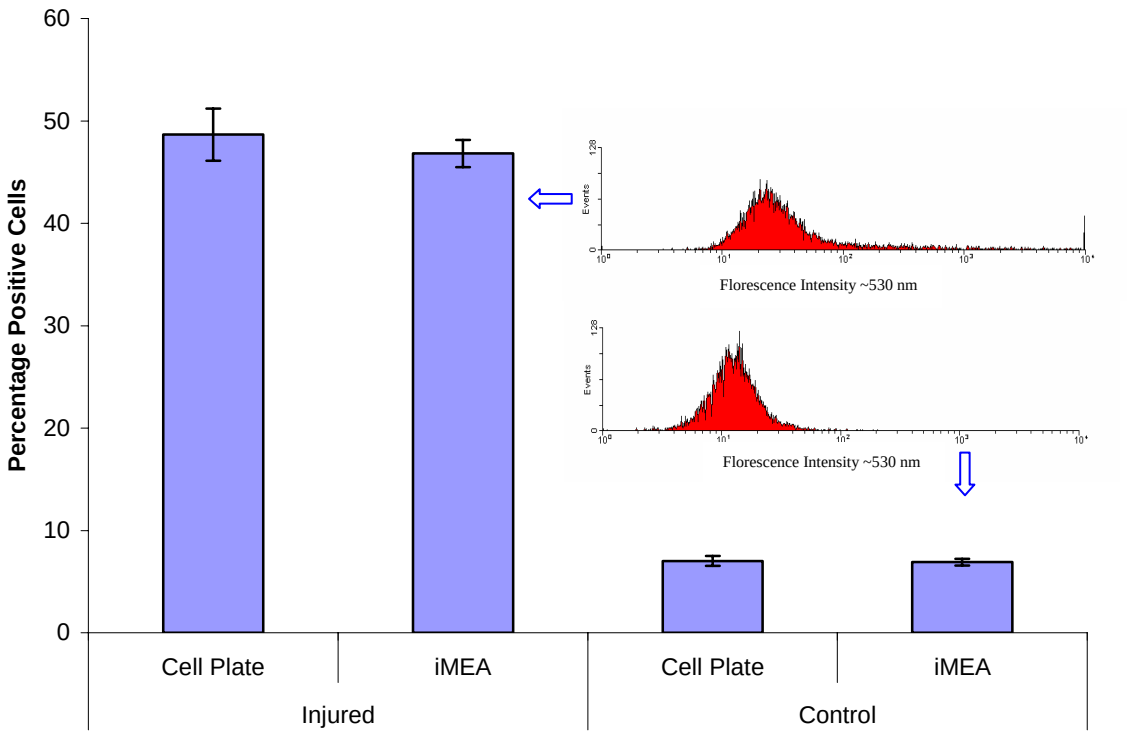

Figure 4.4. Neuronal membrane disruption in cell plates (7 DIV) vs. *i*MEA cultures (10 DIV). Membrane disruptions caused by a mechanical insult generated by the CSID were not significantly different in *i*MEA cultures when compared to cell plate cultures. Cells were injured in the presence of calcein. Histograms on the right show flow cytometry-derived green fluorescence intensity of injured (top) and uninjured (bottom) *i*MEA cultures. Uninjured controls were not used to subtract from injured values in order to show comparison between *i*MEA-cultures vs. cell plate cultures uninjured uptake. See Chapter 3 for methods (n=3)

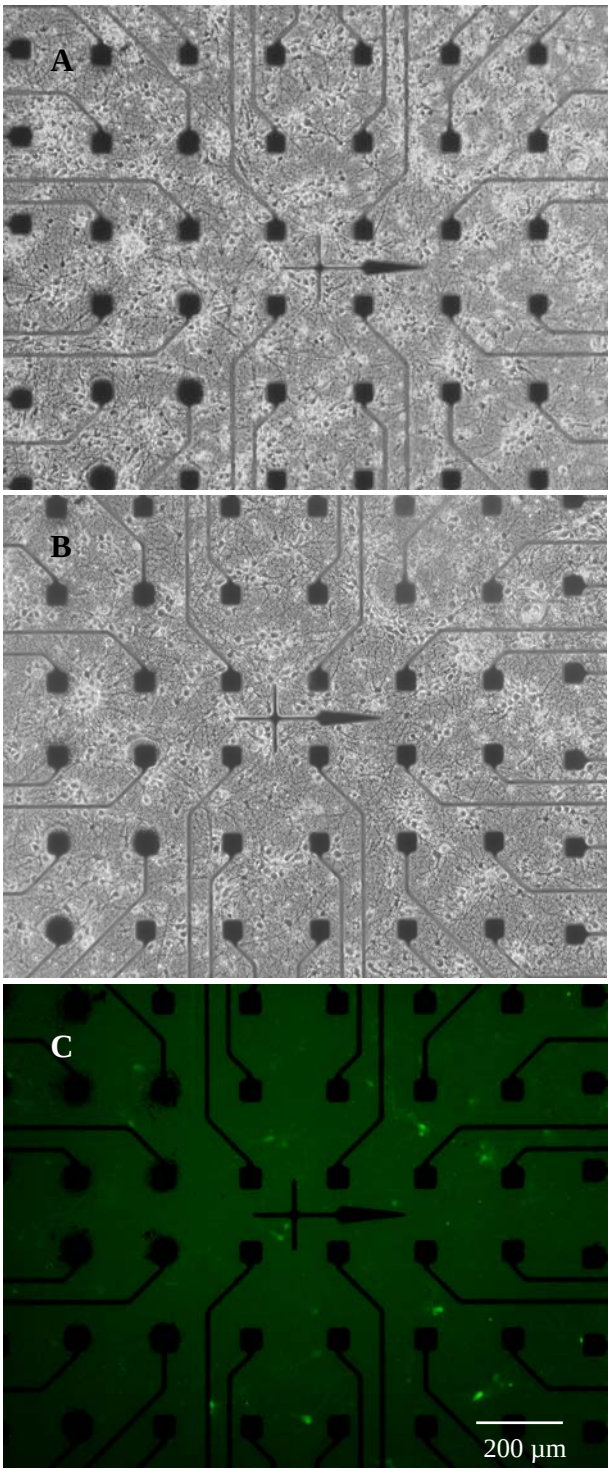

Figure 4.5. Neuronal cultures in *i*MEA before and after mechanical insult. Cultures present a developed neurite arbor at 10 DIV (A). Neurons are able to sustain adhesion after mechanical insult (B). Neuronal plasma membrane disruption is evidenced by the uptake of calcein immediately following injury when cultures are imaged under fluorescence (C).

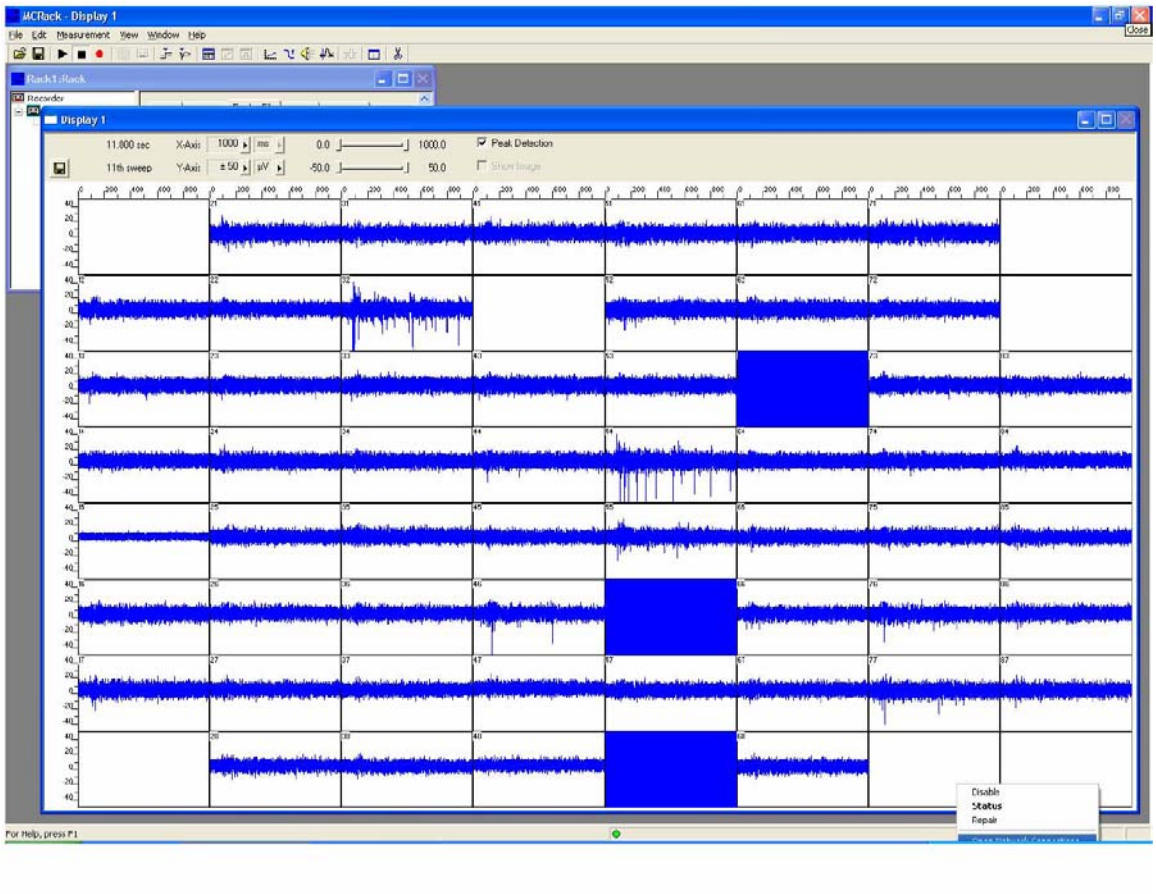

Figure 4.6. Spatial electric activity in 10 DIV neuronal cultures. At that time, electrodes have different levels of electrical activity.

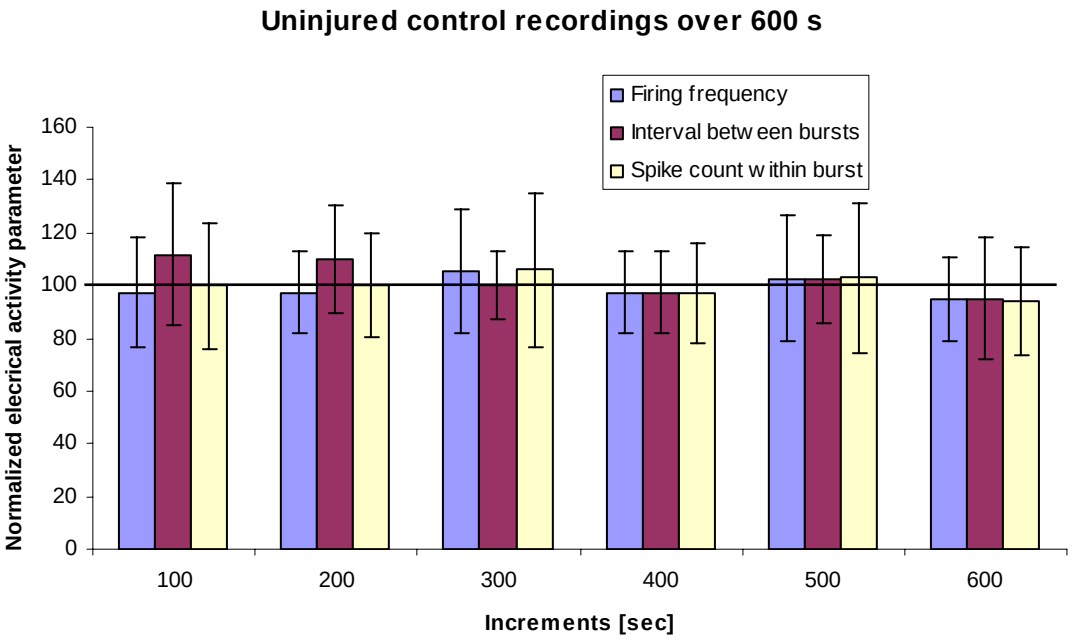

Figure 4.7. Electrical activity parameters do not present significant changes over 600 seconds. Using the criteria described in the Materials and Methods section, individual increments of 100 s are not significantly different than the averaged parameters over 600 s in uninjured controls. This shows that the occurrence of false positives with this method is low. All three parameters were normalized to the average obtained by the 10 minute recording averages (100%).

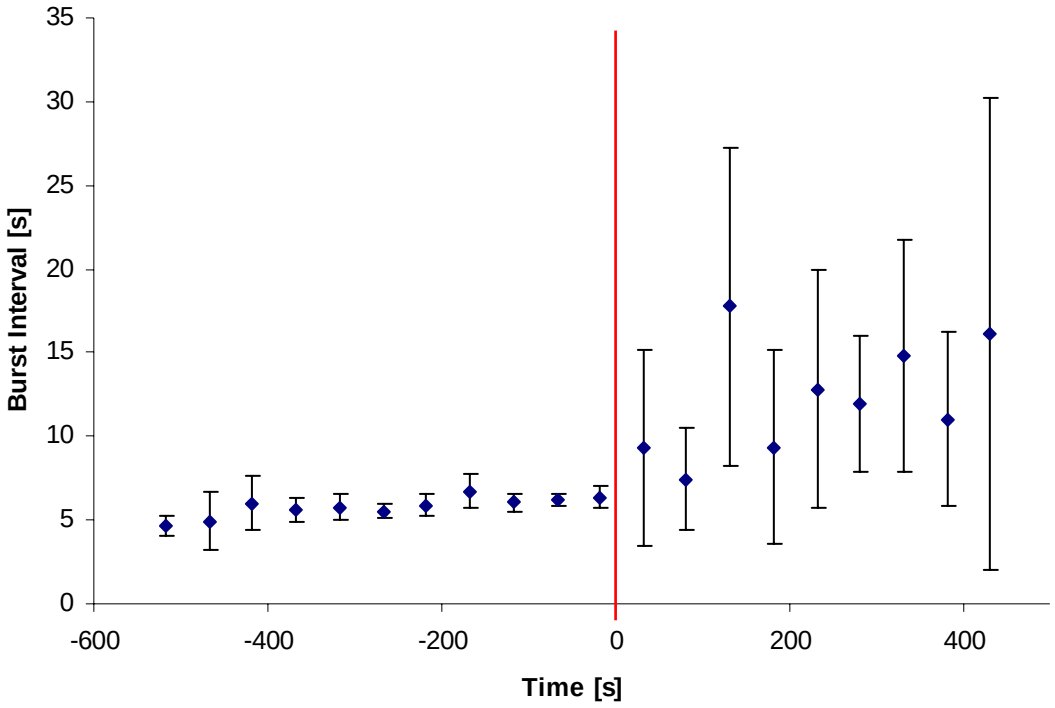

Figure 4.8. Hybrid system allows for continuous extracellular recording before and after injury. As this example shows, variability can increase dramatically following mechanical insult. Electrical activity is relatively constant in this electrode throughout the 10 minute recording before insult was applied. Following insult (time=0; red line) burst intervals became erratic. Each time point represents raw data averaged over 50 seconds.

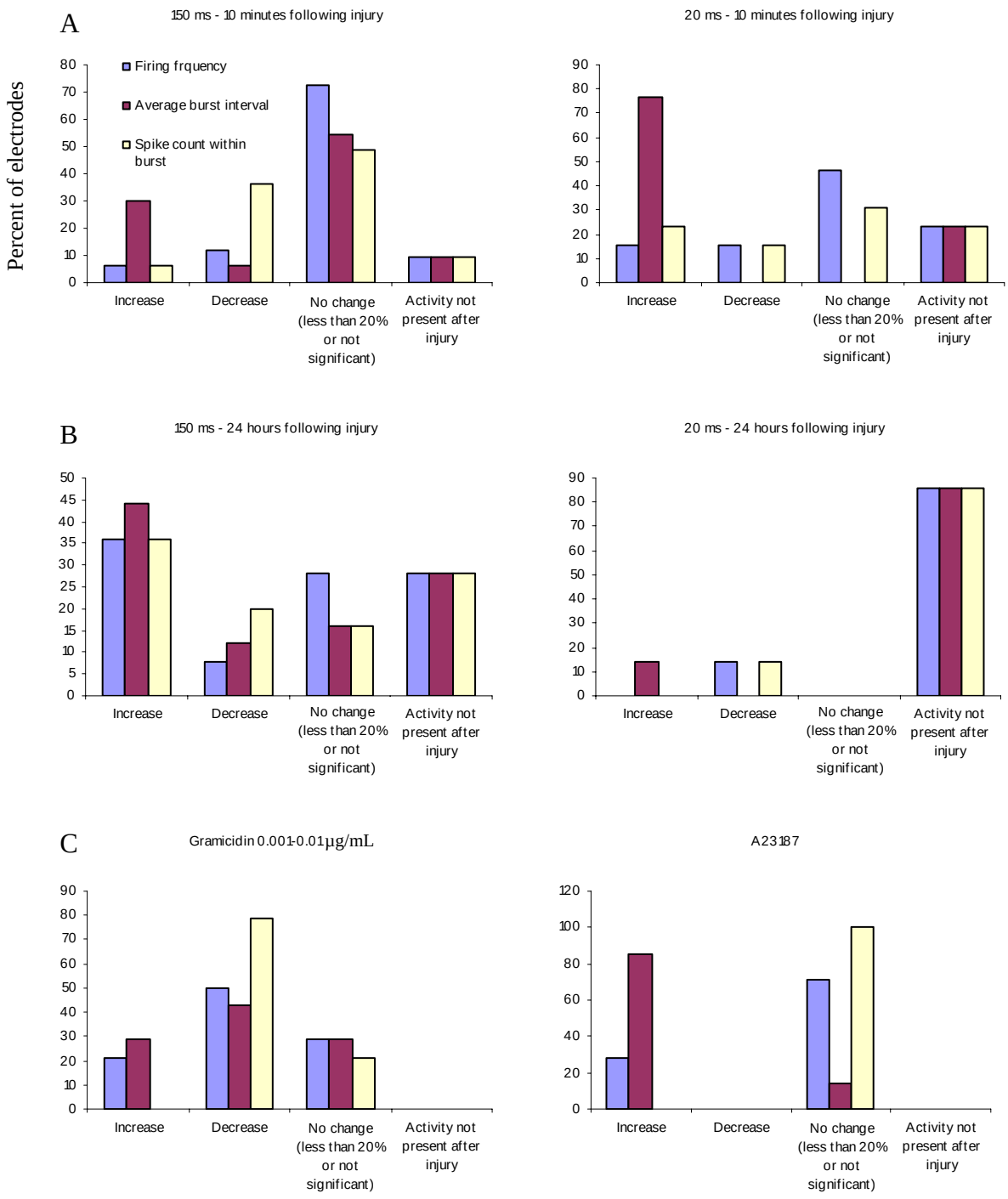

Figure 4.9. Compilation of all electrodes which presented spontaneous activity before treatment. Electrode activities were averaged over 10 minutes before injury and compared to 10 minutes (A) or 24 hours (B) after mechanical insult. Electrodes that did not meet the criterion for significant change were quantified as "No change". (A and B) Outcome of electrode activity following a mechanical insult at 20 ms rise time (left) and 150 ms rise time (right). (C) Effects of ionophore treatments on spontaneous activity 10 minutes following addition to gramicidin (left) or A23187 (right).

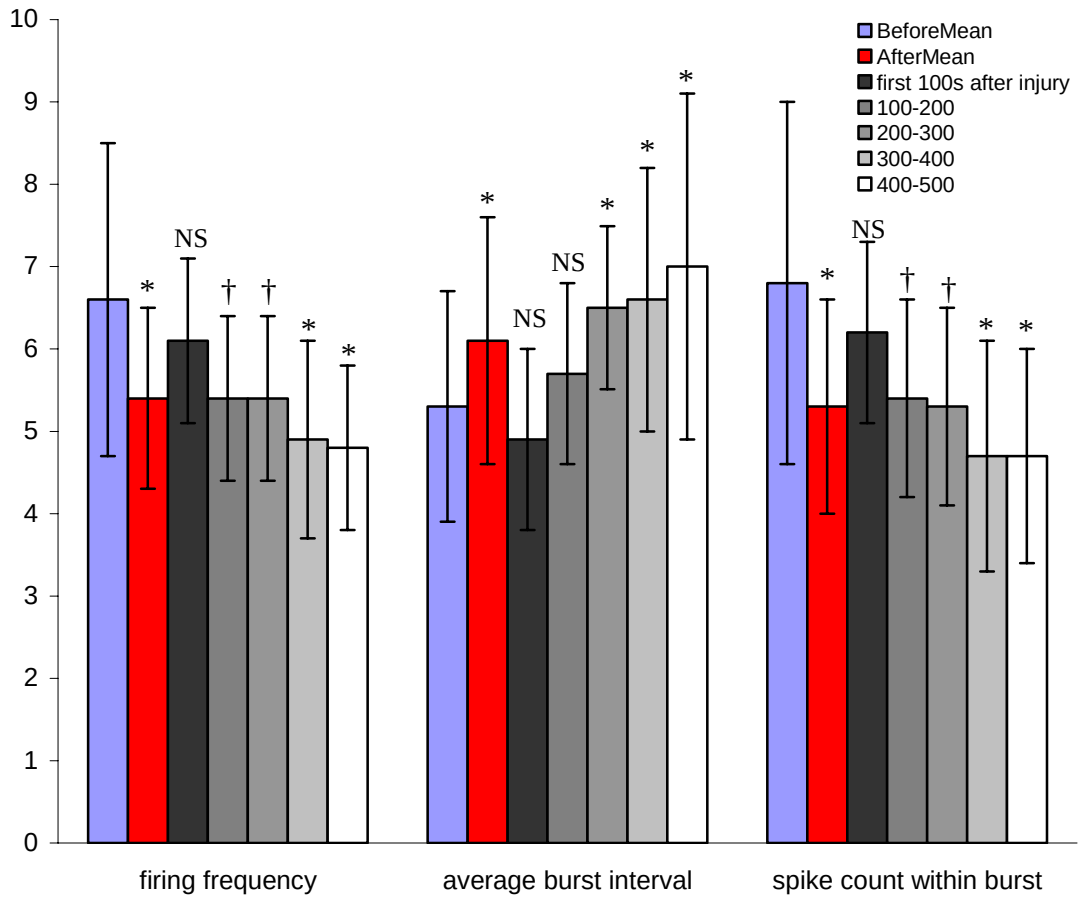

Figure 4.10. Temporal profile of burst intervals averaged over the first 10 minutes and averaged in 100 s increments following injury. Data obtained from one electrode shows increase in burst interval after injury as well as decrease in firing rate within burst and overall firing frequency. Notice that changes occur gradually within the first 10 minutes. Injury rise time was 150 ms. y-axis represent absolute values in units given in the methods section. * $p<0.001$, †$p<0.05$, NS=not significant when compared to parameters before injury.

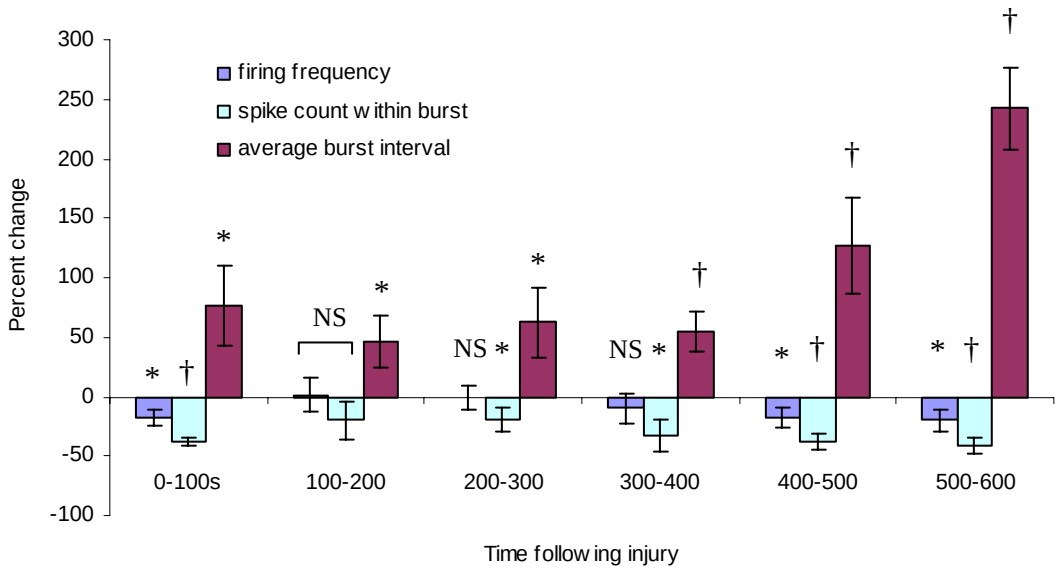

Figure 4.11. Mechanical insult responses cause an immediate and a delayed change in burst interval. Average of all active electrodes within one iMEA following injury. Responses were normalized by the activity recorded before injury (0%). Notice the immediate increase following insult and second further increase from 400 s after insult. Culture was injured at 150 ms rise time. * $p<0.01$, †$p<0.001$, NS=not significantly different than before injury.

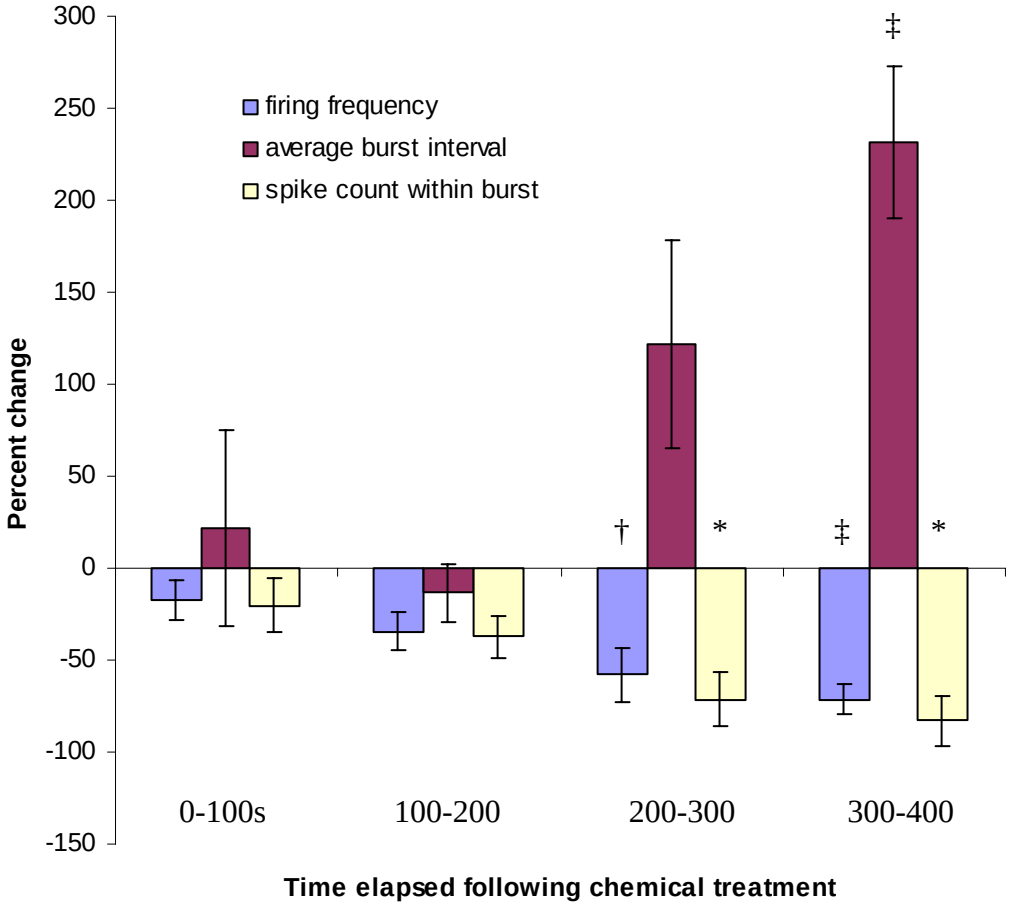

Figure 4.12. Gramicidin treatment (0.01 µg/mL) of neuronal cultures causes acute electrical disturbances. Response is delayed, taking up to 200 seconds to be evident. Data depicts the average of four electrodes within one *i*MEA. * Significantly different than electrical activity from 0-100 s and 100-200 s ($p<0.05$). † Significantly different when compared to 0-100s ($p<0.001$). ‡ Significantly different than 100-200 s ($p<0.05$).

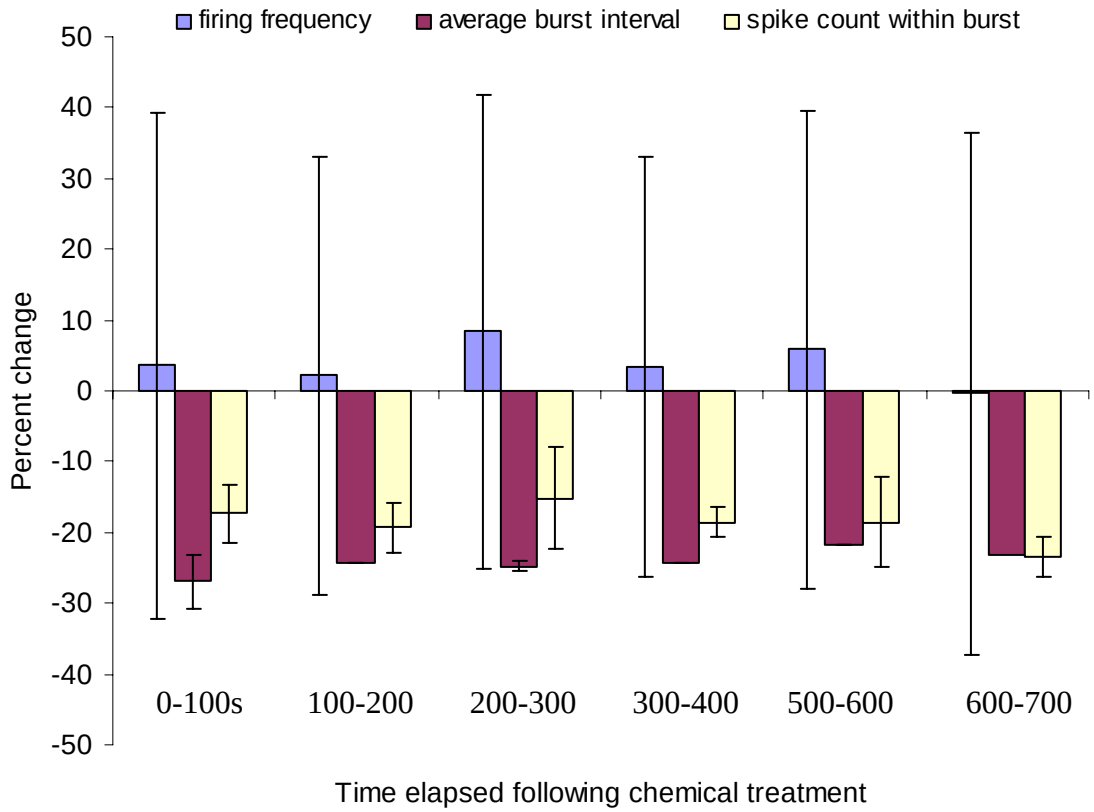

Figure 4.13. Low concentrations of gramicidin cause changes in electrical activity without overwhelming cultures. At 0.0001 µg/mL, gramicidin treatment caused a shift in electrical activity that was constant throughout the recording time. Data was averaged over 3 electrodes and normalized with activity before injury (0 %).

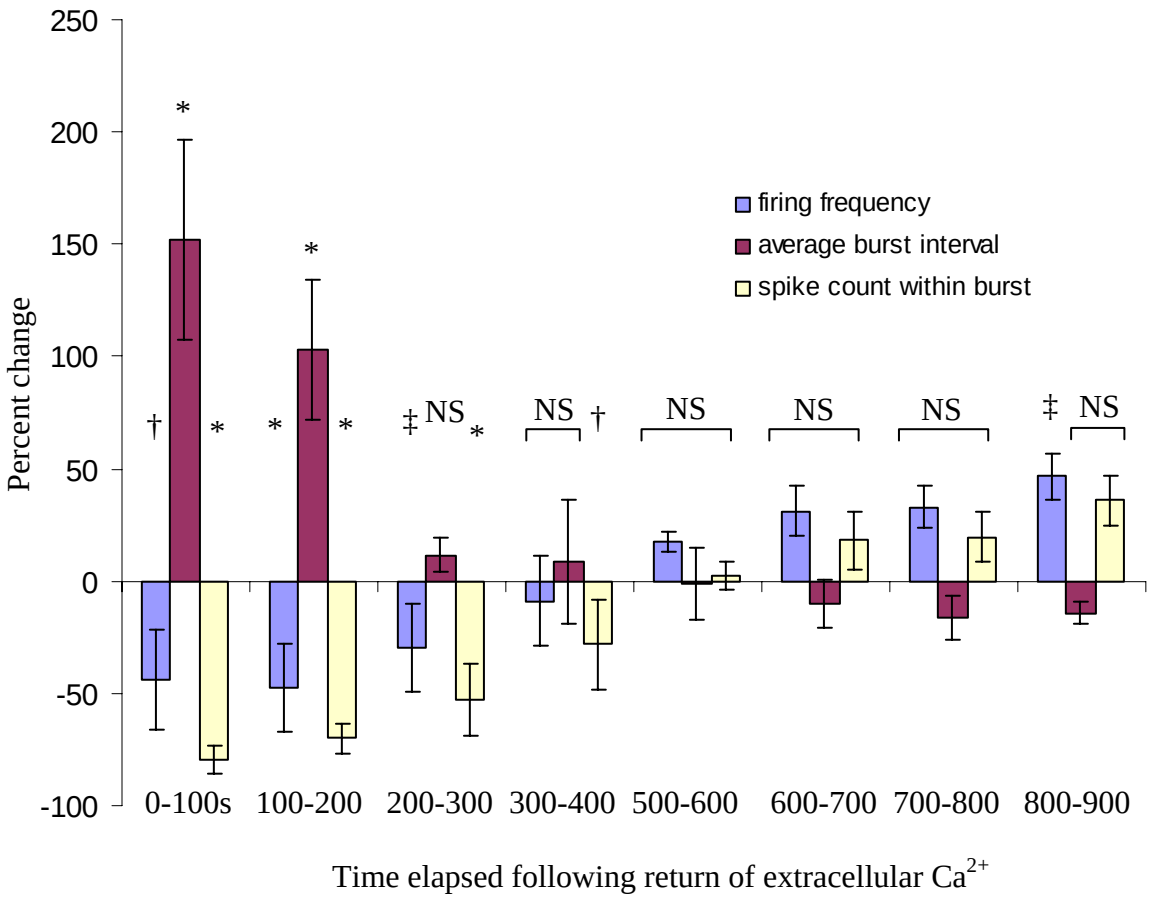

Figure 4.14. The return of extracellular Ca^{2+} causes a slow recovery of electrical activity. Significantly different from electrical activity before removal of extracellular Ca^{2+} * P<0.001, †P<0.01, ‡ P<0.05.

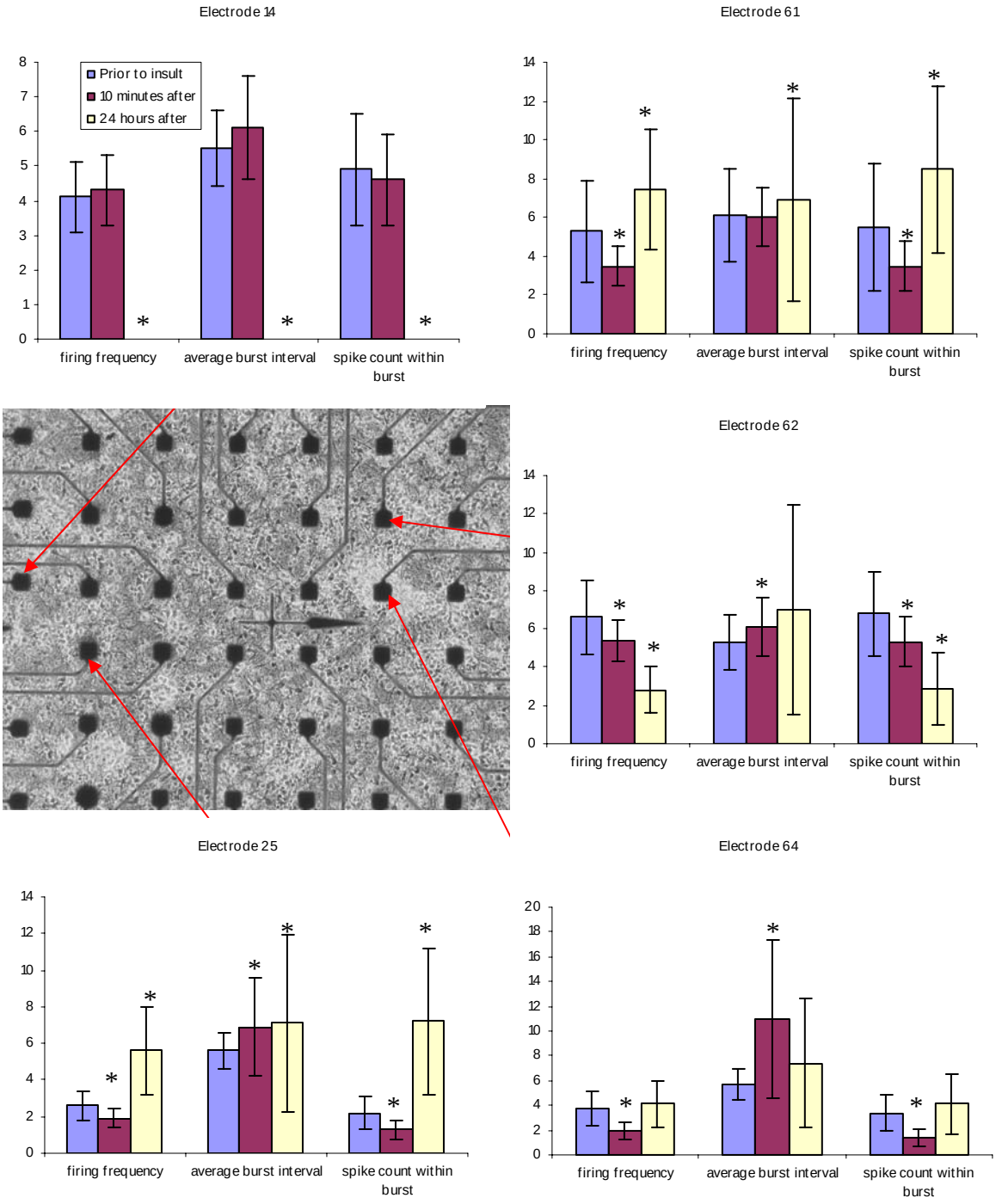

Figure 4.15. Comparison of electrical activity before, immediately after and 24 hours following injury revels heterogeneity within a culture. Injury rise time was 150 ms. Electrical responses can vary widely amongst electrodes within the same iMEA. Increase in variability was present in all parameters at 24 hours following injury, except for electrode 14 which was silent at that time point. y-axis is not normalized and represent absolute values. * Significantly different when compared to recordings before injury ($p<0.001$).

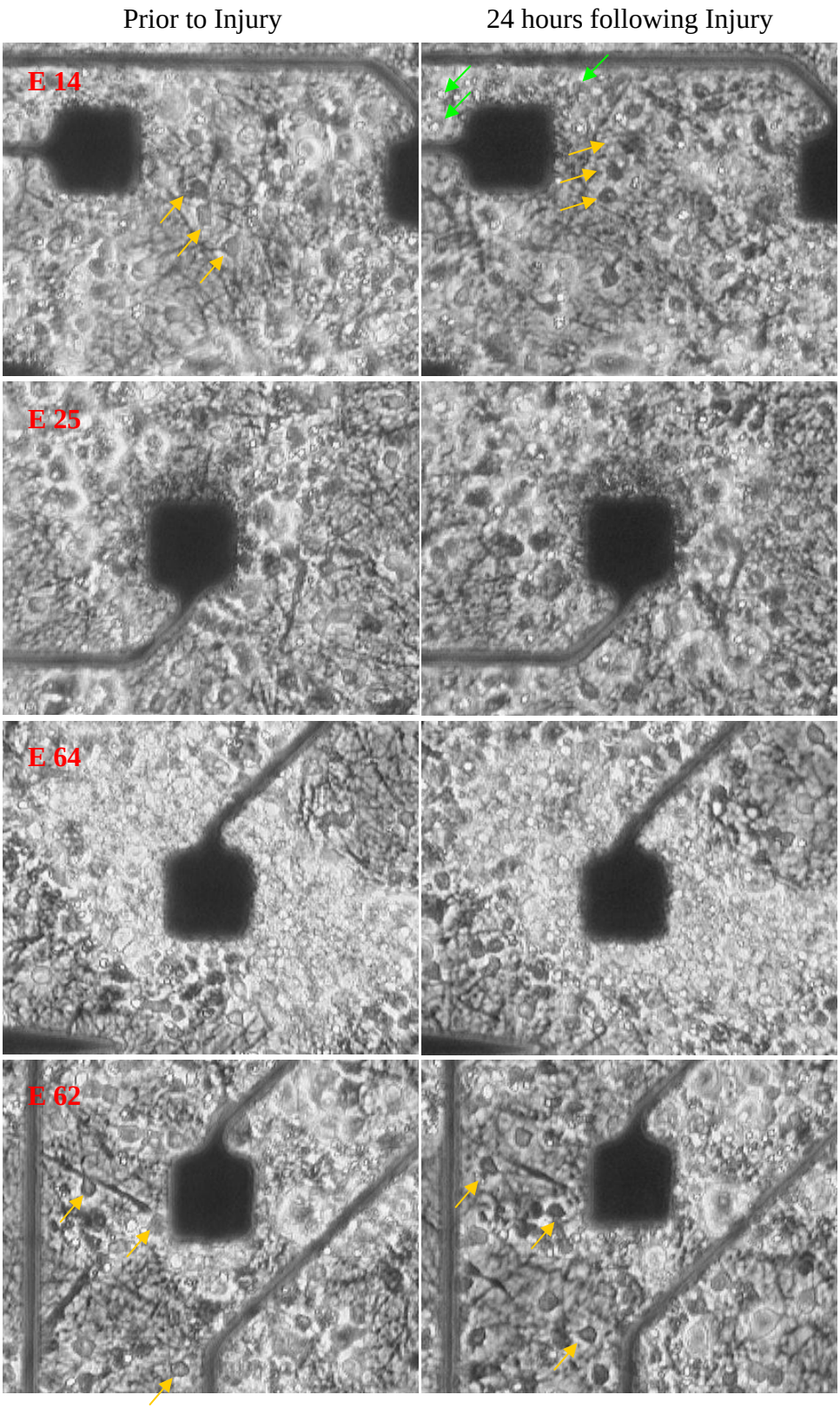

Figure 4.16. Neuronal cultures present remodeling after injury. Orange arrows indicate cell motility. Green arrows indicate evidence of increased in cell death.

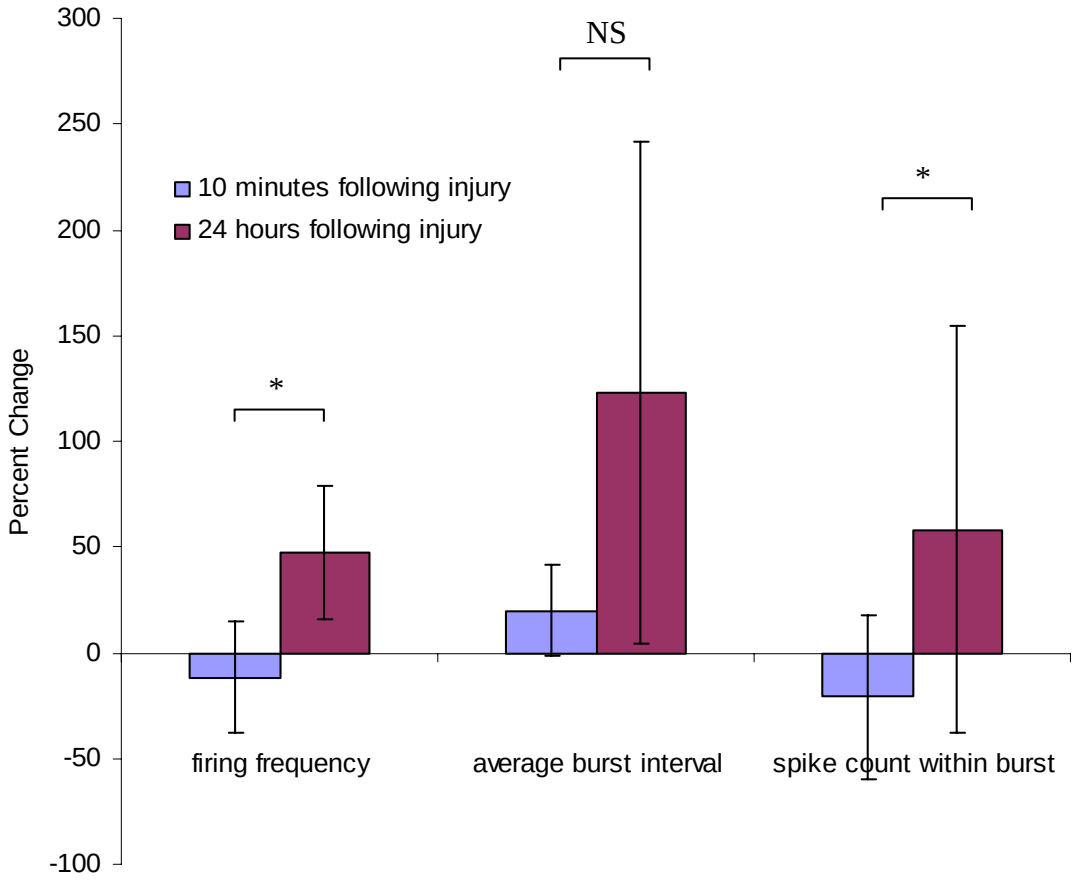

Figure 4.17. Long-term effects of gramicidin treatment. Two of the three parameters assessed were significantly different at 24 hours post chemical insult when compared to immediately following gramicidin treatment (0.01 µg/mL; *$p<0.05$). Baseline (0%) was established based on the electrical activity before injury.

CHAPTER 5

CONCLUSIONS

We have elucidated the presence of neuronal plasma membrane disruptions acutely following TBI. This is the first study of its kind which has assessed acute somata membrane disruptions both in *in vivo* and *in vitro*. The widespread presence of neuronal somata which presented plasma membrane disruption following *in vivo* TBI may offer an explanation and a mechanism for the acute neuronal degeneration reported by other investigators. This is reinforced by the morphological signs of early degeneration of neurons containing high concentrations of the permeability marker in the injured rat brain. Future studies will concentrate on evaluating the biochemical signature of somata containing plasma membrane disruptions with respect to activation of enzymatic cascades known to play a role in cell death and dysfunction in TBI. In addition, separating somata that became affected by the primary mechanical insult and are positive to the permeability marker from the other cell bodies that will subsequently degenerate due to secondary insults such as excitotoxicity will enable further elucidation of the degeneration process. The analysis of plasma membrane susceptibility among different neuronal cell types can further enhance our knowledge of the causes of selective cell death following TBI. The *in vivo* techniques developed in this study can also be used in the investigation of acute electrical profiling of neurons with disrupted membranes using intracellular electrophysiology and acute *ex vivo* slice procedures. Instead of blindly probing for electrical activity of neurons of the injured brain, the comparison of positive and negative cells to a permeability marker can be made. This type of research could

provide new insights into the resealing process in a *in vivo* environment, since plasma membrane integrity can be easily assessed with standard intracellular recording methods.

Using an *in vitro* model of TBI, we have elucidated the characteristics of the neuronal plasma membrane disruptions caused by a mechanical insult such as the size distribution. Using this idealized environment, we have found that the rate in which the mechanical insult is applied affects the percentage of cells within the injured population which present membrane disruptions. We confirmed that, as in other cell types, resealing of neuronal plasma membrane disruptions takes place rapidly and its mechanism is dependent on the presence of extracellular Ca^{2+}. Furthermore, for the first time, a study has evaluated the role of the actin cytoskeleton in the neuronal plasma membrane resealing mechanism. This cytoskeletal component has been previously described as an important and active component in the resealing process in other cell types. We found that unlike other cell types, the actin cytoskeleton in neurons is not as crucial to cell morphology. This was evidenced by the lack of expressive morphological changes relative to other cell types upon treatment of neurons with powerful actin perturbing agents. This difference may be a reflection of the same underlying mechanism that caused resealing in neurons not affected by jasplakinolide treatment as compared to other cell types. We believe that the role of the actin cytoskeleton in neurons is fundamentally different from other cell type such as astrocytes and fibroblasts, which have prominent stress fibers, thereby warranting further investigation in this interesting and potentially important phenomenon.

We have developed a novel device which allows for the uninterrupted reading of extracellular electrical activity of neuronal cultures before and after they are subjected to

a mechanical stress. The results from the experiments have given us insight into what electrically occurs in neuronal cultures following a mechanical insult. For example, we showed that in many instances cultures can present no noticeable morphological traces of injury or degeneration yet display a complete cessation in electrical activity. The techniques developed in this study will give the research of TBI a new dimension in which neuronal health can be evaluated in conjunction with other parameters. Future use of this novel device may provide insights in network dynamics before and after insult with respect to how signals are conducted and relayed from cell to cell. For example, other dimensional configurations of the *i*MEA can be used, with electrodes placed farther apart from each other, to evaluate spread of signals, signal velocity, among others. Collectively, these studies presented in this thesis provide new information to TBI researchers that may ultimately lead to new treatment strategies.

APPENDIX A

IN VITRO MODEL OF TRAUMATIC BRAIN INJURY: VALIDATION

A.1 Introduction

Shear deformation is the main type of deformation during TBI (Holbourn, 1943). We have developed a shearing system for applying large magnitudes of fluid shear stress at high rates to neuronal cultures. The device consists of a cone which rotates at a small distance above a flat plate to which two-dimensional cultures are adhered (Figure A.1). The rotation of the cone induces a velocity gradient perpendicular to the cell plate in the fluid that fills the gap between the cone and plate. Controlled shear stress and shear rate can be applied to the cultures. This device differs from our past fluid-induced shear stress injury apparatus (LaPlaca and Thibault, 1997) in that it produces a uniform shear stress throughout the flat plate and holds a larger number of separate cultures that, once injured, can be used for different assays. The CSID uses a computer-controlled servo-motor system that precisely controls acceleration, velocity, and pulse duration (Fig A.2). Well-controlled combinations of high steady-state shear stress (up to 2000 dynes/cm^2) at short rise times (as short as 20 ms) can be applied so that injury thresholds of cell death and other cellular responses can be investigated. The neuronal permeability experiments, for example, used shear stresses magnitudes of up to 190 dynes/cm^2 at 20 ms rise times. Higher shear stress magnitudes were used in the cell death and cell injury experiments, where shearing buffer viscosity was increased up to 50 fold. Steady-state conditions for similar cone-plate geometry have been shown to be reached in less than 20 ms (Blackman

et al., 2000). In the same study, Blackman et al. also extensively characterized the cone-plate geometry with respect to dynamic shear stress quantification at different radial positions.

A.2 Materials and Methods

A.2.1 Neuronal cell culture and injury

Neonatal neuronal cells were cultured for 7 days and then injured in the CSID (for injury and cell culture details please see Chapter 3). Cell viability assessment was accomplished using ethidium homodimer and calcein-AM (Molecular Probes, Eugene, OR). At the chosen assessment time point after injury, cells were rinsed with Hanks' balanced salt solution (HBSS; Invitrogen, Carlsbad, CA) and then treated with ethidium homodimer (4 μM) and calcein-AM (1 μM) for 30 minutes. Cells were then dissociated and fluorescent intensity was assessed via flow cytometry.

A.2.2 Lactate dehydrogenase assessment

Quantification of release of lactate dehydrogenase (LDH) was accomplished by and LDH quantification kit (Sigma, St. Louis, MO).

A.2.3 Caspase-3 activity assessment

Caspase-3 activity was assessed with a Clevalite kit (Chemicon, Temecula, CA). This kit works by detecting caspase-3-specific substrate (DEVD) in cell extracts.

A.3 Results and Discussion

A.3.1 Neuronal cell death following injury

We have showed that neuronal cell death was dependent on the rate and magnitude of shear stress produced by the CSID (Figure A.3). Similar results have been obtained in different *in vitro* injury models which induce mechanical insult via fluid shear

stress (LaPlaca and Thibault, 1997) or elastic membrane stretch (Geddes and Cargill, 2001). In order to reach the cell death rates shown in Figure A.3 shear stress magnitudes of up to 1200 dynes/cm^2 were employed. Also, rise times (time spent for the motor to reach its final velocity) ranged from 0.45 ms to 45 ms. We therefore classify this regime of injury as moderate to severe, which is more injurious than the regimes employed in the plasma membrane disruption experiments.

A.3.2 Cytosolic lactate dehydrogenase release following injury correlates with cell death

Increase in cytosolic lactate dehydrogenase (LDH) is used as an injury marker since this enzyme is not normally present in cell culture medium or supplements added to cultures such as B-27 (Invitrogen), nor is it secreted by healthy cells. It is, however, readily released from cells when plasma membranes become compromised (LaPlaca et al., 1997). Neuronal injury evoked an increase in LDH release seen as early as 24 hours post-injury (Figure A.4). Micrographs from the same experiment confirm the presence of widespread cell death as early as 12 hours following injury (Figure A.5).

A.3.3 Mechanisms of cell death following injury is not dependent on caspase-3 activation

Cell lysates from the same cell cultures shown in Figure A.4 and A.5 were used to quantify activation of caspase-3. Caspase-3 is known as an executioner caspase found in its active state in cells undergoing apoptosis (Nicholson et al., 1995). Apoptotic cells have been detected within TBI sites *in vivo* experiments days following insult (Rink et al., 1995) as well as in *in vitro* models of TBI (Allen et al., 1999). However, other studies *in vivo* have revealed that apoptosis is probably not as prevalent in TBI (Conti et al., 1998). Injured cells at the 4.5 ms rise time presented a significant increase of activation of the caspase-3 (Figure A.6).

The increase of caspase-3 activation in the longer rise time treatment, however, was not sufficient to explain most of the cell injury seen in the LDH assay, considering that positive control samples using staurosporine, which induces apoptosis in neurons (Krohn et al., 1998), induced massive cell death with concurrent large activation of caspase-3. Therefore, we believe that if a considerable amount of the cell death seen in the mechanically injured samples were apoptotic in nature, there would have been a corresponding increase in caspase-3 activation, comparable to staurosporine samples. The results suggest that most of the cell death due to injury was necrotic in nature. These findings are in agreement with recent publications which show prevalence of necrotic cell death following TBI (Beer et al., 2000; Pike et al., 2000). The onset of necrosis can be due to excessive influx of ions such as Ca^{2+} into cells during and following mechanical injury, as described in TBI *in vitro* models (Geddes and Cargill, 2001; LaPlaca et al., 1997; Weber et al., 1999). The persistence of excess Ca^{2+} in the cytosol can overwhelm the ability of cells to maintain ionic homeostasis, leading to ATP depletion (Lifshitz et al., 2003), cytoskeletal proteolysis (Buki et al., 1999a), and an eventual necrotic death (Pike et al., 2000).

A.4 Conclusions

The results presented here show that the CSID is able to cause neuronal death, and that the process which cells dye is mainly a necrotic one. In order to elucidate the initial biomechanical events that lead to this form of cell death, we propose to investigate possible mechanisms that can initiate this death cascade. In order to do so, we chose to investigate in particular the acute cellular responses that can lead to the delayed mechanisms that lead to death.

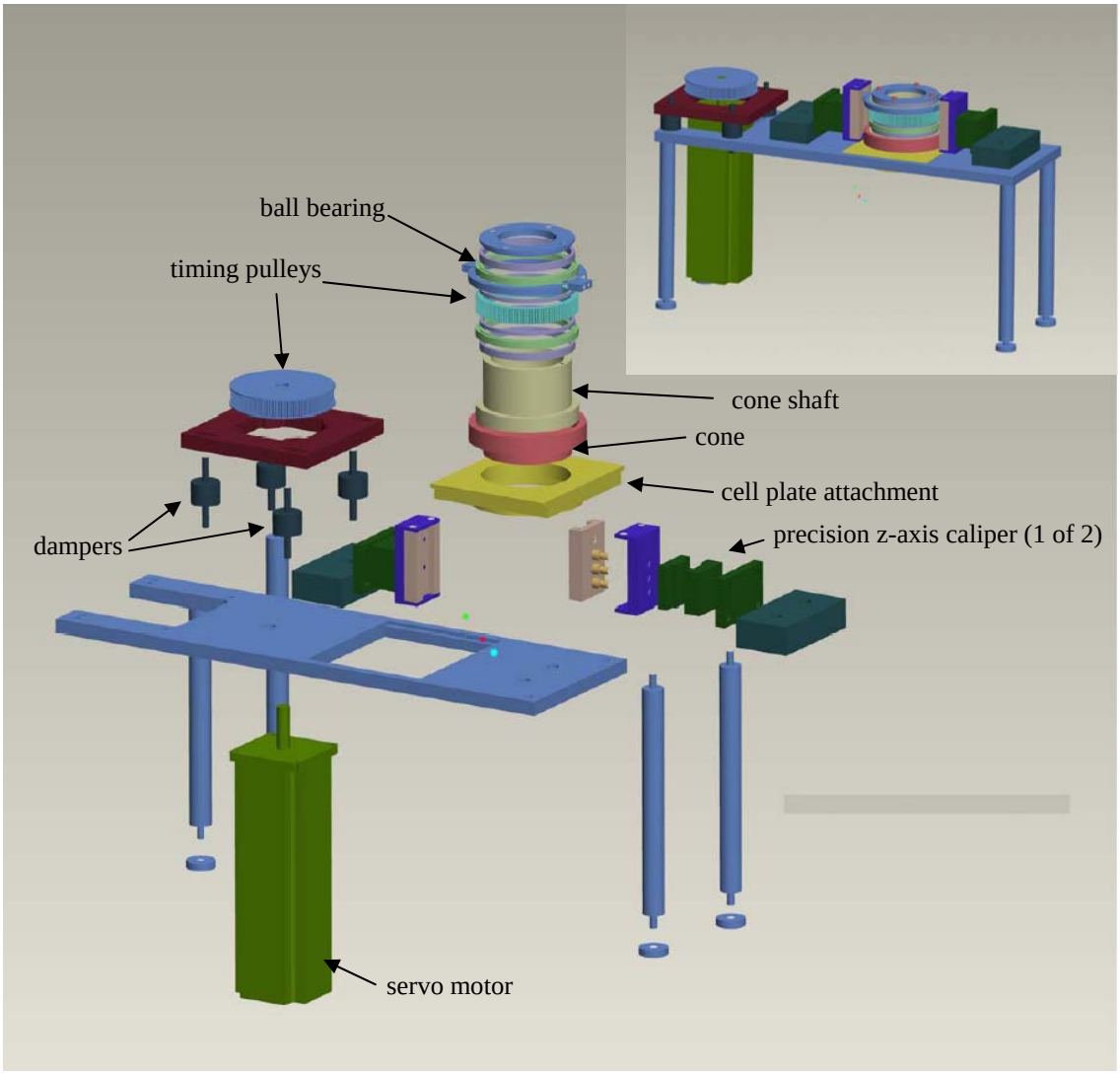

Figure A.1. Cell shearing injury device. Partially exploded view of the components of the CSID and the assembled device (upper right corner). The main components of the CSID are highlighted in the exploded view. Timing belt was not included in the schematics for simplicity.

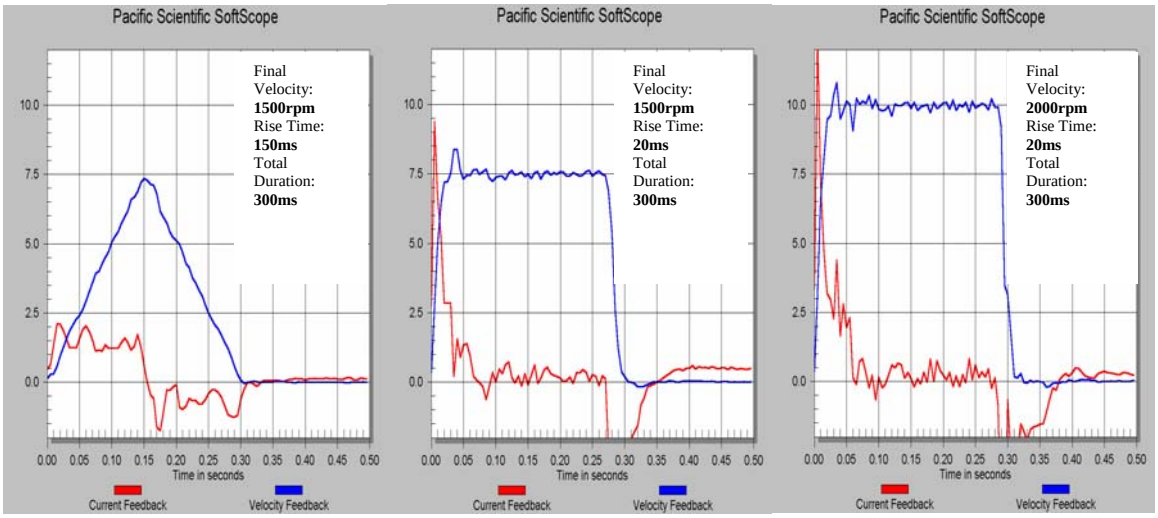

Figure A.2. Samples of servo motor velocity profiles used in the neuronal permeability studies. The blue curve indicates the velocity feedback. The red curve indicates the current used to drive the motor. The y-axis scales for velocity and current are 200 rpm and 2 amperes per unit, respectively. Final velocities of 1500 and 2000 rpm result in steady-state shear stresses of 140 and 190 dynes/cm^2, respectively.

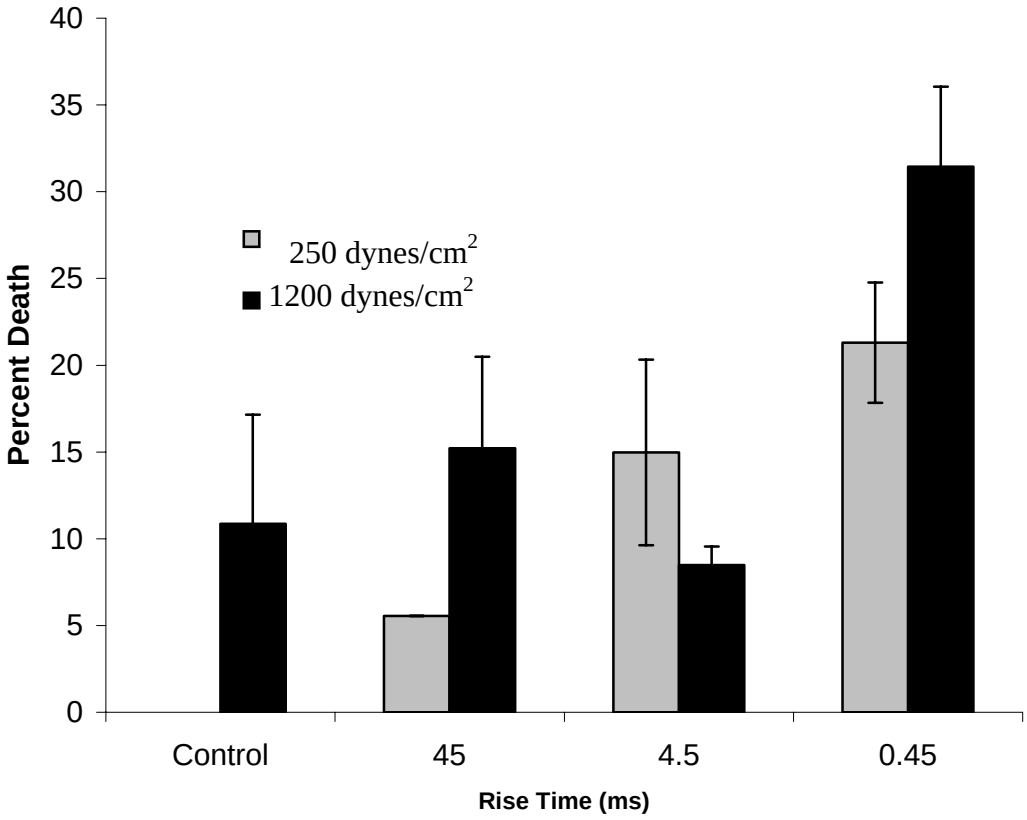

Figure A.3. Percent cell death at 48 hours post insult. Cell death depends on shear stress magnitudes and rise time ($p<0.005$) by 2-way ANOVA ($n=3$). Shear stress magnitude was obtained by varying the viscosity of the shearing buffer. Shearing buffer viscosity of 10 and 50 cP were used, yielding shear stresses values of 250 dynes/cm^2 and 1200 dynes/cm^2, respectively. Length of time of insult was 300 ms. Error bars represent standard deviation (SD).

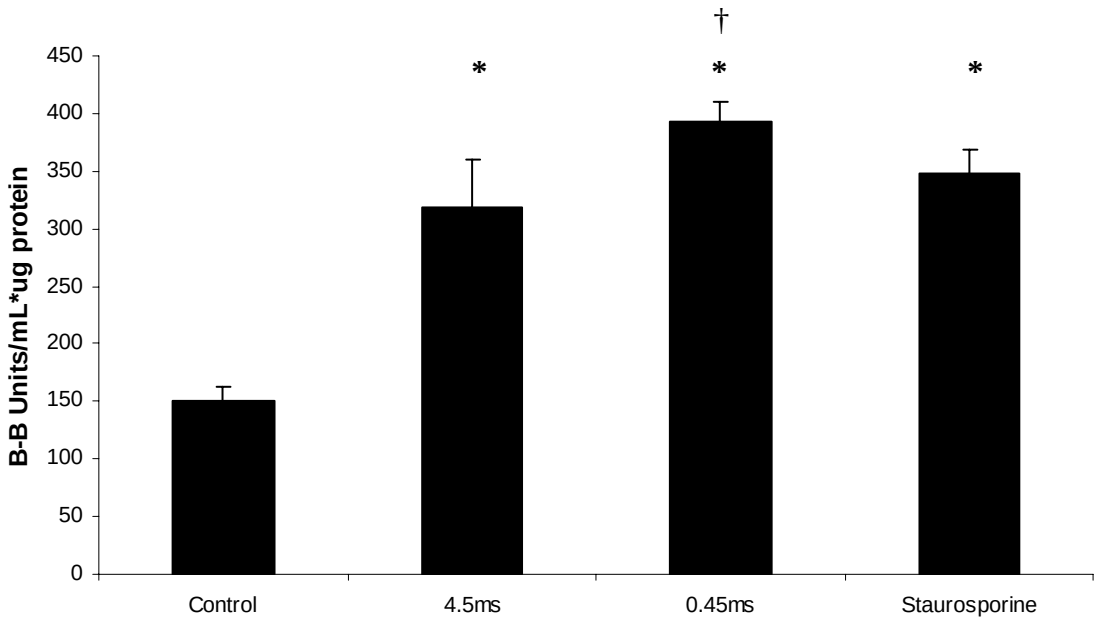

Figure A.4. Lactate dehydrogenase release from neurons at 24 hours post injury. Mechanical and chemical trauma induced an increase of LDH release. LDH release was dependent on the rise time of the insult. * Significantly different $p<0.001$ compared with control. † Significantly different from 4.5ms ($p<0.05$). Shear stress magnitude was 2000 dynes/cm^2, using buffer viscosity of 80cP. Insult length was 400 ms. Error bars represent SD.

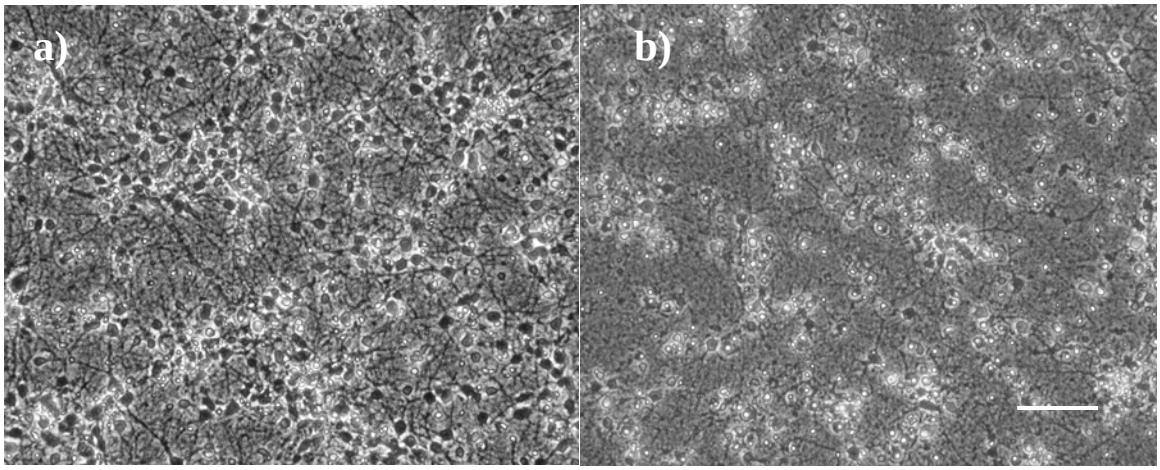

Figure A.5. Phase contrast photo micrograph of neuronal cultures 12 hours after long duration insult (400 ms). (a) control (b) cells injured at 0.45 ms. By 24 hours, dead cells were prevalent, which is indicated by data shown in Figure 4. Shear stress magnitude was 2000 dynes/cm^2, using buffer viscosity of 80cP. Insult length was 400 ms. Scale bar represents 100 μm.

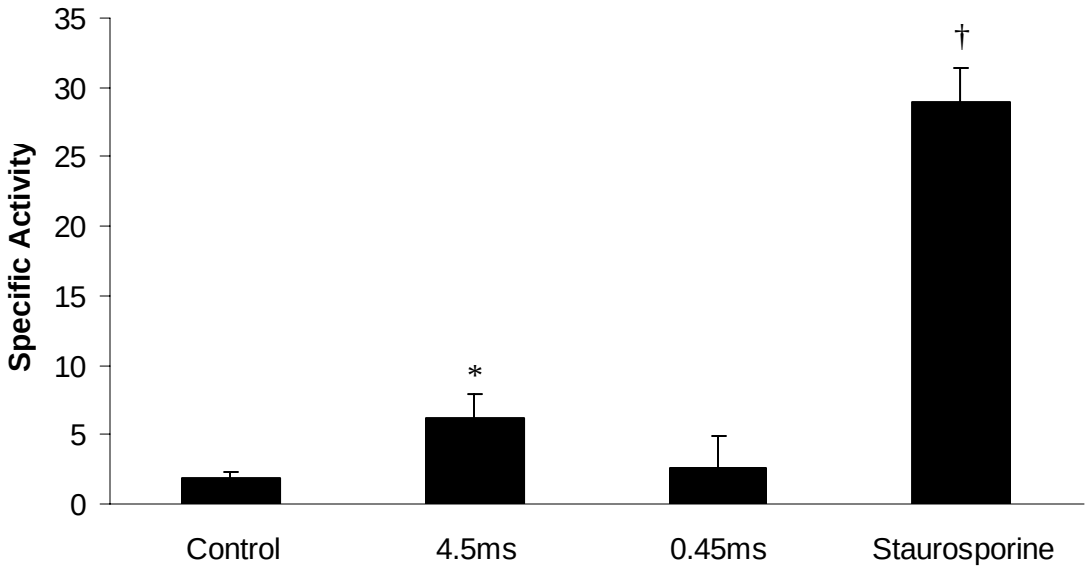

Figure A.6. Caspase-3 specific activity 24 hours post-insult. Caspase-3 activity increased at medium injury level (4.5 ms rise time) but not at high injury level (0.45 ms rise time). * Significantly different from control ($p<0.05$). † Significantly different from all others ($p<0.001$). Shear stress magnitude was 2000 dynes/cm^2, using a buffer viscosity of 80cP. Insult length was 400 ms. Error bars represent SD.

APPENDIX B

ORIGINS OF HETEROGENEITY IN NEURONAL CELLULAR RESPONSES TO MECHANICAL TRAUMA

B.1 Introduction

The heterogeneity of cellular responses in cultured neurons is probably one of the most predominant observations reported in TBI *in vitro* models. This occurs in spite of the care in designing models which produce a constant insult such as biaxial stretch (Geddes et al., 2003) and fluid shear stress (Chapter 3 and 4; Fig B.1). Both *in vitro* models can produce cellular responses that are greatly affected by cell morphology and substrate adhesion.

Stretch-induced injury as well as fluid shear stress-induced injury devices can only apply an even insult if cells are equally attached to the substrate. A common problem observed in neuronal cultures (i.e. cultures of neuronal cells with a low percentage of glial cells; <5%) is the weakening of cell to substrate adhesion as cultures mature. Despite of a good initial attachment to the substrate, neuronal processes have been commonly observed to preferentially adhere to themselves and to coalesce into groups of neurites which can eventually become weakly attached to the substrate. This has been observed especially when longer term cultures (10 days or more) are attempted. Culturing neuronal cells for at least 10-14 days have been shown to yield more mature cells that express adult cellular markers as well as a more developed electrical activity profile (Kamioka et al., 1996; Tateno et al., 2002).

In case of stretch-induced injury, there are inherent difficulties of adhesion between the elastic substrate and neurons.

We have used identically cultured cells as the ones used in the study of plasma membrane disruptions following mechanical trauma (see Chapter 3 for details) to study variations in cell morphology and adhesion differences using scanning electron microscopy techniques. This study objective is to elucidate the potential causes of differential cellular responses to mechanical trauma.

B.2 Materials and Methods

Neonatal neuronal cells were cultured using the same protocol described in Chapter 3 with the exception that the substrate was silicone and not glass. Briefly, cultures (7 DIV) were fixed with 2.5% glutaraldehyde in 0.1M cacodylate buffer (pH 7.4) at 4°C for 24 hours. Cultures were washed in di-H_2O followed by post-fixation of phospholipids by 1% OsO_4 in 0.1M cacodylate buffer, pH 7.4, for 1 hour. A graded series of ethanol (30, 50, 70, 3 x 100%, 15 min each) was used for removal of water from cultures. Exchange with CO_2 was accomplished by a critical point dryer (Polaron E-3000) at critical temperature and pressure. Cells were coated with a 3 nm layer of chromium. Using a low voltage high resolution scanning electron microscope, cultures were viewed at magnifications ranging from 1000X to 20000X.

B.3 Results and Discussion

Acutely, cell morphology and adhesion are probably the only parameters to dictate differential cellular responses to mechanical trauma. These parameters are hypothesized to cause the acute differential plasma membrane disruption obtained from experiments presented in Chapter 3.

This morphology analysis helps us understand and explain why a differential cellular response is expected based on the inherent heterogeneous composition of the population studied (Figure B.2). Although cell morphology and attachment can explain some of the more acute differential cellular responses, they are not the only factors dictating cellular outcome, especially at longer time points. Cellular metabolism and differentiation levels, for example, can also play a role in cellular outcome.

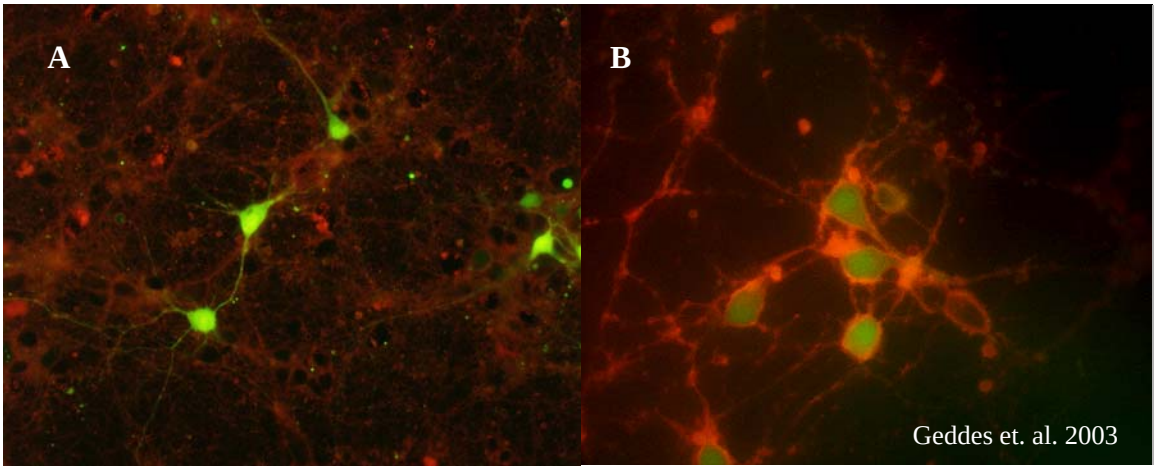

Figure B.1. Two different injury modalities, both uniform, yield heterogeneous responses. Only a sub-population of cells from neuronal cultures injured by uniform fluid shear stress present plasma membrane disruption evidenced by calcein uptake (green) (A). Stretch-induced injury yields similar heterogeneous presence of membrane disruptions marked by carboxyfluorescein uptake (B). Both cultures were counterstained with di-8-ANEPPS.

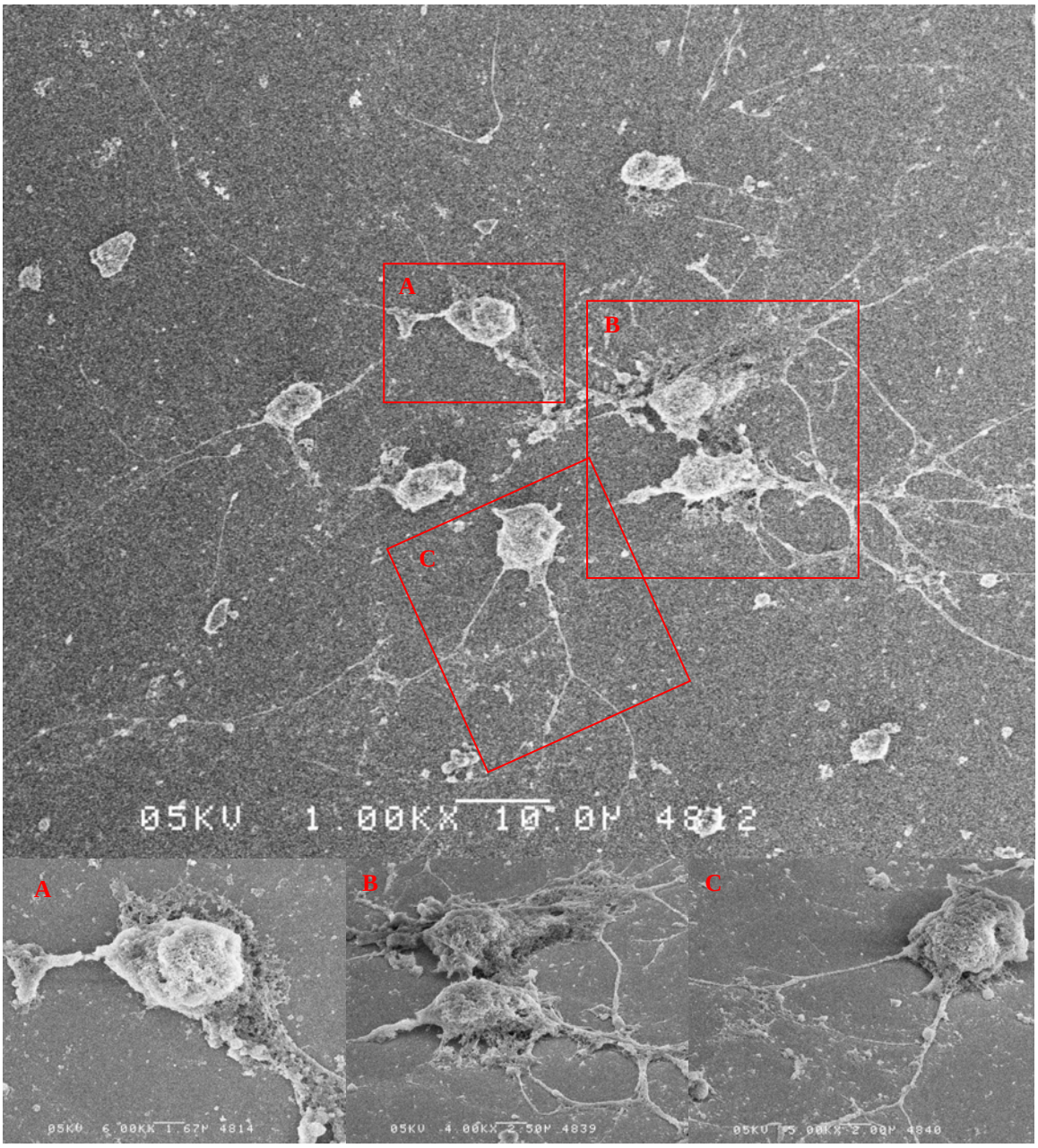

Figure B.2. Heterogeneous cell morphology is found neuronal cultures. Scanning electron micrograph depicts different morphologies and levels of attachment to the substrate in this uninjured cell population. Upper micrograph shows a group of neurons in lower magnification (1000X). Micrographs at the bottom show some of the cells in the upper micrograph at higher magnification. (A) Neuron seen at 6000X presents parts of its soma that sits high from the substrate (where nucleus is located) compared to the skirt like structure (cytoplasmic in nature) seen contacting the substrate. A large neurite (presumed axon) extends from the soma on the right. (B) Two neurons seen at a 40º angle from the substrate at 4000X present numerous neurite extensions and a presumed strong interaction with the substrate. (C) The neuron in this micrograph presents a yet different morphology with visually weaker interactions with the substrate.

REFERENCES

Albensi, B. C., Sullivan, P. G., Thompson, M. B., Scheff, S. W. and Mattson, M. P. (2000). Cyclosporin ameliorates traumatic brain-injury-induced alterations of hippocampal synaptic plasticity. *Exp Neurol* **162**, 385-9.

Allen, J. W., Knoblach, S. M. and Faden, A. I. (1999). Combined mechanical trauma and metabolic impairment in vitro induces NMDA receptor-dependent neuronal cell death and caspase-3-dependent apoptosis. *Faseb J* **13**, 1875-82.

Anderson, A. J. M. a. R. W. G. (1997). Biomechanics of Closed Head Injury. In *Head Injury*, (ed. P. R. a. R. Bullock), pp. 25-37. London: Chapman & Hall.

Beer, R., Franz, G., Srinivasan, A., Hayes, R. L., Pike, B. R., Newcomb, J. K., Zhao, X., Schmutzhard, E., Poewe, W. and Kampfl, A. (2000). Temporal profile and cell subtype distribution of activated caspase-3 following experimental traumatic brain injury. *J Neurochem* **75**, 1264-73.

Blackman, B. R., Barbee, K. A. and Thibault, L. E. (2000). In vitro cell shearing device to investigate the dynamic response of cells in a controlled hydrodynamic environment. *Ann Biomed Eng* **28**, 363-72.

Brana, C., Benham, C. D. and Sundstrom, L. E. (1999). Calpain activation and inhibition in organotypic rat hippocampal slice cultures deprived of oxygen and glucose. *Eur J Neurosci* **11**, 2375-84.

Bubb, M. R., Senderowicz, A. M., Sausville, E. A., Duncan, K. L. and Korn, E. D. (1994). Jasplakinolide, a cytotoxic natural product, induces actin polymerization and competitively inhibits the binding of phalloidin to F-actin. *J Biol Chem* **269**, 14869-71.

Buki, A., Koizumi, H. and Povlishock, J. T. (1999a). Moderate posttraumatic hypothermia decreases early calpain-mediated proteolysis and concomitant cytoskeletal compromise in traumatic axonal injury. *Exp Neurol* **159**, 319-28.

Buki, A., Siman, R., Trojanowski, J. Q. and Povlishock, J. T. (1999b). The role of calpain-mediated spectrin proteolysis in traumatically induced axonal injury. *J Neuropathol Exp Neurol* **58**, 365-75.

Carbonell, W. S. and Grady, M. S. (1999). Evidence disputing the importance of excitotoxicity in hippocampal neuron death after experimental traumatic brain injury. *Ann N Y Acad Sci* **890**, 287-98.

Cargill, R. S., 2nd and Thibault, L. E. (1996). Acute alterations in [Ca2+]i in NG108-15 cells subjected to high strain rate deformation and chemical hypoxia: an in vitro model for neural trauma. *J Neurotrauma* **13**, 395-407.

Carragher, N. O. and Frame, M. C. (2002). Calpain: a role in cell transformation and migration. *Int J Biochem Cell Biol* **34**, 1539-43.

Conti, A. C., Raghupathi, R., Trojanowski, J. Q. and McIntosh, T. K. (1998). Experimental brain injury induces regionally distinct apoptosis during the acute and delayed post-traumatic period. *J Neurosci* **18**, 5663-72.

Detrait, E., Eddleman, C. S., Yoo, S., Fukuda, M., Nguyen, M. P., Bittner, G. D. and Fishman, H. M. (2000a). Axolemmal repair requires proteins that mediate synaptic vesicle fusion. *J Neurobiol* **44**, 382-91.

Detrait, E. R., Yoo, S., Eddleman, C. S., Fukuda, M., Bittner, G. D. and Fishman, H. M. (2000b). Plasmalemmal repair of severed neurites of PC12 cells requires Ca(2+) and synaptotagmin. *J Neurosci Res* **62**, 566-73.

Doebler, J. A. (2000). Effects of neutral ionophores on membrane electrical characteristics of NG108-15 cells. *Toxicol Lett* **114**, 27-38.

Duval, N., Gomes, D., Calaora, V., Calabrese, A., Meda, P. and Bruzzone, R. (2002). Cell coupling and Cx43 expression in embryonic mouse neural progenitor cells. *J Cell Sci* **115**, 3241-51.

Ellis, E. F., McKinney, J. S., Willoughby, K. A., Liang, S. and Povlishock, J. T. (1995). A new model for rapid stretch-induced injury of cells in culture: characterization of the model using astrocytes. *J Neurotrauma* **12**, 325-39.

Evans, M. S., Collings, M. A. and Brewer, G. J. (1998). Electrophysiology of embryonic, adult and aged rat hippocampal neurons in serum-free culture. *J Neurosci Methods* **79**, 37-46.

Gallant, P. E. (1988). Effects of the external ions and metabolic poisoning on the constriction of the squid giant axon after axotomy. *J Neurosci* **8**, 1479-84.

Geddes, D. M. and Cargill, R. S., 2nd. (2001). An in vitro model of neural trauma: device characterization and calcium response to mechanical stretch. *J Biomech Eng* **123**, 247-55.

Geddes, D. M., Cargill, R. S., 2nd and LaPlaca, M. C. (2003). Mechanical stretch to neurons results in a strain rate and magnitude-dependent increase in plasma membrane permeability. *J Neurotrauma* **20**, 1039-49.

Gennarelli, T. A. (1993). Mechanisms of brain injury. *J Emerg Med* **11**, 5-11.

Gennarelli, T. A., Thibault, L. E., Adams, J. H., Graham, D. I., Thompson, C. J. and Marcincin, R. P. (1982). Diffuse axonal injury and traumatic coma in the primate. *Ann Neurol* **12**, 564-74.

Goforth, P. B., Ellis, E. F. and Satin, L. S. (1999). Enhancement of AMPA-mediated current after traumatic injury in cortical neurons. *J Neurosci* **19**, 7367-74.

Gordon, L. M., Sauerheber, R. D., Esgate, J. A., Dipple, I., Marchmont, R. J. and Houslay, M. D. (1980). The increase in bilayer fluidity of rat liver plasma membranes achieved by the local anesthetic benzyl alcohol affects the activity of intrinsic membrane enzymes. *J Biol Chem* **255**, 4519-27.

Graham, D. I., Raghupathi, R., Saatman, K. E., Meaney, D. and McIntosh, T. K. (2000). Tissue tears in the white matter after lateral fluid percussion brain injury in the rat: relevance to human brain injury. *Acta Neuropathol (Berl)* **99**, 117-24.

Grembowicz, K. P., Sprague, D. and McNeil, P. L. (1999). Temporary disruption of the plasma membrane is required for c-fos expression in response to mechanical stress. *Mol Biol Cell* **10**, 1247-57.

Gudi, S., Nolan, J. P. and Frangos, J. A. (1998). Modulation of GTPase activity of G proteins by fluid shear stress and phospholipid composition. *Proc Natl Acad Sci U S A* **95**, 2515-9.

Gurdjian, E. S., Roberts, V. L. and Thomas, L. M. (1966). Tolerance curves of acceleration and intracranial pressure and protective index in experimental head injury. *J Trauma* **6**, 600-4.

Guzman, H. R., Nguyen, D. X., Khan, S. and Prausnitz, M. R. (2001a). Ultrasound-mediated disruption of cell membranes. I. Quantification of molecular uptake and cell viability. *J Acoust Soc Am* **110**, 588-96.

Guzman, H. R., Nguyen, D. X., Khan, S. and Prausnitz, M. R. (2001b). Ultrasound-mediated disruption of cell membranes. II. Heterogeneous effects on cells. *J Acoust Soc Am* **110**, 597-606.

Haidekker, M. A., L'Heureux, N. and Frangos, J. A. (2000). Fluid shear stress increases membrane fluidity in endothelial cells: a study with DCVJ fluorescence. *Am J Physiol Heart Circ Physiol* **278**, H1401-6.

Harris-Warrick, R. M. (2002). Voltage-sensitive ion channels in rhythmic motor systems. *Curr Opin Neurobiol* **12**, 646-51.

Hicks, R., Soares, H., Smith, D. and McIntosh, T. (1996). Temporal and spatial characterization of neuronal injury following lateral fluid-percussion brain injury in the rat. *Acta Neuropathol (Berl)* **91**, 236-46.

Holbourn, A. (1943). Mechanics of Head Injuries. *The Lancet*, 438-441.

Howard, M. J., David, G. and Barrett, J. N. (1999). Resealing of transected myelinated mammalian axons in vivo: evidence for involvement of calpain. *Neuroscience* **93**, 807-15.

Huh, J. W., Raghupathi, R., Laurer, H. L., Helfaer, M. A. and Saatman, K. E. (2003). Transient loss of microtubule-associated protein 2 immunoreactivity after moderate brain injury in mice. *J Neurotrauma* **20**, 975-84.

James, T., Matzelle, D., Bartus, R., Hogan, E. L. and Banik, N. L. (1998). New inhibitors of calpain prevent degradation of cytoskeletal and myelin proteins in spinal cord in vitro. *J Neurosci Res* **51**, 218-22.

Kamioka, H., Maeda, E., Jimbo, Y., Robinson, H. P. and Kawana, A. (1996). Spontaneous periodic synchronized bursting during formation of mature patterns of connections in cortical cultures. *Neurosci Lett* **206**, 109-12.

Kampfl, A., Posmantur, R. M., Zhao, X., Schmutzhard, E., Clifton, G. L. and Hayes, R. L. (1997). Mechanisms of calpain proteolysis following traumatic brain injury: implications for pathology and therapy: implications for pathology and therapy: a review and update. *J Neurotrauma* **14**, 121-34.

Katayama, Y., Becker, D. P., Tamura, T. and Hovda, D. A. (1990). Massive increases in extracellular potassium and the indiscriminate release of glutamate following concussive brain injury. *J Neurosurg* **73**, 889-900.

Ko, K. S., Arora, P. D., Bhide, V., Chen, A. and McCulloch, C. A. (2001). Cell-cell adhesion in human fibroblasts requires calcium signaling. *J Cell Sci* **114**, 1155-67.

Koh, J. Y., Goldberg, M. P., Hartley, D. M. and Choi, D. W. (1990). Non-NMDA receptor-mediated neurotoxicity in cortical culture. *J Neurosci* **10**, 693-705.

Krohn, A. J., Preis, E. and Prehn, J. H. (1998). Staurosporine-induced apoptosis of cultured rat hippocampal neurons involves caspase-1-like proteases as upstream initiators and increased production of superoxide as a main downstream effector. *J Neurosci* **18**, 8186-97.

LaPlaca, M. C., Lee, V. M. and Thibault, L. E. (1997). An in vitro model of traumatic neuronal injury: loading rate-dependent changes in acute cytosolic calcium and lactate dehydrogenase release. *J Neurotrauma* **14**, 355-68.

LaPlaca, M. C. and Thibault, L. E. (1997). An in vitro traumatic injury model to examine the response of neurons to a hydrodynamically-induced deformation. *Ann Biomed Eng* **25**, 665-77.

LaPlaca, M. C. and Thibault, L. E. (1998). Dynamic mechanical deformation of neurons triggers an acute calcium response and cell injury involving the N-methyl-D-aspartate glutamate receptor. *J Neurosci Res* **52**, 220-9.

Lewen, A., Fredriksson, A., Li, G. L., Olsson, Y. and Hillered, L. (1999). Behavioural and morphological outcome of mild cortical contusion trauma of the rat brain: influence of NMDA-receptor blockade. *Acta Neurochir (Wien)* **141**, 193-202.

Lewen, A., Sugawara, T., Gasche, Y., Fujimura, M. and Chan, P. H. (2001). Oxidative cellular damage and the reduction of APE/Ref-1 expression after experimental traumatic brain injury. *Neurobiol Dis* **8**, 380-90.

Lifshitz, J., Friberg, H., Neumar, R. W., Raghupathi, R., Welsh, F. A., Janmey, P., Saatman, K. E., Wieloch, T., Grady, M. S. and McIntosh, T. K. (2003). Structural and functional damage sustained by mitochondria after traumatic brain injury in the rat: evidence for differentially sensitive populations in the cortex and hippocampus. *J Cereb Blood Flow Metab* **23**, 219-31.

Lubke, J., Deller, T. and Frotscher, M. (1997). Septal innervation of mossy cells in the hilus of the rat dentate gyrus: an anterograde tracing and intracellular labeling study. *Exp Brain Res* **114**, 423-32.

Marrese, C. A. (1987). Preparation of Strongly Adherent Platinum Black Coatings. *Analytical Chemistry* **59**, 217-218.

Martin, T. F. (2003). Tuning exocytosis for speed: fast and slow modes. *Biochim Biophys Acta* **1641**, 157-65.

McIntosh, T. K., Vink, R., Noble, L., Yamakami, I., Fernyak, S., Soares, H. and Faden, A. L. (1989). Traumatic brain injury in the rat: characterization of a lateral fluid-percussion model. *Neuroscience* **28**, 233-44.

McNeil, P. L. (2002). Repairing a torn cell surface: make way, lysosomes to the rescue. *J Cell Sci* **115**, 873-9.

McNeil, P. L. and Baker, M. M. (2001). Cell surface events during resealing visualized by scanning-electron microscopy. *Cell Tissue Res* **304**, 141-6.

McNeil, P. L. and Steinhardt, R. A. (1997). Loss, restoration, and maintenance of plasma membrane integrity. *J Cell Biol* **137**, 1-4.

McNeil, P. L. and Terasaki, M. (2001). Coping with the inevitable: how cells repair a torn surface membrane. *Nat Cell Biol* **3**, E124-9.

McNeil, P. L., Vogel, S. S., Miyake, K. and Terasaki, M. (2000). Patching plasma membrane disruptions with cytoplasmic membrane. *J Cell Sci* **113**, 1891-902.

Mills, L. R. and Kater, S. B. (1990). Neuron-specific and state-specific differences in calcium homeostasis regulate the generation and degeneration of neuronal architecture. *Neuron* **4**, 149-63.

Miyake, K., McNeil, P. L., Suzuki, K., Tsunoda, R. and Sugai, N. (2001). An actin barrier to resealing. *J Cell Sci* **114**, 3487-94.

Morrison, B., 3rd, Saatman, K. E., Meaney, D. F. and McIntosh, T. K. (1998). In vitro central nervous system models of mechanically induced trauma: a review. *J Neurotrauma* **15**, 911-28.

Munir, M., Lu, L. and McGonigle, P. (1995). Excitotoxic cell death and delayed rescue in human neurons derived from NT2 cells. *J Neurosci* **15**, 7847-60.

Nawashiro, H., Shima, K. and Chigasaki, H. (1995). Selective vulnerability of hippocampal CA3 neurons to hypoxia after mild concussion in the rat. *Neurol Res* **17**, 455-60.

Newcomb-Fernandez, J. K., Zhao, X., Pike, B. R., Wang, K. K., Kampfl, A., Beer, R., DeFord, S. M. and Hayes, R. L. (2001). Concurrent assessment of calpain and caspase-3 activation after oxygen- glucose deprivation in primary septo-hippocampal cultures. *J Cereb Blood Flow Metab* **21**, 1281-94.

Nicholson, D. W., Ali, A., Thornberry, N. A., Vaillancourt, J. P., Ding, C. K., Gallant, M., Gareau, Y., Griffin, P. R., Labelle, M., Lazebnik, Y. A. et al. (1995). Identification and inhibition of the ICE/CED-3 protease necessary for mammalian apoptosis. *Nature* **376**, 37-43.

Okonkwo, D. O., Pettus, E. H., Moroi, J. and Povlishock, J. T. (1998). Alteration of the neurofilament sidearm and its relation to neurofilament compaction occurring with traumatic axonal injury. *Brain Res* **784**, 1-6.

Ommaya, A. K. and Gennarelli, T. A. (1974). Cerebral concussion and traumatic unconsciousness. Correlation of experimental and clinical observations of blunt head injuries. *Brain* **97**, 633-54.

Pettus, E. H., Christman, C. W., Giebel, M. L. and Povlishock, J. T. (1994). Traumatically induced altered membrane permeability: its relationship to traumatically induced reactive axonal change. *J Neurotrauma* **11**, 507-22.

Pettus, E. H. and Povlishock, J. T. (1996). Characterization of a distinct set of intra-axonal ultrastructural changes associated with traumatically induced alteration in axolemmal permeability. *Brain Res* **722**, 1-11.

Pike, B. R., Zhao, X., Newcomb, J. K., Glenn, C. C., Anderson, D. K. and Hayes, R. L. (2000). Stretch injury causes calpain and caspase-3 activation and necrotic and apoptotic cell death in septo-hippocampal cell cultures. *J Neurotrauma* **17**, 283-98.

Potter, D. A., Tirnauer, J. S., Janssen, R., Croall, D. E., Hughes, C. N., Fiacco, K. A., Mier, J. W., Maki, M. and Herman, I. M. (1998). Calpain regulates actin remodeling during cell spreading. *J Cell Biol* **141**, 647-62.

Prange, M. T. and Margulies, S. S. (2002). Regional, directional, and age-dependent properties of the brain undergoing large deformation. *J Biomech Eng* **124**, 244-52.

Raghupathi, R., McIntosh, T. K. and Smith, D. H. (1995). Cellular responses to experimental brain injury. *Brain Pathol* **5**, 437-42.

Rami, A., Ferger, D. and Krieglstein, J. (1997). Blockade of calpain proteolytic activity rescues neurons from glutamate excitotoxicity. *Neurosci Res* **27**, 93-7.

Rink, A., Fung, K. M., Trojanowski, J. Q., Lee, V. M., Neugebauer, E. and McIntosh, T. K. (1995). Evidence of apoptotic cell death after experimental traumatic brain injury in the rat. *Am J Pathol* **147**, 1575-83.

Saatman, K. E., Murai, H., Bartus, R. T., Smith, D. H., Hayward, N. J., Perri, B. R. and McIntosh, T. K. (1996). Calpain inhibitor AK295 attenuates motor and cognitive deficits following experimental brain injury in the rat. *Proc Natl Acad Sci U S A* **93**, 3428-33.

Saito, K., Miyake, K., McNeil, P. L., Kato, K., Yago, K. and Sugai, N. (1999). Plasma membrane disruption underlies injury of the corneal endothelium by ultrasound. *Exp Eye Res* **68**, 431-7.

Sattler, R. and Tymianski, M. (2000). Molecular mechanisms of calcium-dependent excitotoxicity. *J Mol Med* **78**, 3-13.

Sawyer, D. B., Koeppe, R. E., 2nd and Andersen, O. S. (1989). Induction of conductance heterogeneity in gramicidin channels. *Biochemistry* **28**, 6571-83.

Shapovalov, V. L., Kotova, E. A., Rokitskaya, T. I. and Antonenko, Y. N. (1999). Effect of gramicidin A on the dipole potential of phospholipid membranes. *Biophys J* **77**, 299-305.

Shi, R., Qiao, X., Emerson, N. and Malcom, A. (2001). Dimethylsulfoxide enhances CNS neuronal plasma membrane resealing after injury in low temperature or low calcium. *J Neurocytol* **30**, 829-39.

Singleton, R. H. and Povlishock, J. T. (2004). Identification and characterization of heterogeneous neuronal injury and death in regions of diffuse brain injury: evidence for multiple independent injury phenotypes. *J Neurosci* **24**, 3543-53.

Singleton, R. H., Zhu, J., Stone, J. R. and Povlishock, J. T. (2002). Traumatically induced axotomy adjacent to the soma does not result in acute neuronal death. *J Neurosci* **22**, 791-802.

Spira, M. E., Dormann, A., Ashery, U., Gabso, M., Gitler, D., Benbassat, D., Oren, R. and Ziv, N. E. (1996). Use of Aplysia neurons for the study of cellular alterations and the resealing of transected axons in vitro. *J Neurosci Methods* **69**, 91-102.

Stewart, M. P., McDowall, A. and Hogg, N. (1998). LFA-1-mediated adhesion is regulated by cytoskeletal restraint and by a Ca2+-dependent protease, calpain. *J Cell Biol* **140**, 699-707.

Sutton, R. L., Lescaudron, L. and Stein, D. G. (1993). Unilateral cortical contusion injury in the rat: vascular disruption and temporal development of cortical necrosis. *J Neurotrauma* **10**, 135-49.

Tateno, T., Kawana, A. and Jimbo, Y. (2002). Analytical characterization of spontaneous firing in networks of developing rat cultured cortical neurons. *Phys Rev E Stat Nonlin Soft Matter Phys* **65**, 051924.

Terasaki, M., Miyake, K. and McNeil, P. L. (1997). Large plasma membrane disruptions are rapidly resealed by Ca2+-dependent vesicle-vesicle fusion events. *J Cell Biol* **139**, 63-74.

Thurmond, D. C., Gonelle-Gispert, C., Furukawa, M., Halban, P. A. and Pessin, J. E. (2003). Glucose-Stimulated Insulin Secretion Is Coupled to the Interaction of Actin with the t-SNARE (Target Membrane Soluble N-Ethylmaleimide-Sensitive Factor Attachment Protein Receptor Protein) Complex. *Mol Endocrinol* **17**, 732-42.

Togo, T., Alderton, J. M., Bi, G. Q. and Steinhardt, R. A. (1999). The mechanism of facilitated cell membrane resealing. *J Cell Sci* **112 (Pt 5)**, 719-31.

Togo, T., Krasieva, T. B. and Steinhardt, R. A. (2000). A decrease in membrane tension precedes successful cell-membrane repair. *Mol Biol Cell* **11**, 4339-46.

Tymianski, M. and Tator, C. H. (1996). Normal and abnormal calcium homeostasis in neurons: a basis for the pathophysiology of traumatic and ischemic central nervous system injury. *Neurosurgery* **38**, 1176-95.

Villa, P. G., Henzel, W. J., Sensenbrenner, M., Henderson, C. E. and Pettmann, B. (1998). Calpain inhibitors, but not caspase inhibitors, prevent actin proteolysis and DNA fragmentation during apoptosis. *J Cell Sci* **111**, 713-22.

Wakatsuki, T., Schwab, B., Thompson, N. C. and Elson, E. L. (2001). Effects of cytochalasin D and latrunculin B on mechanical properties of cells. *J Cell Sci* **114**, 1025-36.

Weber, J. T., Rzigalinski, B. A., Willoughby, K. A., Moore, S. F. and Ellis, E. F. (1999). Alterations in calcium-mediated signal transduction after traumatic injury of cortical neurons. *Cell Calcium* **26**, 289-99.

Wolf, J. A., Stys, P. K., Lusardi, T., Meaney, D. and Smith, D. H. (2001). Traumatic axonal injury induces calcium influx modulated by tetrodotoxin-sensitive sodium channels. *J Neurosci* **21**, 1923-30.

Yakovlev, A. G., Knoblach, S. M., Fan, L., Fox, G. B., Goodnight, R. and Faden, A. I. (1997). Activation of CPP32-like caspases contributes to neuronal apoptosis and neurological dysfunction after traumatic brain injury. *J Neurosci* **17**, 7415-24.

Yoshino, A., Hovda, D. A., Kawamata, T., Katayama, Y. and Becker, D. P. (1991). Dynamic changes in local cerebral glucose utilization following cerebral conclusion in rats: evidence of a hyper- and subsequent hypometabolic state. *Brain Res* **561**, 106-19.

Zhang, L., Rzigalinski, B. A., Ellis, E. F. and Satin, L. S. (1996). Reduction of voltage-dependent Mg2+ blockade of NMDA current in mechanically injured neurons. *Science* **274**, 1921-3.